

University of Kentucky

UKnowledge

Theses and Dissertations--Biology

Biology

2014

THE INTERACTIONS BETWEEN JAK/STAT SIGNALING LIGANDS IN DROSOPHILA MELANOGASTER

Qian Chen

University of Kentucky, qian.chen@uky.edu

[Right click to open a feedback form in a new tab to let us know how this document benefits you.](#)

Recommended Citation

Chen, Qian, "THE INTERACTIONS BETWEEN JAK/STAT SIGNALING LIGANDS IN DROSOPHILA MELANOGASTER" (2014). *Theses and Dissertations--Biology*. 23.
https://uknowledge.uky.edu/biology_etds/23

This Doctoral Dissertation is brought to you for free and open access by the Biology at UKnowledge. It has been accepted for inclusion in Theses and Dissertations--Biology by an authorized administrator of UKnowledge. For more information, please contact UKnowledge@lsv.uky.edu.

STUDENT AGREEMENT:

I represent that my thesis or dissertation and abstract are my original work. Proper attribution has been given to all outside sources. I understand that I am solely responsible for obtaining any needed copyright permissions. I have obtained needed written permission statement(s) from the owner(s) of each third-party copyrighted matter to be included in my work, allowing electronic distribution (if such use is not permitted by the fair use doctrine) which will be submitted to UKnowledge as Additional File.

I hereby grant to The University of Kentucky and its agents the irrevocable, non-exclusive, and royalty-free license to archive and make accessible my work in whole or in part in all forms of media, now or hereafter known. I agree that the document mentioned above may be made available immediately for worldwide access unless an embargo applies.

I retain all other ownership rights to the copyright of my work. I also retain the right to use in future works (such as articles or books) all or part of my work. I understand that I am free to register the copyright to my work.

REVIEW, APPROVAL AND ACCEPTANCE

The document mentioned above has been reviewed and accepted by the student's advisor, on behalf of the advisory committee, and by the Director of Graduate Studies (DGS), on behalf of the program; we verify that this is the final, approved version of the student's thesis including all changes required by the advisory committee. The undersigned agree to abide by the statements above.

Qian Chen, Student

Dr. Douglas Harrison, Major Professor

Dr. David Westneat, Director of Graduate Studies

THE INTERACTIONS BETWEEN JAK/STAT SIGNALING LIGANDS IN DROSOPHILA
MELANOGASTER

DISSERTATION

A dissertation submitted in partial fulfillment of the
requirements for the degree of Doctor of Philosophy
in the Department of Biology and
College of Arts and Sciences
University of Kentucky
Lexington, KY 40506

By

Qian Chen

Adviser: Dr. Douglas Harrison, Associate Professor of Biology

University of Kentucky

Lexington, KY 40506

2014

Copyright © Qian Chen 2014

ABSTRACT OF DISSERTATION

THE INTERACTIONS BETWEEN JAK/STAT SIGNALING LIGANDS IN *DROSOPHILA* MELANOGASTER

The development of multi-cellular organisms requires extensive cell-cell communication to coordinate cell functions. However, only a handful of signaling pathways have emerged to mediate all the intercellular communications; therefore, each of them is under an array of regulations to achieve signaling specificity and diversity. One such signaling pathway is the **Janus Kinase/ Signal Transducer and Activator of Transcription (JAK/STAT)** pathway, which is the primary signaling cascade responding to a variety of cytokines and growth factors in mammals and involved in many developmental processes. This signaling pathway is highly conserved between mammals and *Drosophila*, but the *Drosophila* JAK/STAT pathway possesses only three ligands: Unpaired (Upd), Upd2 and Upd3. Co-localized expression patterns of the ligands at several developmental stages raise the possibility that they physically interact. This work was aimed at testing the protein-protein interactions between Upd-family ligands and exploring possible outcomes of ligand oligomerization.

Physical interactions between Upd-family ligands were tested using a Bimolecular Fluorescence Complementation (BiFC) assay. The data suggested that homotypic interactions of Upd2 and Upd3 were stronger than their respective heterotypic interactions with Upd, and the homotypic interaction between Upd molecules was the weakest. In addition, the homotypic interaction of Upd3 was confirmed using yeast two-hybrid interaction assays. To identify protein domains critical for Upd3/Upd3 interaction, a series of poly-alanine substitutions were made to target the 6 conserved domains of Upd3. All 6 substitutions altered the strength of Upd3/Upd3 interaction and drastically reduced Upd3-induced JAK signaling activity. In addition, poly-alanine substitutions of some domains also affected Upd3 extracellular localization or protein accumulation.

Potential outcomes of interactions between Upd-family ligands were tested both *in vitro* and *in vivo*. The interaction between Upd and Upd3 did not significantly change the level of JAK signaling activity. However, loss of Upd3 restricted the distribution of Upd in egg chambers and consequently altered the follicle cell composition. Therefore, Upd/Upd3 interaction is likely to affect the range rather than the intensity of JAK signaling in egg chambers. In summary, this study suggested the possibility of ligand oligomerization as a mechanism for regulating signaling pathways in order to achieve signaling specificity and diversity during development.

Key Words: JAK/STAT signaling, Upd-family ligands, protein interaction, BiFC, follicle cells

THE INTERACTIONS BETWEEN JAK/STAT SIGNALING LIGANDS IN DROSOPHILA
MELANOGASTER

By

Qian Chen

Dr. Douglas Harrison

Director of Dissertation

Dr. David Westneat

Director of Graduate Studies

May 07 2014

This work is dedicated to my parents, Hongyin Chen and Wenhua, Li.

ACKNOWLEDGEMENTS

I would like to thank many people for their insights, instructions and supports throughout my graduate study. This dissertation would not be completed without their help.

First and foremost, I would like to express my sincere gratitude and appreciation to my advisor, Dr. Doug Harrison, who guided me into the fascinating world of fly genetics and development. He always supported and encouraged me. His wisdom, broad knowledge and guidance kept me on track with my project.

Secondly, I would like to thank Drs. Brian Rymond, Rebecca Kellum and Subba R. Palli for their service on my advisory committee. I benefited greatly from their expertise and advices throughout the study.

I would like to thank all past and present lab members in the Harrison lab: Dr. Susan Harrison, Dr. Liqun Wang, Dr. Travis Sexton, Dr. Claire Venard, Linzhu Han, Dustin Perry, Lingfeng Tang and Michelle Giedt, for the exchange of scientific ideas and encouragement they gave to me. I felt lucky to have worked with such a group of enthusiastic and supportive people in the lab.

I want to give a special thank to members in Dr. Rymond's lab, especially to Dr. Daipayan Banerjee, Dr. Min Chen and Swagata Ghosh, for their tremendous help on all the yeast studies. It would not be possible for me to complete this part of the project without their step by step instructions and suggestions.

I also would like to thank all other faculty members, staff and students in the Biology Department. I appreciate their academic influence and efforts that made the department a really inspiring and pleasant place to work in.

Finally, I wish to give my thanks to my fiancé, Peng Jiang, and my parents for their love and support.

Table of Contents

Chapter 1: Background	1
JAK/STAT signaling pathway	1
Upd-family ligands	4
Potential physical interactions among Upd-family ligands.....	6
Chapter 2: Physical interaction between Upd-family ligands.....	13
Introduction	13
Results	16
Homotypic and heterotypic interactions of Upd-family ligands are detected in BiFC	16
Homotypic interaction of Upd3 was detected in yeast two-hybrid	20
Interaction domains in Upd3	22
Discussion	26
BiFC and yeast two-hybrid assays showed different sensitivities in detecting interactions between Upd-family ligands	26
Upd-family ligand oligomers might have different binding capacities to the receptor	28
Chapter 3: Biological significance of interaction between Upd-family ligands	40
Introduction	40
Result	44
Upd and Upd3 may be weakly synergistic in cell culture	44
Functional domains in Upd3	47
No synergy was exhibited between Upd and Upd3 in vivo	50
Upd exhibited narrower distribution in upd3 mutant egg chambers	51
Loss of Upd3 caused stronger impact on Upd distribution than JAK signaling intensity	54
Upd3 might affect the concentration gradient of JAK signaling through complex mechanisms	56
Discussion	60
No strong synergistic effect was detected between Upd and Upd3	60
JAK signaling stimulation is controlled by complex regulatory machinery	61
Chapter 4: Conclusions and Discussion	77
Interactions between Upd-family ligands are mediated by weak strength	77
Interactions between Upd-family ligands are likely to happen intracellularly.....	79
Functional domains of Upd-family ligands	80

Upd3 facilitates the establishment of the Upd concentration gradient in egg chambers	83
Chapter 5: Materials and Methods.....	88
Cell culture maintenance	88
Bimolecular Fluorescence Complementation (BiFC)	88
Yeast two-hybrid assay	89
Upd3 alanine substitution constructs	89
Luciferase Assay	91
Cellular fractionation	92
Fly strains and markers	92
Generation of misexpression clones.....	93
Immunological staining.....	93
Image capture and processing.....	94
Reference	95
VITA.....	104

List of figures

Figure 1.1 Activation of the JAK/STAT signaling pathway.....	10
Figure 1.2 Amino acid sequence alignment between Upd-family ligands.....	11
Figure 1.3 Secondary structure predictions of Upd-family ligands.....	12
Figure 2.1 A schematic representation of the BiFC experiment.....	31
Figure 2.2 Optimization of a cell system for relatively high exogenous gene expression	32
Figure 2.3 BiFC results.....	33
Figure 2.4 Quantification of the BiFC results between Upd and Upd3.....	34
Figure 2.5 Physical interactions of Upd2 with Upd and Upd3.....	35
Figure 2.6 Yeast two-hybrid results of the Upd3 Δ SS homotypic interaction.....	36
Figure 2.7 Yeast two-hybrid analyses of all possible interactions between Upd and Upd3.....	37
Figure 2.8 Yeast two-hybrid results of truncated Upd3.....	38
Figure 2.9 Comparison of the Upd3 interaction strength with alanine substituted Upd3 mutants.....	39
Figure 3.1 A schematic diagram of follicular cell specification during egg chamber development.....	64
Figure 3.2 Optimization of the luciferase assay.....	65
Figure 3.3 JAK signaling activation stimulated by different proportions of Upd and Upd3.....	66
Figure 3.4 Different ligand expression strategies caused distinct JAK signaling activation.....	67
Figure 3.5 Functional domains in Upd3.....	68
Figure 3.6 Ectopic border cell formation caused by the overexpression of Upd-family ligands.....	69
Figure 3.7 Upd localization on different stages of egg chambers.....	70

Figure 3.8 Upd3 expression affects Upd distribution in egg chambers.....71

Figure 3.9 Posterior cell population is reduced in *upd3* null mutants.....72

Figure 3.10 Loss of *upd3* changes anterior follicle cell fates.....73

Figure 3.11 Upd3 has a stronger effect on JAK signaling activity range than signaling intensity.....74

Figure 3.12 Potential mechanisms underlying the Upd3 effect on Upd distribution in egg chambers.....75

Figure 3.13 *upd3* overexpression outside of polar cells.....76

Chapter 1: Background

JAK/STAT signaling pathway

During the development of multi-cellular organisms, cells need to be able to constantly perceive and respond to signals from their microenvironment to determine their identities and carry out coordinated functions. Remarkably, however, all the intercellular communication is sufficiently accomplished by only a small number of signaling pathways. Each of these signaling pathways is typically involved in diverse developmental processes and they together are orchestrated in an intricate program to ensure normal development of the whole organism. A comprehensive understanding of how signaling cascades achieve the highly diverse, yet specific regulation of cell behaviors is pivotal to decipher developmental programs in various multi-cellular organisms. This study focuses on one of these fundamental pathways, the JAK/STAT signaling pathway. It is the primary signaling cascade in response to a variety of cytokines and growth factors in mammals, and dysfunction of this pathway has been associated with a wide range of diseases in human. The aim of this study is to gain a better understanding of the mechanisms utilized by JAK signaling to achieve signaling specificity and diversity during development and identify principles that apply more broadly to other signaling pathways.

The JAK/STAT signaling pathway was first identified through the study of transcriptional activation in response to interferon α (IFN- α) and interferon γ (IFN- γ) (Darnell and Stark 1994). It was soon realized after its discovery that this signaling cascade can be activated by numerous other cytokines as well as growth factors in mammals. Murine knockout models of several JAK signaling components generated over the years have provided precious insight into the function of the pathway. JAK signaling pathway is essential for many processes during the development of the immune system, including hematopoiesis and lymphoid development (Kiu and Nicholson 2012). Consistently, the majority of human diseases that are related to the misregulation of this pathway are lymphohematopoietic neoplastic diseases. For example, overactivation

of STAT3 has been associated with certain types of myeloma, lymphoma and chronic myelogenous leukemia, and JAK3 mutation is implicated in severe combined immunodeficiency (SCID) (Igaz et al. 2001). However, JAK signaling functions are not limited to the immune system. It is also involved in embryogenesis (Takeda et al. 1997), mammary gland development (Cui et al. 2004), sexually dimorphic growth (Udy et al. 1997), and many other developmental processes. The functional diversity of JAK signaling in various development processes is accompanied by its different actions at the cellular level. It is able to control cell proliferation, differentiation, migration, and apoptosis according to different environmental cues. The JAK/STAT signaling pathway has drawn extensive attention from the biomedical research field for its essentialism in development and potential to become a therapeutic target. In addition, JAK signaling can be used as a model to understand how signaling pathways achieve functional pleiotropy, in general.

The JAK signaling cascade is carried out by a series of phosphorylation events on specific tyrosine residues, catalyzed by JAK kinase activity. JAK is constantly associated with the receptor through a receptor binding domain located at the N-terminus of the protein. The tyrosine kinase domain is located to the C-terminus of the protein, adjacent to a pseudokinase domain, which lacks catalytic activity but can regulate the enzymatic activity of the kinase domain (Leonard and O'Shea 1998). JAK signaling is initiated by ligand binding to the receptor, which triggers the dimerization of receptors (Kiu and Nicholson 2012). Receptor dimerization brings the associated pair of JAK proteins in close proximity (Figure 1.1). The two JAKs trans-phosphorylate each other and the phosphorylated JAK then phosphorylates receptors at specific tyrosine sites. The phosphotyrosine on the receptor serves as a docking site for STAT, the transcriptional factor of this pathway, to recruit it from the cytosol to the cell membrane. Once it is bound to the receptor, STAT also gets phosphorylated by JAK. Phosphorylated STATs then disassociate from the receptor, form homo- or heterodimers and translocate into the nucleus to initiate downstream gene expression. Besides signaling activators, JAK/STAT signaling is also tightly controlled by several negative regulators. Major

negative regulators of the pathway include the suppressor of cytokine signaling (SOCS) proteins (Kershaw et al. 2013), protein inhibitor of activated STAT (PIAS) family members (Liu et al. 1998) and various protein tyrosine phosphatases (PTP) (Klingmüller et al. 1995). Negative regulators of the pathway utilize different mechanisms to down-regulate JAK signaling at various steps of the signaling activation, such as dephosphorylating proteins, blocking protein interaction interfaces and suppressing target gene expression. Moreover, protein modification, ubiquitination (Ungureanu et al. 2002) and signaling crosstalk with other pathways (Shuai and Liu 2003) also contribute to the fine-tuning of the JAK signaling pathway.

The JAK/STAT signaling pathway is conserved in flies, zebrafish and mammals (Hou et al. 2002, Arbouzova and Zeidler 2006). The mammalian JAK signaling pathway is highly complicated. It contains four JAKs, seven STATs and an even greater variety of ligands and receptors. The complexity of the pathway is beneficial to the signaling specificity (Kisseleva et al. 2002), but hinders the studies towards the understanding of the basic regulatory mechanism of the pathway. By contrast, *Drosophila* offers a much simpler streamlined pathway. The *Drosophila* JAK/STAT signaling pathway consists of only one JAK (Hopscotch) (Binari and Perrimon 1994), one STAT (STAT92e) (Hou et al. 1996), one receptor (Domeless) (Brown et al. 2001, Chen et al. 2002) and three ligands (Unpaired (Upd), Upd2 and Upd3) (Harrison et al. 1998, Hombría et al. 2005, Wright et al. 2011). In spite of the less complex arrangement, *Drosophila* JAK signaling is also involved in many developmental processes, including hematopoiesis (Harrison et al. 1995), immune responses (Agaisse and Perrimon 2004), ovarian follicle cell differentiation (McGregor et al. 2002, Xi et al. 2003), and stem cell maintenance (López-Onieva et al. 2008, Issigonis et al. 2009, Jiang et al. 2009, Lin et al. 2010). The low level of redundancy in conjunction with the rich genetic toolbox developed for this organism makes *Drosophila* an excellent model for studying the basic regulatory machinery of the JAK/STAT signaling pathway.

Upd-family ligands

Upd was the first ligand to be identified that stimulates the *Drosophila* JAK/STAT signaling pathway. It was discovered through the observation that *upd* mutants cause similar embryonic defects to those seen in *hop* and *stat92e* mutants (Harrison et al. 1998). This is a unique embryonic phenotype characterized by the loss of pair-rule gene expression in the fifth and the posterior portion of the fourth stripes, not resembling the stereotypical mutant phenotype of any segmentation gene (Nüsslein-Volhard and Wieschaus 1980). Upd2 and Upd3 were identified subsequently because of their sequence similarity to Upd.

All three ligands can be found in the 12 *Drosophila* species that have been sequenced. They are clustered in a 70 kb region on the X-chromosome, where *upd3* sits between *upd* and *upd2* and has an opposite transcriptional orientation. In *Drosophila melanogaster*, the overall sequence similarity of amino acids among the three ligands is about 40% (Sexton 2009), but conserved amino acids are scattered across the sequences, resulting in only a few short conserved domains (Figure1.2). Homologs of Upd-family ligands are also found in other arthropods, including *Anopheles gambiae* (African malaria mosquito), *Nasonia vitripennis* (jewel wasp), *Tribolium castaneum* (red flour beetle), *Apis mellifera* (honey bee) and *Harpegnathos saltator* (ant) (Wang 2009, Loehlin and Werren 2012). Upd-family ligands do not show homology at the primary sequence level to any mammalian cytokine, but they resemble the secondary structures of cytokines belonging to the four-helical bundle protein family (Harrison et al. 1998), which is the biggest structural group of mammalian cytokines. Members of this family are characterized by stretches of α -helices, arranged into an up-up-down-down topology. Cytokines in this family can be further distinguished into type I or type II cytokines based on the presence of certain motifs on their receptors (Sprang and Fernando Bazan 1993). All three Upd-family ligands have stretches of α -helices (Figure1.3) as predicted by the PSIPRED server (Krüger et al. 2013) and they most resemble the structures of type I cytokines (Boulay et al. 2003).

The three Upd-family ligands presumably undergo a series of post-translational modifications as they are transported in the secretory pathway. It has been shown that Upd is led into the secretory pathway through its signal peptide located at the N-terminus of the protein and gets glycosylated at multiple sites during secretion (Harrison et al. 1995). Glycosylation occurs on most membrane bound and secreted proteins and it could be critical for protein stability, transportation and localization. After secretion, Upd binds to at least one heparan sulfate proteoglycan (HSPG) that resides in the extracellular matrix (ECM), Dally (Hayashi et al. 2012). This ECM association is critical for establishing the Upd concentration gradient and controlling the subsequent JAK signaling activation in egg chambers. Fewer studies have been focused on post-translational modifications of Upd2 and Upd3. Both ligands contains multiple glycosylation sites predicted by the NetNGlyc Server (Hombría et al. 2005). A signal peptide of Upd3 located at the very N-terminus of the protein is predicted by the Signal P program (Petersen et al. 2011), but no signal peptide is predicted in Upd2 sequence, despite the fact that it is also a secreted protein (Figure1.3). To directly visualize their localization, the three ligands were tagged with green fluorescent protein (GFP) at the C-terminus and expressed in cell culture (Hombría et al. 2005, Wright et al. 2011). Upd3 showed a similar “halo” localization pattern surrounding cells as Upd and given the known ECM localization of Upd, Upd3 is likely to be also located to the ECM after secretion. Upd2, however, was mostly diffused into the medium and its localization in the ECM was barely detectable. On the other hand, in flies, Upd2 is able to travel a long distance from the fat body to the brain under well-fed conditions to stimulate insulin-like peptide secretion (Rajan and Perrimon 2012). Therefore, Upd2 appears to be is a more freely diffusible ligand than Upd and Upd3.

All three ligands are able to stimulate the JAK/STAT signaling pathway (Harrison et al. 1998, Agaisse et al. 2003, Hombría et al. 2005). In cell culture studies, Upd stimulated higher JAK signaling intensity compared to the other two ligands in autocrine and paracrine manners, whereas Upd2 stimulated the highest signaling when conditioned medium was used (Wright et al. 2011). Careful genetic analyses have been

taken *in vivo* to understand the potential functional redundancy between the three ligands. In some developmental processes, JAK signaling seems to be regulated by only one of the ligands. For example, Upd2 is the only ligand out of this family that controls the release of insulin-like peptides to maintain physiological homeostasis of the organism (Rajan and Perrimon 2012). Upd3, on the other hand, takes on an independent role in regulating immune responses under septic challenges (Agaisse et al. 2003). During this process, *upd3* is expressed in hemocytes and turns on JAK signaling in fat body cells to activate the expression of antimicrobial peptides as a defense strategy in *Drosophila* towards infection. However, in many other developmental processes, functions of the three ligands overlap. During oogenesis, both Upd and Upd3 are necessary for border cell specification (Silver et al. 2005, Sexton 2009). Mutation of *upd* causes retardation of border cell migration, as well as reduction in the numbers of border cells in the migratory cluster. Mutation of *upd3* also results in reduced numbers of border cells, although cell migration seems to be not affected. Overlapping functions were also observed between Upd and Upd2 during embryogenesis. Upd null mutants are lethal and have severe patterning defects in embryos. Mutation of *upd2* alone did not cause any obvious defect in embryos, but it exacerbates the spiracle and head skeleton defects observed in *upd* mutants (Hombría et al. 2005), indicating that Upd2 functions semi-redundantly to Upd during embryogenesis. Upd-family ligands are involved in many more developmental processes than discussed here, such as sex determination (Wawersik et al. 2005) and stem cell maintenance (Tulina and Matunis 2001, Singh et al. 2007), but whether only one or multiple ligands are involved in many of these processes has not been extensively studied.

Potential physical interactions among Upd-family ligands

In contrast to the mammalian counterpart, the *Drosophila* JAK signaling pathway utilizes only three ligands. It is therefore bewildering to see how *Drosophila* JAK signaling relies on only three ligands to interpret diverse environmental information and respond specifically. One potential mechanism for providing the necessary specificity

from only three ligands is ligand oligomerization, by which signaling pathways expand the reservoir of ligands without increasing the size of the genome. *In situ* hybridization of the three ligands has shown that the expression of *upd2* and *upd3* co-localizes with the expression of *upd* at several developmental stages. *upd2* and *upd* are expressed in the same striped pattern in embryos (Gilbert et al. 2005, Hombría et al. 2005), whereas *upd3* and *upd* are both expressed in polar cells of egg chambers and the posterior region of eye discs (Wang 2009). However, no overlapping expression between *upd2* and *upd3* has been found. The co-localized expression pattern raises the possibility that Upd2 and Upd3 may physically interact with Upd.

Crystal structure studies on isolated mammalian cytokines and cytokine-receptor complexes have revealed that some cytokines function as dimers. Covalent or non-covalent interactions are formed between several cytokines of the four-helical bundle protein family that the Upd-family most resembles, such as IL-5, IFN- β and M-CSF (macrophage colony stimulating factor) (Karpusas et al. 1997, Kothe 1997, Kusano et al. 2012). However, the functional consequences of these cytokine dimerization events are not the same. Some cytokines rely on protein dimerization to make active ligands, such as IL-5. IL-5 dimers are stabilized by two intermolecular disulfide bonds formed between two pairs of conserved cysteine residues. Mutations of these two cysteine sites abolished IL-5 ability in signaling induction (Milburn et al. 1993, Kusano et al. 2012). IL-5 belongs to a cytokine sub-family comprised of also IL-3 and GM-CSF (Granulocyte-macrophage colony-stimulating factor). Although no similar disulfide bond is found in IL-3 and GM-CSF, structural studies have also suggested potential homotypic interactions of these two ligands, which may be stabilized by van der Waals forces and hydrogen bonds (Hansen et al. 2008, Dey et al. 2009). Neutralizing antibodies and large deletions of the proposed interaction interface of IL-3 block its activity. Moreover, site-specific amino acid substitutions made in this region cause either loss of function or gain of function modification of its signaling activity (Lokker et al. 1991, Olins et al. 1995). By contrast, some cytokine dimers may function as antagonists of their monomers and attenuate signaling activity. The IL-6 receptor comprises two subunits: an α subunit that

is bound by IL-6 and a gp130 subunit that is bound by STAT3 for signal transduction. IL-6 dimers bind to the α subunit of the receptor with a higher affinity than monomers, but they have lower ability to incorporate the gp130 subunit into the complex. As a result, IL-6 dimers have lower signaling potency as assessed by STAT3 phosphorylation and can potentially antagonize the function of monomers (Ward et al. 1996). Finally, some cytokines can form not only homodimers but also heterodimers, but different dimers may or may not cause different signaling induction. For example, human M-CSF has multiple mRNA splicing variants that give rise to protein products of various sizes. Homodimers and heterodimers are formed between a long form of M-CSF containing 221 amino acids and a short form containing 158 amino acids when mixed together *in vitro*. The three types of dimers do not show any functional difference in a M-CSF dependent cell proliferation assay (Koths 1997).

Besides signaling intensity, ligand oligomerization could also control the signaling activity range, an important aspect of ligand function that has not been extensively studied with cytokines in the simplified cell culture system. In this respect, *Drosophila* BMP signaling sets an excellent example to illustrate how ligand oligomerization can affect signaling activity in both ways, during the establishment of the dorsal-ventral axis in embryos (Wang and Ferguson 2005, O'Connor et al. 2006). Two BMP signaling ligands are involved in this process. Decapentaplegic (Dpp) is expressed uniformly in the dorsal half of the embryo and Screw (Scw) is produced throughout the entire embryo. Despite their broad expression patterns, heterodimers of Dpp and Scw are restricted to the dorsal-most region through proteolytic actions of three extracellular modulators: Short gastrulation (Sog), Twisted gastrulation (Tsg) and Tolloid (Tld). Homodimers of Dpp and Scw are located in the dorsal lateral region. On the other hand, heterodimers stimulate 10 fold higher BMP signaling activity compared to either of the homodimers, as measured by the phosphorylation level of the downstream transcription factor Mad. The specific localization pattern and distinct signaling potency of different ligand dimers consequently establish a sharp biphasic BMP signaling, which specifies cells at the dorsal half of embryos to undergo one of two cell fates. Dorsal midline cells that receive high

levels of BMP signaling stimulation from heterodimers are specified into extraembryonic amnioserosa, whereas dorsal-lateral cells that receive moderate levels of signaling stimulation from homodimers become dorsal ectoderm. A mathematical simulation based on these experimental results showed that the regulatory mechanism involving protein dimers provides better patterning robustness in response to protein abundance differences than those relying on monomers only (Shimmi et al. 2005).

The three Upd-family ligands might function as homo- and hetero-oligomers to activate the pathway in tissues where overlapping expression between Upd-family ligands was detected, such as embryos and egg chambers. Ligand oligomerization can possibly be an important factor in regulating the signaling activity range, signaling intensity or both. The work described in this thesis focused on testing for physical interactions between Upd-family ligands and exploring the functional consequences of such interactions.

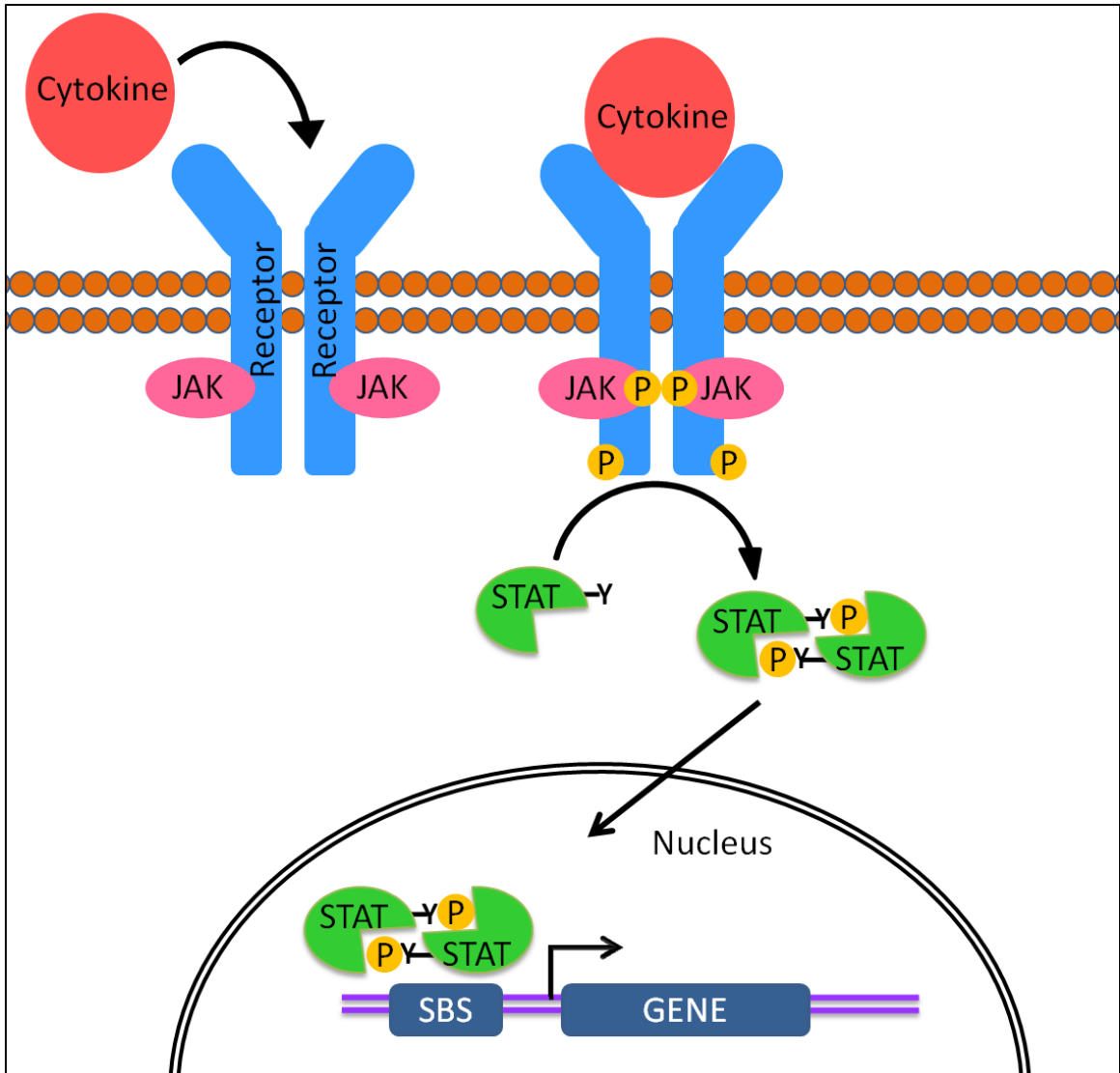


Figure 1.1. Activation of the JAK/STAT signaling pathway. JAK signaling is initiated by the binding of ligands to the receptor, resulting in trans-phosphorylation between the receptor associated JAKs. The phosphorylated JAKs then phosphorylate the receptors to generate docking sites for STATs. STATs are recruited from the cytosol to the cell membrane and also get phosphorylated by JAK. The phosphorylated STATs form dimers and translocate into the nucleus, where they bind specifically to STAT binding sites (SBS) and initiate downstream gene expression.

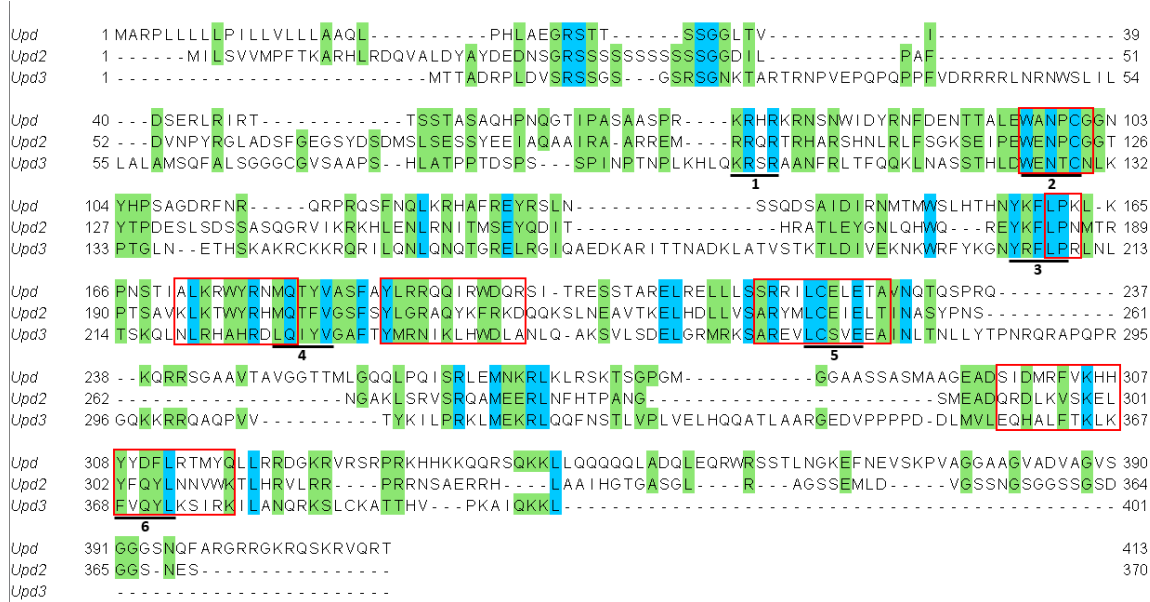


Figure 1.2. Amino acid sequence alignment between Upd-family ligands. The predicted amino acid sequences of the three Upd-family ligands are shown. Identical amino acids shared between two proteins are highlighted in green and those shared between all three proteins are highlighted in cyan. Conserved blocks that were subjected to functional analysis in this study are underlined and numbered. Red boxes show the 6 conserved domains identified in a previous study comparing Upd homologs from 6 arthropod species, including *Drosophila* (Loehlin and Werren 2012).

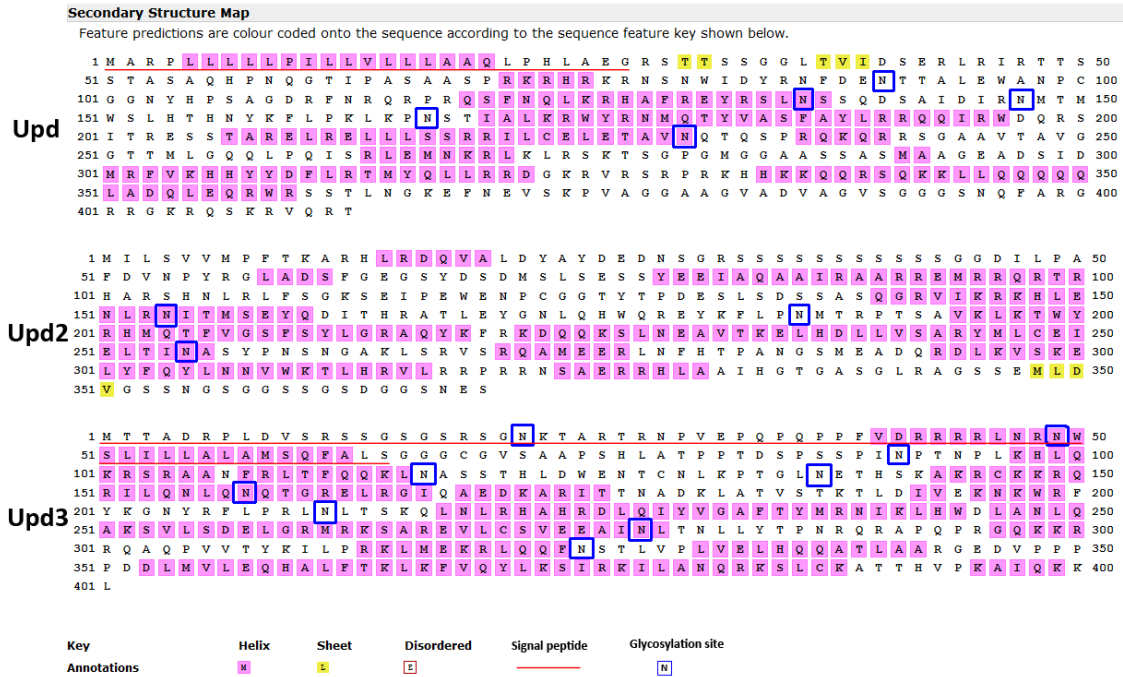


Figure 1.3. Secondary structure predictions of Upd-family ligands. All three ligands in the Upd-family are predicted to form stretches of α -helices and little or no β -sheet. Predicted signal peptides are underlined in red. There was no signal peptide predicted in the Upd2 sequence. Predicted N-glycosylation sites are outlined in blue.

Chapter 2: Physical interaction between Upd-family ligands

Introduction

Protein interactions are involved in every cellular process, and they are often the key to understanding biological regulations. However, there is not a universal method that can genuinely report protein interactions under every given biological context. Consequently, several methods have been developed to detect protein interactions and the list of techniques is still growing. Conventional biochemical assays (Phizicky and Fields 1995), including protein affinity chromatography and co-immunoprecipitation, have been used as standard techniques to detect protein interactions for years. However, the disadvantage of these *in vitro* assays is also obvious: protein interactions are not analyzed in their natural environment. Losing cell context could result in false positive or false negative interactions. To overcome this problem, multiple *in vivo* methods have been developed (Villalobos et al. 2007), including yeast two-hybrid (Krogan et al. 2006), Fluorescence Resonance Energy Transfer (FRET) and the more recently developed Bimolecular Fluorescence Complementation (BiFC) (also referred to as split GFP assay) (Hu et al. 2002). Among these, fluorescence based methods allow direct visualization of protein interactions in cell compartments and are thus able to reveal the subcellular localization of protein interactions at the same time. Based on these reasons, interactions between Upd-family ligands were tested using two *in vivo* assays. One is a fluorescence based assay, BiFC, and the other is a conceptually different but widely used yeast two-hybrid assay.

Both BiFC and yeast two-hybrid are protein fragment complementation assays. This type of interaction assays is based on the fact that certain fragments of some proteins have the ability to re-associate into a functional unit when they are brought in close proximity. Such proteins include ubiquitin (Johnsson and Varshavsky 1994), β -galactosidase (Rossi et al. 1997), dihydrofolate reductase (Pelletier et al. 1998) and the one utilized in the BiFC, green fluorescent protein and its spectral variants. BiFC was first established in mammalian cell culture (Hu et al. 2002) and has been adapted into plants

(Atmakuri et al. 2003), worms (Hiatt et al. 2008) and flies (Gohl et al. 2010). In BiFC assays, two proteins of interest are fused to an N-terminal and a C-terminal fragment of GFP variants respectively. The truncated GFP variant fragments have no fluorescence ability by themselves, but if interaction happens between the two proteins to which they have been fused, the two GFP variant fragments can be brought in proximity and spontaneously reconstruct a functional fluorophore (Figure 2.1). Over ten combinations of protein complementation can be formed between different fragments of GFP variants and this results in fluorescence at a variety of wavelengths, enabling simultaneous comparisons of multiple pairs of protein interactions (Hu and Kerppola 2003, Grinberg et al. 2004). In comparison to other complementation based interaction assays, BiFC allows direct visualization of protein interaction without any exogenous fluorogenic or chromogenic agent. FRET is another fluorescence-based *in vivo* assay. Compared to FRET, BiFC offers both higher sensitivity and convenience. In FRET assays, fluorophores that are attached to the proteins of interest have to be placed within 100Å of one another, since this is the maximum distance over which energy transfer between fluorescent molecules can be detected (dos Remedios and Moens 1995). To fulfill this requirement, proteins usually need to be overexpressed to maximize the chance of protein collision. By contrast, BiFC is able to detect protein interactions at their endogenous expression levels and no structural information is required.

Despite its advantages, BiFC assays have been reported to have high background signal produced by spontaneous association between the truncated fluorescence tags (Kodama and Hu 2010, Nakagawa et al. 2011, Horstman et al. 2014). Therefore, a yeast two-hybrid assay was used to confirm the results from BiFC. Yeast two-hybrid has long been routinely used to detect specific protein interactions, and it has also been adapted into high throughput studies to dissect the protein interactome of the whole genome (Uetz et al. 2000, Ito et al. 2001, Giot et al. 2003). In yeast two-hybrid assays, the two proteins of interest are fused respectively to the DNA binding domain and the activation domain of a yeast transcriptional factor, GAL4. The DNA binding domain carries the fusion protein to the promoter of reporter genes. The activation domain recruits

necessary proteins to the transcriptional machinery. Only when the two proteins of interest physically interact, a functional transcriptional complex can be formed at the promoter sequence to initiate the expression of reporter genes. The yeast two-hybrid assay also has limitations in detecting some protein interactions, because the yeast nucleus, where the assay takes place, could be a hostile environment for some proteins and the truncated GAL4 tags can sometimes interfere with the interaction (Parrish et al. 2006). Nonetheless, by using both BiFC and yeast two-hybrid assays, a more confident conclusion should be drawn on interactions between Upd-family ligands. In addition, critical protein domains that mediate the interactions between Upd-family ligands were explored using these two methods.

Results

Homotypic and heterotypic interactions of Upd-family ligands are detected in BiFC

To detect interactions between Upd-family ligands using a BiFC assay, the N-terminal half of Venus (1-173aa, VN) and the C-terminal half of CFP (155-238aa, CC) were fused to the C-termini of Upd-family proteins. This particular combination of GFP variants was chosen since it showed the highest signal to noise ratio in a previous study performed in mammalian cells (Shyu et al. 2006). Another fluorescent molecule, Cherry, driven by a highly active actin5C promoter, was co-expressed in cells to serve as an internal control to monitor the consistency of plasmid transfection and protein production between transfection groups.

Each BiFC fusion protein was expressed under the control of the UAS/GAL4 binary expression system (Duffy 2002), and the actin5C driven cherry was delivered by a separate plasmid. This presented the technical challenge of co-transfecting four plasmids into cells, especially given that *Drosophila* cells generally have low transfection efficiency in comparison to mammalian cells. Individual mammalian cells are able to uptake approximately 10^5 to 10^6 copies of plasmids during transfection, through either liposome vehicles (Tseng et al. 1997) or calcium phosphate precipitation (Batard et al. 2001). Although less than 10% of these plasmids can remain intact and are located to the nucleus, the amount of plasmid transfected into mammalian cells is significantly higher than the amount that enters the nucleus of *Drosophila* cells. *Drosophila* cells can only incorporate hundreds of plasmid copies in the genome during transfection (Rio and Rubin 1985, Johansen et al. 1989). On the other hand, fluorescent signals from GFP can only be detected when the protein concentration is higher than approximately 2×10^5 molecules/cell (Tseng et al. 1997). Therefore, when using a fluorescent molecule as a marker to estimate transfection rate, mammalian cells can achieve 90% transfection efficiency (Maurisse et al. 2010), whereas a maximum of only 30-40% has been detected in *Drosophila* cells (Yang and Reth 2012). To establish a *Drosophila* cell system with relatively high exogenous gene expression, transfection efficiency was optimized by

comparing different cell lines, transfection reagents, and GAL4 drivers. Six cell lines were available in the lab, including embryonic S3 (Schneider 1972) and Kc167 (Cherbas et al. 1988) cells, imaginal disc derivative clone8 (Peel and Milner 1990) and ML-DmD32 (Ui et al. 1987) cells, blood cell derivative mbn2 cells (Gateff et al. 1980), and a *Spodoptera frugiperda* (armyworm) cell line, Sf9 (Vaughn et al. 1977). Transfection efficiency was tested by expressing *actin-cherry* in all *Drosophila* cell lines and *pie-GFP* in the Sf9 cell line. Cell confluency, plasmid concentration and the amount of transfection reagent were adjusted to achieve the highest transfection efficiency in individual cell lines. Mediated by the transfection reagent Effectene (Qiagen), Kc167 and mbn2 cells showed the highest transfection rate compared to other cell lines, which was over 30%. In comparisons between the two, Kc167 cells adhered more readily to the bottom of cell culture dishes and grew in monolayer, whereas mbn2 cells usually took weeks to adhere in monolayer and resume their normal growth rate after thawing. Therefore, Kc167 cells were easier to handle and more reliable on generating consistent results. S3 cells grew the fastest and also stayed in monolayer but showed only about 15% transfection rate. Clone 8 cells had the most unique fibroblast-like morphology, with long arms and small cell bodies, which does not resemble its wing disc columnar epithelial cell origin. This morphological change is likely due to alterations in cell microenvironment from the *in vivo* tissue to cell culture (Peel and Milner 1990). Clone 8 cells had a low transfection efficiency of about 12%. ML-DmD32 showed the lowest transfection efficiency about 5% and a very slow growth rate. The armyworm cell line Sf9 had a transfection rate about 26%. Besides effectene, two other transfection reagents, Cellfectin (Life Technologies) and X-tremeGene (Roche) were also tested on mbn2 and Kc167 cells respectively, but neither resulted in higher transfection efficiency than Effectene (Figure 2.2 A). Three GAL4 drivers were compared for their ability to drive the expression of UAS-GFP in mbn2 and Kc167 cells. Two of these GAL4 drivers, *armadillo*-GAL4 (arm-GAL4) and Cs1.L7-GAL4 (derived from a presumed ubiquitous promoter from the *su* (Hw) gene (unpublished)), drive constitutive expression of exogenous genes but the third one, *metallothionein*-GAL4 (MT-GAL4), drives gene expression only in the presence of heavy

metal ions, such as copper used in this study. Among the three, arm-GAL4 drove the highest level of GFP expression in both Kc167 and mbn2 cells (Figure 2.2 B). Finally, the endogenous expression levels of Upd-family ligands in these cell lines was considered, since endogenous ligands can potentially interfere with interactions between BiFC fusion proteins and potentially reduce the sensitivity of the assay. Sf9 does not endogenously express any Upd-family ligand. All *Drosophila* cell lines, except for clone 8 cells, showed only low levels of Upd-family ligand expression in a previous transcription profiling study of 25 *Drosophila* cell lines (Cherbas et al. 2011). Taking all these factors into account, the *Drosophila* BiFC experiment was performed in Kc167 cells, using Effectene to mediate plasmid transfection and arm-GAL4 to drive the expression of BiFC fusion proteins.

After plasmid transfection, cells were observed under the microscope. However, only low levels of BiFC signals were detected in cells, possibly because most ligands were secreted into and diluted by the medium. In order to enhance the BiFC signal, cells were treated briefly with monensin before fluorescence microscopy in the subsequent BiFC experiments. Monensin is an ionophore, which blocks intracellular protein transport and sequester secreted proteins in the Endoplasmic reticulum (ER)/Golgi network. Dpp was used as the negative control in this experiment. Dpp is synthesized and transported through the same secretory pathway along with Upd-family ligands but should not be able to form physical interactions with any of them. Images were taken under a standard fluorescence microscope using the same exposure setting for all groups. Actin-cherry was detected in around 22% of cells in all groups, indicating the consistency in plasmid transfection. BiFC signals were detected in only a small subset of Cherry positive cells and they were localized into puncta in the cytosol of many, but not all cells (Figure 2.3).

Between different ligand combinations, BiFC signals varied in both signal intensity and frequency (Figure 2.3). Co-expression of different combinations of Upd-family ligands resulted in stronger and more frequent BiFC signals than Dpp negative

controls. Among different types of Upd and Upd3 interactions, the homotypic interaction of Upd3 had the strongest and most frequent BiFC signals, followed by the heterotypic interaction between Upd and Upd3, and the homotypic interaction of Upd was the weakest. To test if BiFC fusion proteins were expressed at similar levels, cells expressing individual fusion proteins were lysed and the cell lysate was subjected to immunoblotting analysis using anti-GFP polyclonal antibodies. BiFC fusion proteins, including UpdVN, UpdCC, Upd3VN, Upd3CC, DppVN and DppCC, were shown approximately at their predicted molecular weights, which are 68.5 kD, 58.1 kD, 67.1 kD, 56.7 kD, 87.5 kD and 77.1 kD, respectively (Figure 2.4B). Notably, all Upd and Upd3 fusion proteins showed multiple bands on the immunoblot. Some of these bands appearing at higher than predicted molecular weights might be caused by glycosylation (Harrison et al. 1998). However, those bands that were shown at lower molecular weights were likely due to protein degradation. Protein degradation might happen inside the cell or during cell lysate preparation, but because no such lower band was observed with Dpp fusion proteins, it indicates that protein degradation of Upd and Upd3 was likely to occur inside cells. Protein degradation could have weakened the BiFC signals in the experimental groups. The percentage of BiFC positive cells in the transfected cell population, which was marked by Cherry, was used as a quantitative measurement of interaction strength and compared between groups. Since the reconstructed BiFC molecules have intrinsically much weaker fluorescent signal than intact fluorescent proteins (Hu et al. 2002), BiFC signals in most cells were much dimmer than Cherry fluorescent signals. To objectively count the number of BiFC positive cells, a signal threshold was set using the ImageJ program and only cells with signal intensity above the threshold were counted as positives. Five to seven pictures were taken for each ligand combination and each picture generally contained over 100 Cherry positive cells. The numbers of BiFC and Cherry positive cells from all pictures of the same experimental group were combined, and the BiFC/Cherry percentage was calculated. Homotypic and heterotypic interactions between Upd and Upd3 were tested independently six times using the BiFC assay. All types of interactions between Upd and

Upd3 always produced higher percentage of BiFC signals in comparison to Dpp controls, but the raw number of the BiFC/Cherry ratio for each ligand combination varied between trials. To normalize the data obtained from the six trials, the average BiFC/Cherry ratio of the four Dpp negative controls was calculated for individual trials as a baseline measurement of the BiFC signal. Then the fold change of each ligand combination compared to the baseline signal was calculated (Figure 2.4). All four possible combinations between Upd and Upd3 showed significantly higher signal than the Dpp negative controls (One-way ANOVA with Bonferroni post-hoc test). Between Upd and Upd3 interactions, homotypic interaction of Upd3 showed a trend to be the strongest interaction group, whereas the homotypic interaction of Upd was the weakest. However, the difference between different types of Upd and Upd3 interactions was not statistically significant.

Upd2 is expressed in a similar striped pattern as Upd in embryos (Hombría et al. 2005, Wang 2009). However, no overlapping expression has been observed between Upd2 and Upd3. The ability of Upd2 to interact with Upd and Upd3 was also tested using the BiFC assay. Both Upd2VN and Upd2CC BiFC fusion proteins were expressed at similar levels as other BiFC fusion proteins, and Upd2 proteins also showed multiple bands on an immunoblot (Figure 2.5 B). This experiment has been repeated only twice, but some trends started to emerge. Similar to what was observed between Upd and Upd3, homotypic interaction of Upd2 was stronger than its heterotypic interaction with Upd. However, the BiFC signal generated by co-expressed Upd2 and Upd3 was not significantly different from Dpp controls (Figure 2.5 A), suggesting that Upd2 and Upd3 might not be able to physically interact.

Homotypic interaction of Upd3 was detected in yeast two-hybrid

Homotypic and heterotypic interactions between Upd and Upd3 were also tested in a yeast two-hybrid assay. In this assay, the signal peptides of these two proteins needed to be removed in order to change their location from the secretory pathway to the nucleus in yeast cells. The signal peptide at the N-terminus of Upd was

experimentally confirmed (Harrison et al. 1998), but the signal peptide predicted for Upd3 by the Signal P program (Dyrløv Bendtsen et al. 2004) has not been verified. Therefore, both a full length Upd3 and a truncated Upd3 protein lacking the predicted signal peptide (Upd3 Δ SS) were tested in the yeast two-hybrid assay. Upd Δ SS, Upd3, and Upd3 Δ SS coding sequences were fused to the C-terminus of the GAL4 activation domain (AD) and the DNA binding domain (BD), in frame with a nuclear localization signal at the N-terminus of the fusion proteins. Empty vectors containing GAL4 AD or GAL4 BD were used as negative controls to assess the background activity of the reporters.

The yeast host cell used in this study, PJ69-4A, contains three reporter genes in the genome, including *HIS3*, *ADE2* and *lacZ* (James et al. 1996). Each reporter gene is driven by a separate highly inducible promoter. The *HIS3* reporter gene is under the control of a *GAL1* promoter and downstream of a *LYS2* gene, which enhances the stringency of the *HIS3* expression. The *ADE2* gene is controlled by a *GAL2* promoter and the *lacZ* gene is controlled by a *GAL7* promoter. The use of three independent reporters prevents false positives due to the leaky expression from certain promoters. Protein interactions can be assayed based on cell growth on histidine or adenine deficient plates, and the strength of interactions can be quantitatively measured based on β -galactosidase activities. Plasmids containing the two proteins of interest were sequentially transformed into yeast cells. Successful transformants were selected from leucine and tryptophan double deficient plates (-Leu/-Trp) and then were grown on three selective plates, including a histidine deficient (-His) plate, a adenine deficient (-Ade) plate and a histidine deficient plus 5mM 3-Amino-1,2,4-triazole (3AT) (-His + 5mM 3AT) plate, to assess protein interactions. 3AT is a competitive inhibitor of the *HIS3* gene product and can enhance the stringency of the -His selection. Two yeast splicing factors, Spp382 and Prp43, that have been shown to interact were used as positive controls (Pandit et al. 2006).

Upd3 Δ SS homotypic interaction was shown on all three selective plates. On the -His plate, although low levels of leaky expression from the *HIS3* gene were detected in

the negative controls, cells co-expressing Upd3 Δ SS-AD and Upd3 Δ SS-BD showed significantly better growth. The addition of 3AT on the –His + 5mM 3AT plate completely eliminated the background expression of *HIS3* in the negative controls and further supported the homotypic interaction between Upd3 Δ SS proteins. –Ade appeared to be the most stringent selection among the three to detect the Upd3 Δ SS/ Upd3 Δ SS interaction. Cells co-expressing Upd3 Δ SS-AD and Upd3 Δ SS-BD grew very slowly on the – Ade plate. Even though the Upd3 Δ SS/Upd3 Δ SS interaction was detected by all three selective plates, it was shown to be a much weaker interaction compared to the one between Spp382 and Prp43. Upd3 Δ SS/Upd3 Δ SS expressing cells grew much slower than Spp382/Prp43 expressing cells in all three selective plates. Moreover, the color of colonies on the -Trp-Leu plate also indicated the difference in the interaction strength. In general, *ade2* mutants form red colonies on the -Trp-Leu plate, whereas wild-type cells form white colonies. Intermediate expression of the *ADE2* gene gives various shades of the pink color to colonies. Spp382/Prp43 positive control cells were completely white, indicating strong interactions between the two proteins. In contrast, Upd3 Δ SS/Upd3 Δ SS expressing cells showed a similar pink color compared to that of the empty vector controls, indicating weak interactions (Figure2.6). Except for the homotypic interaction of Upd3 Δ SS, no other type of interactions between Upd and Upd3 was detected by the yeast two-hybrid assay. When the full length Upd3 containing its signal sequence was used in this assay, no interaction was detected (Figure2.7), possibly because it failed to be located into the nucleus.

Interaction domains in Upd3

Since the homotypic oligomerization of Upd3 molecules was detected by both the BiFC and the yeast two-hybrid assays, effort was taken to find the critical domains for this interaction. Previously, no study has been done regarding functional domains of the three ligands, probably because no region has been implicated with a potential function. The three ligands do not contain any classic functional domain, and although they possess similar secondary structural features to type I mammalian cytokines, they do not share homology to any cytokine at the primary sequence level. However,

sequence alignment between the three ligands revealed 6 short conserved domains (Figure 1.2), which strikingly overlap with the conserved domains between Upd homologs from several insect species, including mosquito, wasp, beetle, honey bee, ant and fly (Loehlin and Werren 2012). The only difference between the results from the two sequence alignments was that no conserved domain was identified among Upd homologs at the corresponding region of the first conserved domain identified among Upd-family ligands. These six conserved domains among Upd-family ligands were selected as candidates to be tested for functions in the Upd3 homotypic interaction.

Before testing individual domains, interactions were tested on big truncations of Upd3 in order to narrow down the candidate region. Two Upd3 truncations were made by deleting two conserved domains from either the N-terminus or the C-terminus of Upd3 Δ SS, resulting in N-Upd3 Δ SS, which contains domain 1 to 4, and C-Upd3 Δ SS, which contains domain 3 to 6 (Figure 2.8 diagram). Interactions of the two truncated Upd3 proteins with full length Upd3 Δ SS were tested in a yeast two-hybrid assay. Three successful transformants of each interaction group were isolated from the –Trp-Leu plate and grown on a –His selective plate to test for interaction. All three transformants expressing Upd3 Δ SS / Upd3 Δ SS were able to grow on the –His plate, confirming the homotypic interaction between Upd3 Δ SS proteins. In contrast, of the three transformants expressing Upd3 Δ SS /N- Upd3 Δ SS, only one barely grew on the –His plate, suggesting that the loss of domains 5 and 6 reduced, but did not abolish the homotypic interaction of Upd3 (Figure 2.8 (2)). On the other hand, C-Upd3 Δ SS did not show interaction with the full length Upd3 Δ SS, suggesting that domain 1 or 2 might be essential for the homotypic interaction of Upd3 (Figure 2.8 (3)). Since the interaction strength between wild-type Upd3 was shown to be very weak in the previous yeast two-hybrid assay, the negative results from the Upd3 truncated proteins did not necessarily indicate complete loss of the interaction. Instead, the truncations might attenuate the interaction to a level that was lower than the detective limit of the assay. Overall, loss of the region containing domains 1 and 2 seemed to have a stronger effect on the Upd3 homotypic interaction compared to loss of the C-terminal region containing domains 5

and 6. However, no conclusion can be made on the role of domains 3 and 4 based from these results.

Since no region was ruled out for mediating the Upd3 homotypic interaction based on the truncation study, the six conserved domains were tested individually in a second yeast two-hybrid assay. Five amino acids at the core of each conserved domain were substituted with alanine residues. Alanine was chosen because it is small and chemically inert, and it is the least likely amino acid to cause any conformational or electrostatic change in a protein (Morrison and Weiss 2001). The six Upd3 alanine substitution mutants were fused with the GAL4 DNA binding domain and their interaction with the wild-type Upd3 Δ SS protein fused with the GAL4 activation domain was assessed individually. Only substitutions into domain 2 sustained the Upd3 Δ SS homotypic interaction when tested on a –His plate. Substitutions in each of the other domains abolished the interaction (Figure 2.9 A). When tested on the –His+5mM 3AT plate, domain 2 substitution mutants displayed a faster growth rate than wild-type Upd3 Δ SS, suggesting an even stronger interaction than wild-type Upd3 Δ SS. To get a quantitative assessment of the effects of the domain substitutions in the Upd3 homotypic interaction, the interaction strength of each domain substitution mutant with wild-type Upd3 Δ SS was also tested on the basis of the β -galactosidase activity from the *lacZ* reporter gene (Figure 2.9 B). Transformants containing various protein combinations were grown on a nonselective plate until big patches of cells were formed. The galactosidase substrate, X-gal, was then applied evenly to the cells. Surprisingly, after a long incubation period, no blue color was detected in Upd3 Δ SS/Upd3 Δ SS expressing cells, but it was shown lightly in Upd3^{AS2} Δ SS/Upd3 Δ SS expressing cells, confirming that Upd3^{AS2} might have stronger interaction strength than wild-type Upd3. No blue color was observed in colonies expressing any other domain substitution mutant.

In addition to the yeast two-hybrid assay, the interaction strength of Upd3 domain substitution mutants with wild-type Upd3 was also tested using BiFC. The

experiment was repeated four times and the results were normalized relative to wild-type Upd3 (Figure 2.9 C). Consistent with the results of the yeast two-hybrid assays, Upd3^{AS2} had slightly stronger interaction strength compared to wild-type Upd3. All other Upd3 substitution mutants showed reduced interaction strength, and among them, Upd3^{AS1} and Upd3^{AS5} still had significantly stronger interaction strength with wild-type Upd3 than the Dpp negative control ($p < 0.05$, two-tailed T-test with Bonferroni correction). However, Upd3^{AS3}, Upd3^{AS4} and Upd3^{AS6} showed BiFC signals at levels similar to that of Dpp.

Discussion

BiFC and yeast two-hybrid assays showed different sensitivities in detecting interactions between Upd-family ligands

Physical interactions between Upd-family ligands were detected in both BiFC and yeast two-hybrid assays, but some discrepancies were seen in the results of the two assays. The BiFC assay detected all possible homotypic and heterotypic interactions between Upd-family ligands, except for Upd2 with Upd3. The yeast two-hybrid assay was only used to test interactions involving Upd and Upd3, and it detected the Upd3 homotypic interaction, but not the Upd homotypic interaction or the heterotypic interaction between the two.

The discrepancies between results could be due to several technical limitations of the two assays. First of all, one general concern about yeast two-hybrid assays is that interactions between non-nuclear proteins are tested in an abnormal environment, which could lead to false positive or false negative results (Criekinge and Beyaert 1999). Upd and Upd3 are secreted proteins and in the BiFC experiment, protein interactions between the two ligands were localized into punctate structures inside cells, suggesting that protein complexes might be naturally formed in the ER/Golgi network within the secretory pathway. In addition, studies have suggested that ligand oligomerizations in other signaling pathways indeed occur specifically during the process of secretion. For example, heterodimers of Dpp and Scw were formed when they were co-expressed from cells, but not when they were mixed together in conditioned medium (Shimmi et al. 2005). The essential role of the secretory pathway in ligand interactions might be attributed to its associated microenvironment, such as pH and the presence of certain chaperone proteins, which could contribute to the proper folding of the ligands. Moreover, protein modifications that normally occur during secretion, including the formation of disulfide bonds, protein phosphorylation and glycosylation, are likely to be altered in a different organism. Both Upd and Upd3 have several predicted glycosylation sites. The lack of glycosylation on these two proteins when produced in yeast cells could

also affect protein folding or stability (Opdenakker et al. 1995). All the above mentioned factors might reduce the interaction strength between Upd-family ligands in the yeast two-hybrid assay, and as a result, only the Upd3 homotypic interaction, the strongest interaction observed in BiFC, was detected. Notably, even the Upd3 homotypic interaction exhibited very weak interaction strength in comparison to the prp43/Spp382 positive control, suggesting that the yeast two-hybrid assay is not a very sensitive method in detecting physical interactions between Upd-family ligands.

In contrast, the BiFC is not very stringent to detect Upd-family ligand interactions. Theoretically, a functional BiFC molecule can only be formed when the two proteins of interest physically interact. However, a low frequency of BiFC signals was detected in the Dpp negative controls, which was likely to be caused by spontaneous association between the GFP variant tags without interactions between the two proteins to which they were fused. Similar high background signals have also been reported in mammalian BiFC experiments (Kodama and Hu 2010, Nakagawa et al. 2011), suggesting it might be a drawback of the BiFC experiment, in general. Moreover, different from the mammalian BiFC, in which endogenous promoters were used to drive the expression of fusion proteins, a highly active and constitutive arm-GAL4 driver was used in this study, in order to compensate for the low transfection efficiency of *Drosophila* cells. The presumably high expression levels of the BiFC fusion proteins might further elevate the background signal. Nonetheless, real signals derived from ligand interactions can be distinguished from noise based on fluorescence frequency and intensity, and the low stringency of the BiFC assay allowed the detection of weak or transient protein interactions. Therefore, not only the Upd3 homotypic interaction, but other types of interactions between Upd and Upd3 were also detected in the BiFC experiment.

Compared to the previously established BiFC in mammalian cell culture, the *Drosophila* BiFC exhibited signals at much lower frequencies (Hu et al. 2002). Interactions between two transcriptional factors, bJun and Fos, resulted in BiFC signals detected in more than 90% of cells in mammalian culture. In contrast, BiFC signals were

only observed in a very small fraction of cells in this study. There are several potential reasons for the low BiFC frequency in *Drosophila* cells. First of all, it is easier to incorporate exogenous DNA fragments into mammalian cells than *Drosophila* cells. Secondly, the UAS-GAL4 expression system used in this study required one additional plasmid, which exacerbated the difficulty of plasmid transfection and limited the number of cells that received all necessary plasmids for the BiFC assay. Moreover, the truncated fluorescence tags might influence protein folding and interaction. In the mammalian BiFC assay, both N-terminal and C-terminal fusions of the fluorescence tags were attempted to determine the better tagging strategy that had the minimum disturbance on protein interactions. However, since the N-terminal signal peptides of Upd-family ligands are essential for protein localization, fluorescence tags were only fused to their C-termini. When the CFPC155 and VenusN173 tags were switched between interaction partners, slight differences in the BiFC signal were observed, although it did not change the conclusion of the experiment. For instance, Dpp tagged with CFPC155 showed higher background signals than what were observed when it was tagged with VenusN173, suggesting that the fluorescence tags did affect protein behaviors in the BiFC experiment. Finally, because Upd-family ligands are naturally secreted, there were presumably fewer proteins accumulated inside cells in comparison to the transcriptional factors assayed in the mammalian study; this is likely to be another factor in the low BiFC signals in this study.

Upd-family ligand oligomers might have different binding capacities to the receptor

Although ligand interactions are formed in both JAK and BMP signaling, the two pathways are likely to use different mechanisms to distinguish signaling information from different ligand oligomers. In the BMP pathway, signaling is transduced through a tetrameric receptor complex, composed of two type I receptors, Saxophone (Sax) and Thickveins (Tkv), and one type II receptor, Punt. During embryogenesis, Dpp and Scw bind to Tkv and Sax respectively (Shimmi et al. 2005) and therefore, information carried by different dimers of Dpp and Scw is transduced through different type I receptor dimers. Eventually, heterodimers of the Dpp and Scw stimulate 10 fold higher BMP

signaling than homodimers. The mechanism of how different type I receptor dimers lead to different signaling intensities is not very clear, but one possibility is that they might bind to the type II receptor with distinct binding affinities (Haerry 2010). In contrast, all three Upd-family ligands activate the JAK pathway through one single receptor, Dome. A structurally related short transmembrane protein, Eye transformer (Kallio et al. 2010) (aka Latran (Makki et al. 2010)), has also been identified as a receptor of this pathway, but it antagonizes Dome activity and is thus not likely to be involved in JAK signaling activation. In order to convey different stimulus information to the cell, Upd-family oligomers have to be able to distinguish themselves in some ways when they bind to Dome. It is possible that they can cause different conformational changes of Dome and consequently influence Dome dimerization and the subsequent signaling activation. Alternatively, different ligand oligomers might exhibit distinct binding affinities to Dome, and the ones that bind more effectively might be able to elicit a quicker response of signaling activation.

The different binding capacities of ligand oligomers with Dome could be derived from the structural difference in the three ligands and/or it could also be influenced by other molecules at the cell membrane. For example, although Eye transformer does not lead to signaling activation, this short receptor might preferentially bind to certain ligand oligomers and consequently prohibit their binding to Dome. In addition, the numerous proteoglycans present in the ECM might also be involved in the interaction between ligand oligomers and Dome. After secretion, Upd binds to Dally, a HSPG molecule in the ECM, which stabilizes Upd at the cell membrane (Hayashi et al. 2012). Upd3 is also located to the ECM and it possibly can bind to the same HSPG molecule, however, with a different affinity. Different binding affinities of Upd and Upd3 to Dally would result in different stabilities of ligand oligomers in the ECM. Oligomers that are more stable in the ECM are expected to have more chance to encounter receptors and eventually cause higher signaling activation. On the other hand, more mobile oligomers would result in lower signaling activation. Alternatively, ligand oligomers might distinguish themselves by binding to different ECM molecules. Similar to Dally, many

ECM molecules stabilize ligands at the cell membrane and enhance the binding between ligands and receptors. In contrast, some other ECM molecules promote the mobility of ligands and consequently attenuate ligand binding to receptors (Nybakken and Perrimon 2002). If oligomers preferentially bind to different ECM molecules, it can also result in different stabilities of oligomers at the cell membrane and consequently cause different JAK signaling activities.

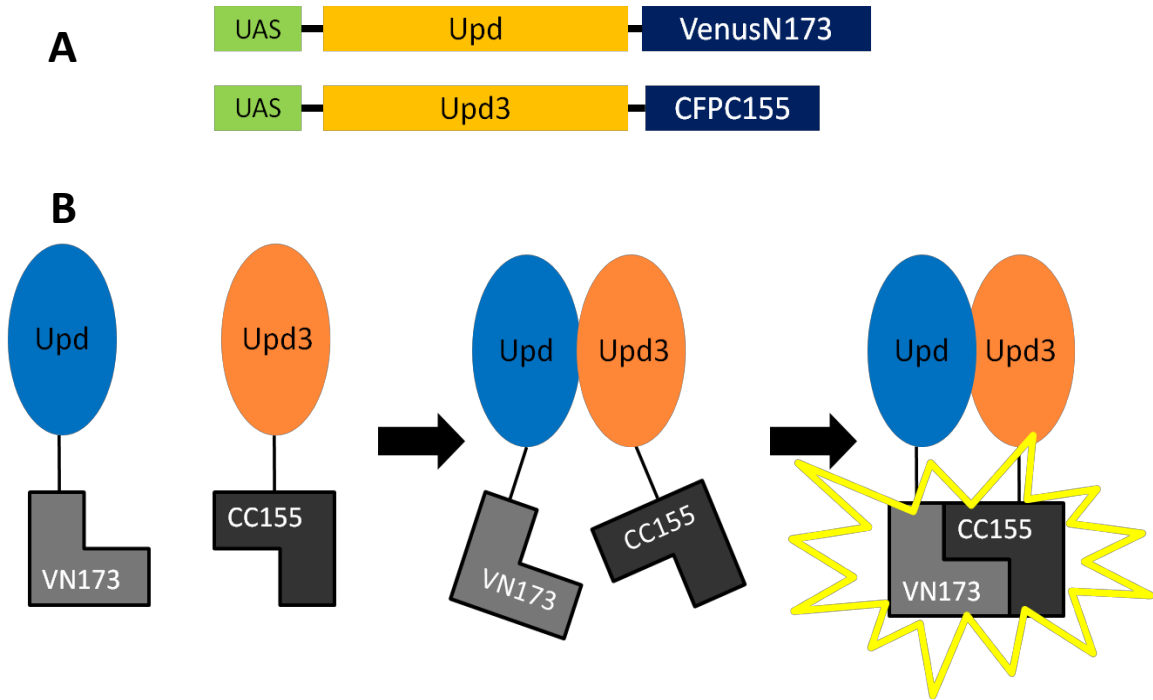
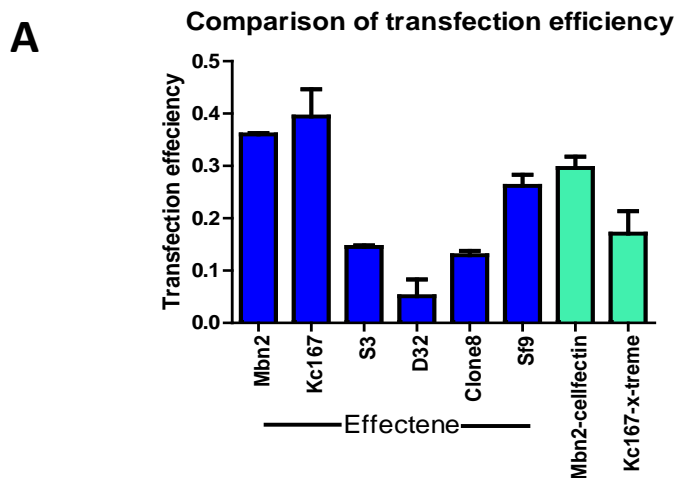


Figure 2.1. A schematic representation of the BiFC experiment. (A) A schematic of DNA constructs of BiFC fusion proteins. The N-terminus of Venus and the C-terminus of CFP are tagged to the C-terminal ends of Upd and Upd3, downstream of an Upstream Activation Sequence (UAS) site. **(B)** A schematic representation of the principle of the BiFC experiment to detect physical interactions between Upd-family ligands. Physical interactions between ligands would bring the two nonfluorescent fragments in close proximity to restore a functional fluorophore.



B

	GAL4	GFP/Cherry	Cherry/Total
Kc167	arm	0.52	0.30
	mt	0.36	0.23
	cs1.L7	0.18	0.30
Mbn2	arm	0.68	0.39
	mt	0.63	0.33
	cs1.L7	0.27	0.30

Figure 2.2. Optimization of a cell system for relatively high exogenous gene expression.

(A) Plasmid transfection rate was compared among different cell lines. Effectene was used to mediate plasmid transfection in all cell lines indicated by blue bars. Transfection rates of *Drosophila* cell lines, including mbn2, Kc167, S3, D32 and clone8, were assessed by calculating the percentage of cells that expressed actin-cherry, and the transfection rate of Sf9 was assessed using pie-GFP. Plasmid transfection in mbn2 and Kc167 cells was also tested using Cellfectin and x-tremeGene transfection reagents (green bars), respectively, and the transfection rates were lower than the ones mediate by Effectene. Error bars, SD. **(B)** Three GAL4 drivers were used (see text for details) to drive the expression of UAS-GFP in Kc167 and mbn2 cells. *actin-cherry* was co-expressed to monitor the transfection rate. The numbers of GFP positive, Cherry positive and total cells were counted. Ratios of GFP/Cherry and Cherry/total were shown.

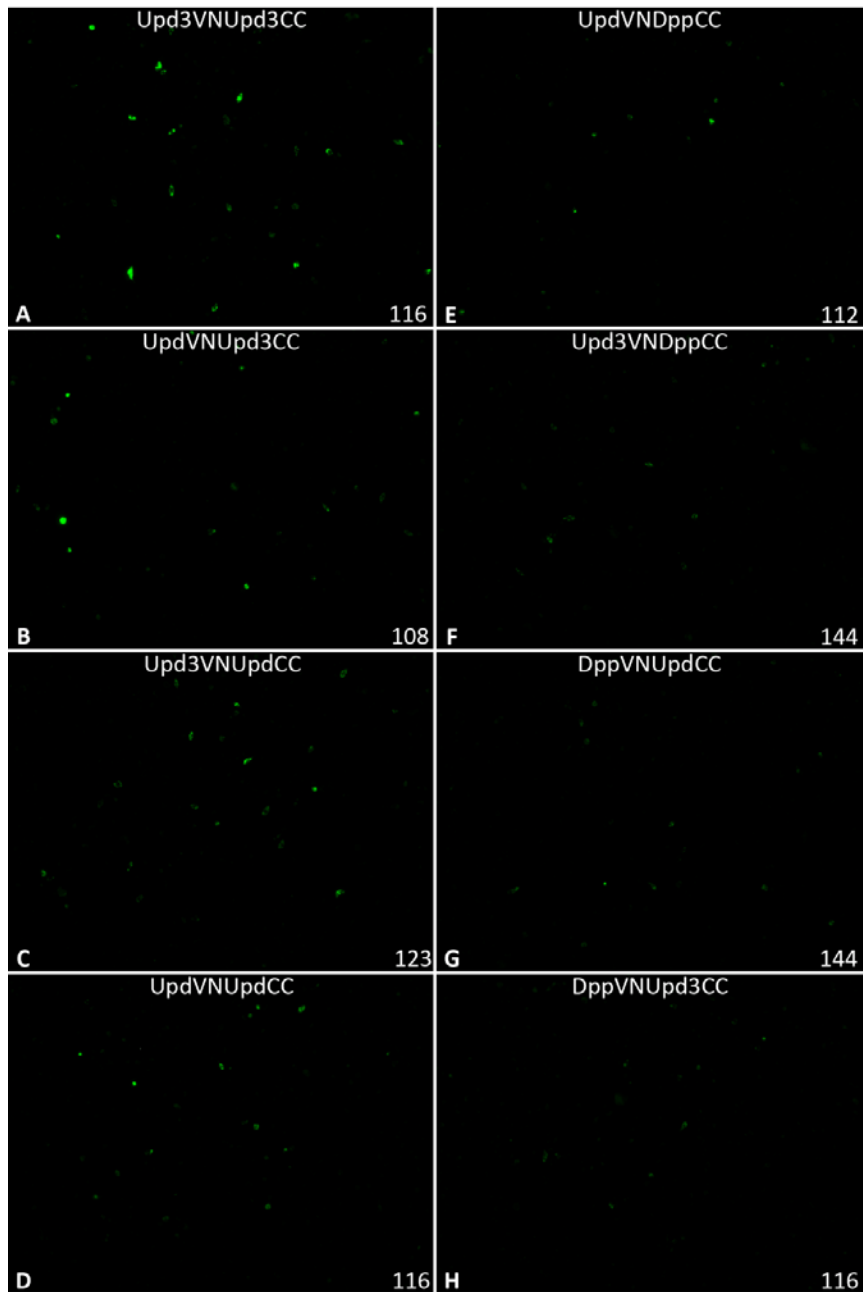


Figure 2.3. BiFC results. Combinations of BiFC fusion proteins, as indicated at the top of individual panels, were expressed in Kc167 cells along with Cherry (not shown). Representative pictures taken at 200x magnification were shown. Green fluorescent signals are results of the reconstitution of the BiFC nonfluorescent fragments, indicating interactions between the ligands. The number of Cherry positive cells in the same picture was indicated at the right bottom corner of each image.

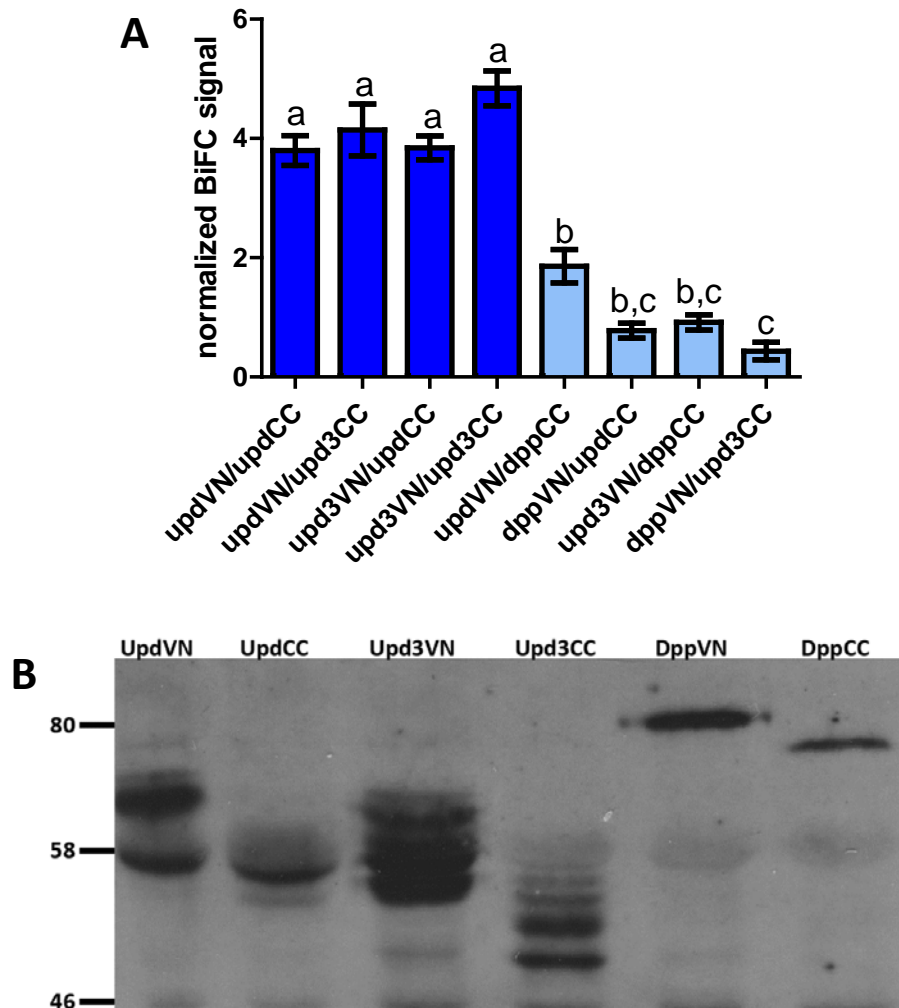


Figure 2.4. Quantification of the BiFC results between Upd and Upd3. (A) Actin-cherry was co-expressed with BiFC fusion proteins to identify cells that were transfected. The percentage of BiFC positive cells over Cherry positive cells was calculated for each ligand combination. The mean BiFC/Cherry ratio of the four Dpp negative controls (light bars) was taken as a measurement of the baseline signal and fold changes of BiFC/Cherry ratios compared to the baseline signal were compared between ligand combinations (dark bars). Data presented are mean values from 6 independent experiments with standard error (indicated by error bars). Groups labeled with the same letter are not significantly different (one-way ANOVA with Bonferroni post-hoc test). **(B)** The expression of BiFC fusion proteins was detected by rabbit anti-GFP polyclonal antibodies on western blot.

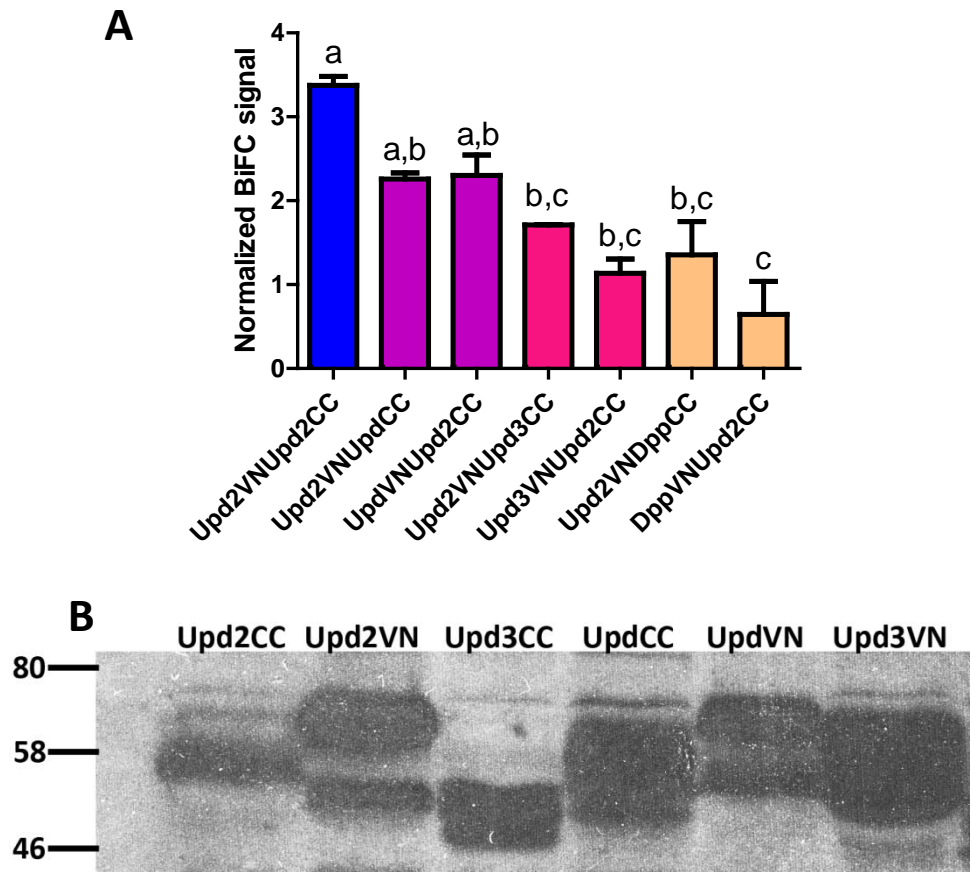


Figure 2.5. Physical interactions of Upd2 with Upd and Upd3. (A) Physical interaction of Upd2 to Upd and Upd3 was tested using BiFC. Homotypic interaction of Upd2 showed stronger signal than heterotypic interaction between Upd and Upd2. Heterotypic interaction between Upd2 and Upd3 was not statistically significant from Dpp controls. Data presented are mean values from two independent experiments with standard error. Groups labeled with the same letter are not significantly different (one-way ANOVA with Bonferroni post-hoc test). **(B)** Expression of involved fusion proteins in this experiment was tested by western blot analysis.

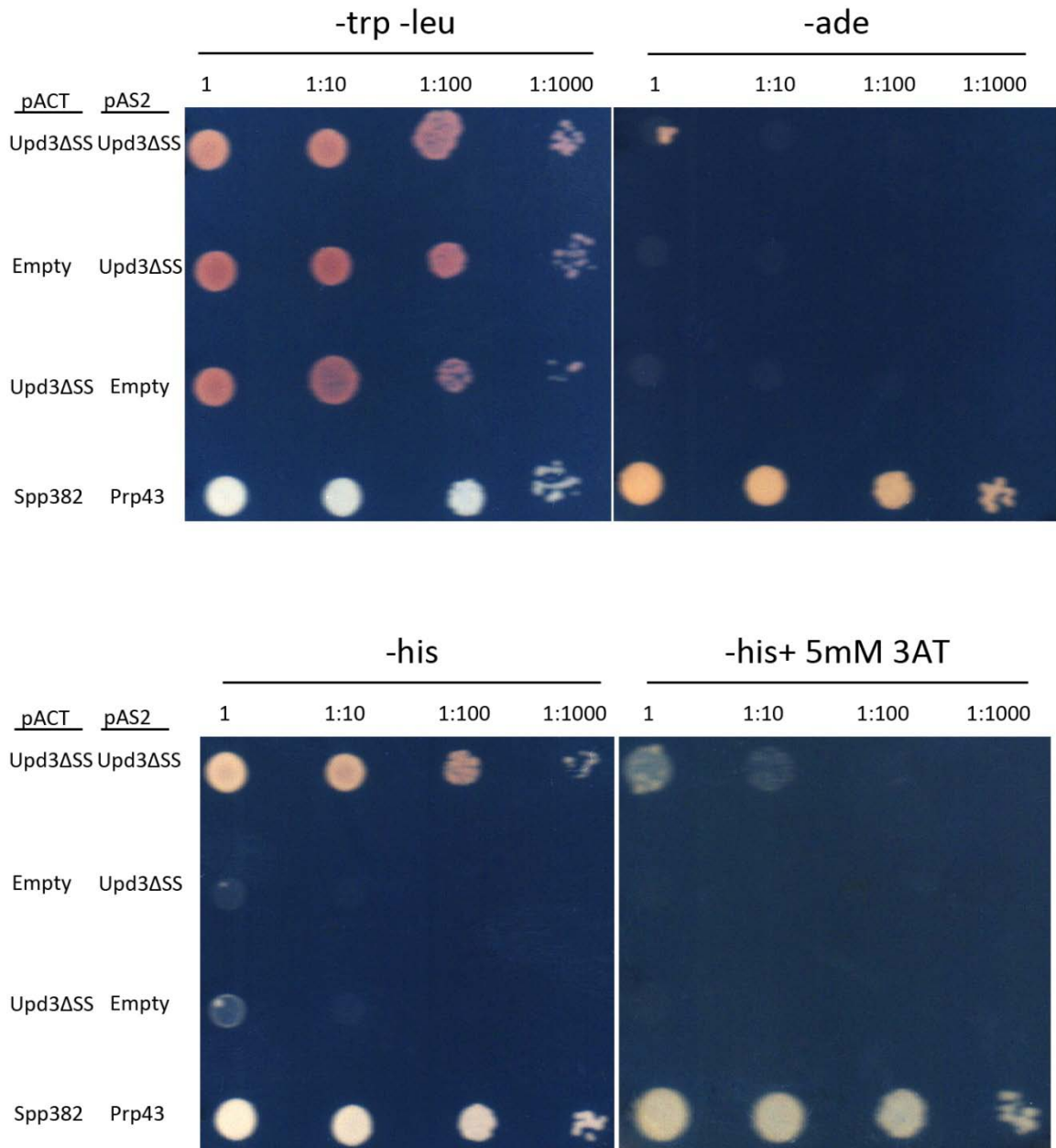


Figure 2.6. Yeast two-hybrid results of the Upd3ΔSS homotypic interaction. A series of diluted cells were grown on different selective plates. Empty vectors were used as negative controls and Spp382/Prp43 was a positive control. A –Trp-Leu plate was used to select successful transformants containing both pACT and pAS2 plasmids. Upd3ΔSS/Upd3ΔSS homotypic interaction was shown on –His, –His+5mM 3AT and –Ade plates.

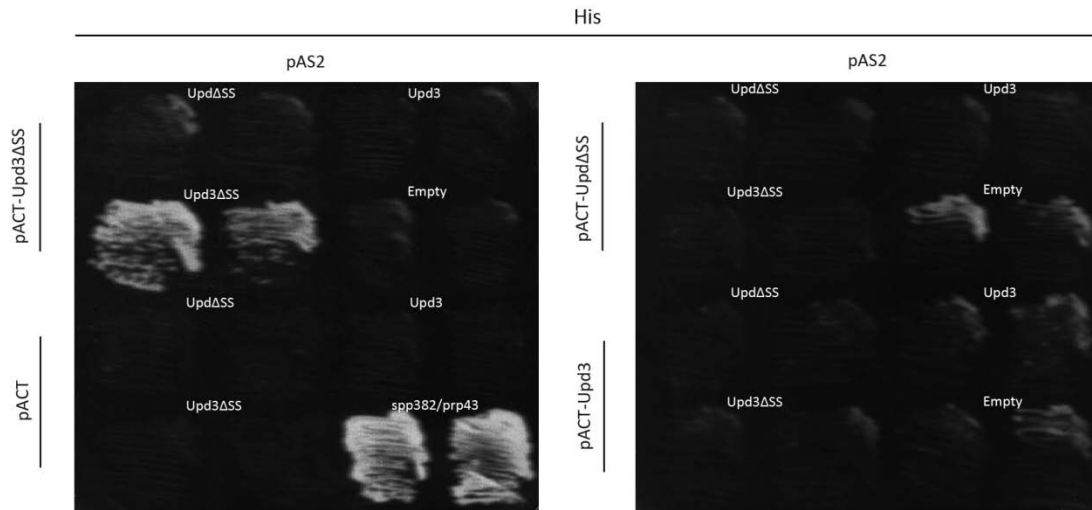


Figure 2.7. Yeast two-hybrid analyses of all possible interactions between Upd and Upd3. Cells expressing different combinations of Upd Δ SS, Upd3 and Upd3 Δ SS were streaked on –His plates to test for ligand interactions. Only Upd3 Δ SS/ Upd3 Δ SS showed positive interaction. Spp382/Prp43 is a positive control.

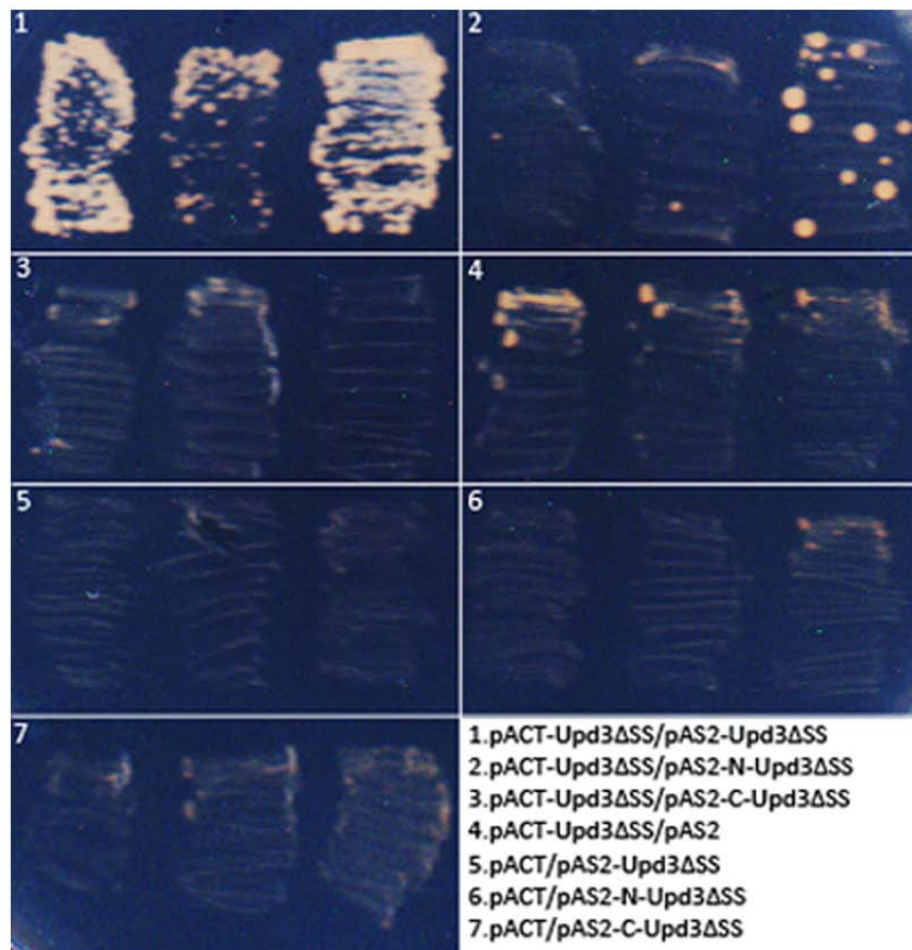
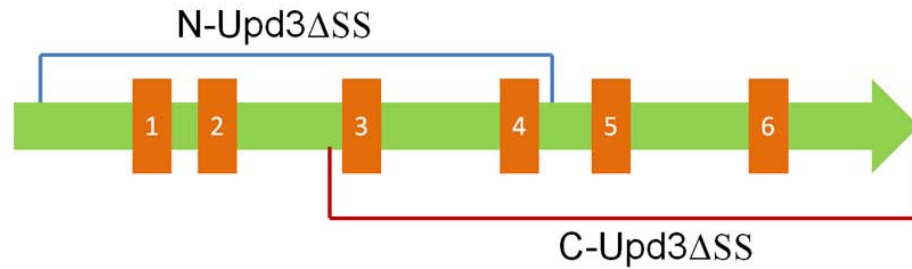


Figure 2.8 Yeast two-hybrid results of truncated Upd3. N-terminal and C-terminal truncations of Upd3 were made as shown in the schematic. The interactions between wild-type Upd3 and Upd3 truncations were tested in triplicate by growth on a – His selective plate. One of the three colonies expressing Upd3ΔSS /N-Upd3ΔSS showed slow growth on the plate (2), suggesting a weaker interaction compared to wild-type Upd3 (1). The C-terminal half of Upd3 (3) did not show interaction with wild-type Upd3. Empty vectors were used as negative controls (4-7).

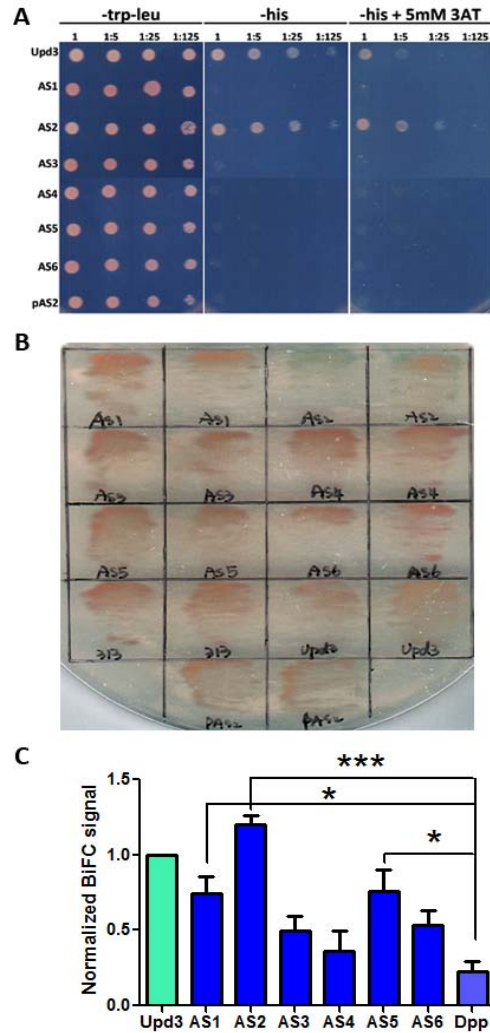


Figure 2.9 Comparison of the Upd3 interaction strength with alanine substituted Upd3 mutants. Interactions between alanine substituted Upd3 mutants and wild-type Upd3 were compared using yeast two-hybrid (A and B) and BiFC (C) assays. **(A)** Upd3^{AS2} showed slightly stronger interaction compared to wild-type Upd3. All other mutants abolished the Upd3/Upd3 interaction. **(B)** Interaction strength between Upd3 mutants and wild-type Upd3 was compared using X-gal staining. Only Upd3^{AS2} showed some blue color, indicating the activation of the *lacZ* gene. **(C)** In the BiFC assay, Upd3^{AS2} exhibited slightly higher interaction strength compared to wild-type Upd3. Upd3^{AS1} and Upd3^{AS5} were able to stimulate significantly higher signal than Dpp. Upd3^{AS3}, Upd3^{AS4} and Upd3^{AS6} failed to elicit higher BiFC signal than Dpp. Error bars, SEM; p<0.0001 one-way ANOVA; * p<0.05, *** p<0.0001 T-test with Bonferroni correction.

Chapter 3: Biological significance of interaction between Upd-family ligands

Introduction

Numerous mechanisms have been generated during the long history of evolution to regulate signaling pathways in order to achieve signaling specificity and robustness. In general, signaling pathways are shaped at three levels: signaling intensity, activity range and kinetics. The formation of homotypic and heterotypic interactions between ligands can be involved in the regulation of signaling pathways at some of these levels. First of all, different ligand oligomers might be able to result in distinct signaling intensities and regulate the pathway in a quantitative manner. For example, both mammalian and *Drosophila* BMP signaling ligands form heterodimers, which stimulate higher signaling intensity than homodimers in a variety of biological processes (Butler and Dodd 2003, Shimmi et al. 2005, Buijs et al. 2012). Synergistic and inhibitory effects have also been observed between several mammalian cytokines (Bartee and McFadden 2013), although no evidence has shown that they were mediated by ligand interactions. Secondly, ligand oligomers might have different localization patterns in tissues and consequently affect the signaling range. Heterodimers of *Drosophila* BMP signaling ligands are transported over a longer distance than homodimers by extracellular proteins during embryogenesis and wing vein development (O'Connor et al. 2006). Additionally, oligomerization is also necessary for chemokine distribution in mammals. Chemokines are a family of small cytokines that induce chemotaxis in neighboring cells. Oligomerization of chemokines help to concentrate them in localized areas and create a chemotactic gradient, which is the directional cue for the migration of responsive cells (Campanella et al. 2006). Monomers of several chemokines showed higher affinity to receptors than oligomers, but they were defective in promoting cell migration (Proudfoot et al. 2003). Finally, different ligands might result in different signaling persistence. For example, TGF α and EGF stimulate EGFR signaling through the same receptor. A single exposure of TGF α elicits shorter EGFR signaling activation than the one stimulated by EGF. Repetitive exposure of TGF α , however, is able to stimulate continuous signaling activation due to a quicker turnover rate of the receptor compared to the one under EGF stimulation

(Ouyang et al. 1999). The underlying mechanism causing the difference in receptor turnover is the different sensitivity of the two ligands to pH changes. TGF α is less stable than EGF in acidic environments. In consequence, TGF α quickly changes its conformation and releases activated receptors in the endosome, enabling receptors to be more rapidly dephosphorylated and recycled back to the membrane. However, to the best of my knowledge, there has been no report showing oligomerization of ligands involved in the regulation of signaling persistence. In this study, whether JAK signaling intensity, the activity range, or both are regulated by the oligomerization of Upd-family ligands were tested using *in vitro* and *in vivo* approaches.

In *Drosophila* cell culture, signaling intensities stimulated by different ligands were compared using luciferase assays. In addition, the six Upd3 alanine substitution mutants were also subjected to luciferase assays, in order to test if any of the conserved domains is critical for signaling activation. The luciferase assay was chosen for the *in vitro* study because of its ease of use and ability to provide a quantitative measurement of signaling induction. However, it is always a challenge to extrapolate what happens in the intact organism from results of *in vitro* studies. Moreover, Upd and Upd3 are both associated with the ECM adjacent to the producing cell in culture (Wright et al. 2011), so the different localization patterns of oligomers, if exist, are hard to detect *in vitro*.

Therefore, the potential functional consequences from different Upd-family oligomers were also explored *in vivo*, using *Drosophila* oogenesis as the model system. Oogenesis is one of the most intensively studied processes during *Drosophila* development and it requires precisely controlled JAK signaling activity. Each *Drosophila* ovary consists of 16 ovarioles, which are chains of continuously developing egg chambers (Bastock and St Johnston 2008) (Figure 3.1). The development of an egg chamber initiates from the anterior end of the ovariole in a structure called the germarium, where germline and somatic stem cells reside. After stem cell differentiation and several rounds of division, an egg chamber pinches off from the germarium as a 16-cell germline cyst surrounded by a monolayer of somatic follicle cells.

One of the germline cells eventually becomes the oocyte and the remainder becomes supporting nurse cells. The morphology of the mature egg and the future embryo is determined during the development of the egg chamber, and it relies extensively on the reciprocal interaction between germline and somatic follicle cells. The JAK/STAT signaling pathway plays a pivotal role in specifying follicular epithelial cell fates. The first two differentiated follicle cell types are polar cells and stalk cells, which are specified during the encapsulation of the 16-cell cyst in the germarium. The differentiation of other follicle cells starts from stage 7 and it ends up with five distinct cell fates: border, stretched, centripetal, main body and posterior cells. Each cell type has its specific morphology and location in egg chambers. Upd is expressed in polar cells and it generates a concentration gradient along egg chambers after secretion (Hayashi et al. 2012). It functions as a classical morphogen to control follicular epithelial cell fate based on its concentration (Xi et al. 2003). At the anterior of egg chambers, the group of cells that is located closest to the source of Upd receiving the highest amount of JAK activity becomes border cells. At stage 9, an ecdysone signal triggers border cells to undergo an epithelial-to-mesenchymal transition and migrate towards the oocyte (Bai et al. 2000). Border cells eventually reach the anterior of the oocyte at stage 10 and form a structure called the micropyle, which is needed for sperm entry. As the Upd concentration declines towards the middle of the egg chamber, follicular epithelial cells are specified into stretched cells and centripetal cells. Stretched cells, as the name suggests, adopt a distinctive squamous morphology, and they cover nurse cells. Centripetal cells can be most easily recognized at stage 10 when they invaginate between nurse cells and the oocyte to provide a physical separation. Cells at the middle of egg chambers receiving the lowest JAK signaling adopt the default main body cell identity. The initial symmetric A/P polarity established by JAK signaling is broken by posterior EGFR signaling activated by the Gurken ligand from the oocyte (Ray and Schüpbach 1996). The posterior terminal cell fate is thus determined by both EGFR and JAK signaling. The composition of follicular epithelial cells is very sensitive to changes in JAK signaling activity. A systematic decrease in JAK signaling, caused by hypomorphic mutations of *upd* or *hop*, results in

reduction of border cell numbers and expansion of the main body cell population (Xi et al. 2003). On the other hand, elevation of JAK signaling activity in centripetal or stretched cells by overexpressing *hop* or *upd* induces ectopic border cell formation (Silver and Montell 2001, Xi et al. 2003). Therefore, anterior follicle cells were used in this study as a qualitative measurement to compare the JAK signaling intensities stimulated by different ligand oligomers. On the other hand, the distribution of ligands was also assessed in egg chambers using immunohistology.

Result

Upd and Upd3 may be weakly synergistic in cell culture

Signaling intensities stimulated by individual Upd-family ligands have been compared previously in autocrine, paracrine and endocrine fashion using luciferase assays in cell culture (Hombria et al. 2005, Wright et al. 2011). In these studies, Upd stimulated the highest JAK activity in autocrine and paracrine manner, whereas Upd2 exceeded the other two in endocrine stimulation when conditioned medium was used. Potential synergistic and inhibitory effects between Upd-family ligands have also been tested through an endocrine luciferase assay (Wright et al. 2011). GFP tagged Upd-family ligands were expressed individually in cells and the conditioned medium containing equal molar amount of ligands, measured by a anti-GFP ELISA (Enzyme-linked immunosorbent assay), was used separately or in combinations to stimulate the pathway. In their study, combining any two of the ligands or all three together did not exhibit either synergistic or inhibitory effect. Rather, Upd-family ligands seemed to function in a simple additive manner, suggesting that the three ligands stimulate the pathway independently. However, there is a caveat to this previous study. As mentioned in the previous chapter, interactions between ligands might only happen in the protein secretory pathway but not in the conditioned medium, and ligand oligomerization could be a prerequisite for exhibiting synergy between ligands. In the example of Dpp and Scw, the two ligands lose the synergistic effect on stimulating the BMP signaling pathway when they are mixed in the conditioned medium, since no heterodimer can be formed (Shimmi et al. 2005). The potential synergistic or inhibitory effect between Upd and Upd3 was therefore re-examined using a paracrine luciferase assay, in which the two ligands were co-expressed from one population of cells and co-cultured with a second population of cells containing a JAK signaling reporter, 6x2xDrafluc-firefly luciferase. This JAK reporter is comprised of 12 tandem copies of the STAT binding site, derived from two STAT binding sites at the promoter region of *Draf* (Muller et al. 2005), placed upstream of a firefly luciferase coding sequence. A constitutive actin-Renilla luciferase reporter was co-expressed with the 6x2xDrafluc-

firefly luciferase reporter to serve as an internal control. Ligands used to stimulate the reporter activity were tagged with the VenusN173 tag at their C-terminus and expressed under the control of arm-GAL4. Cells expressing no exogenous Upd-family ligands were used as the negative control in this experiment to indicate the endogenous JAK activity level.

Cell lines to be used in this paracrine luciferase assay have to meet several criteria. The reporter cell should contain endogenous JAK signaling components to be able to respond to exogenous ligand stimulation, but on the other hand, lower levels of endogenous activity are preferred for more sensitive responses. The ligand-producing cells should have a high transfection rate to produce large amounts of exogenous ligands but also show low levels of endogenous ligand expression. Finally, the two cell lines have to be able to grow healthily together. Three *Drosophila* cell lines that fit these criteria, S3, mbn2 and Kc167 cells, were first tested in combinations to detect JAK signaling activation upon Upd stimulation. Among all possible combinations of the three cell lines, when S3 was used as the ligand producing cell line or Kc167 was used as the reporter cell line, JAK signaling had relatively low induction (Figure 3.2 A). This is possibly because S3 cells have a low transfection rate as shown in the previous chapter and Kc167 cells might have relatively high endogenous JAK activity compared to the other two lines. The strongest signaling induction was achieved when Kc167 expressed the ligands and mbn2 expressed the reporters, and therefore this combination of cell lines was chosen for all luciferase assays throughout the study. In addition to the choice of cell lines, the length of the incubation periods during plasmid transfection and the co-culture was also optimized. Cells were incubated with the plasmid transfection reagent for either one or two days, and after that, the ligand producing cells and the reporter cells were co-cultured for one, two or three days. Longer incubation of cells with the transfection reagent caused slightly lower signaling induction, probably because the transfection reagent had a mild toxic effect on cells. Increasing the co-culture period enhanced JAK activation, but on the other hand, it also resulted in high variability in results (Figure 3.2B). In all subsequent luciferase assays of this chapter, cells were

incubated with the transfection reagent for one day, and the two populations of cells were subsequently co-cultured together for two or three days depending on the purpose of the experiment. The optimized system was first tested for the ability to show linear JAK signaling induction upon various amount of Upd stimulation. In this experiment, varying numbers of Upd expressing Kc167 cells were co-cultured with a constant number of reporter mbn2 cells, with differences in total cell density between groups being compensated by the addition of untransfected Kc167 cells. The resulting JAK signaling induction was correlated with the number of Upd producing cells included in the co-culture, suggesting that the system is capable of showing JAK signaling induction in a dosage dependent way up to the level of Upd stimulation (Figure3.2C).

Potential synergistic or inhibitory effect between Upd and Upd3 was then tested using the established luciferase assay. Holding the total amount of plasmid constant, plasmids expressing either Upd or Upd3 were transfected into Kc167 cells individually or in combination, with an Upd: Upd3 ratio of 1:3, 1:1 or 3:1. Ligand expressing cells and reporter cells were co-cultured for two days before a portion of the co-cultured cells was lysed for measuring the luciferase activity. The remaining co-cultured cells were subjected to western blot analysis. According to the western blot result, protein production was roughly consistent with the amount of plasmids used in transfection (Figure3.3B). The luciferase assay showed similar results to those of Wright et al. regarding individual ligand stimulation; Upd stimulated higher JAK signaling intensity than Upd3 (Figure3.3A) (Wright et al. 2011). Compared to the baseline signaling level as measured from the mock group, Upd caused a 45 fold signaling induction, whereas Upd3 caused only about 13 fold induction. However, the two ligands did not function in a simple additive manner when they were co-expressed. Under the assumption of independent function, combinations of the two ligands were predicted to stimulate intermediate signal intensities at various levels (shown as gray bars in Figure 3.3A). However, all three combinations of the two ligands stimulated JAK signaling to a similar or even higher level than that of stimulation by Upd alone. Even the group with an Upd: Upd3 ratio of 1:3 resulted in a slightly higher signaling activation than Upd alone. The

discrepancy in results between this experiment and the previous one (Wright et al. 2011) might be caused by the different strategies used in signaling activation (paracrine versus endocrine) or ligand expression (co-expression versus separate expression). To test these two possibilities, co-expressed and separately expressed Upd and Upd3 were used in parallel to stimulate JAK signaling activation in a paracrine fashion. Separate expression of the ligands with an Upd: Upd3 ratio of 1:3 resulted in an intermediate signal between individual ligand inductions, consistent with the idea of an additive effect between the two ligands (Figure 3.4). In contrast, co-expression of this ligand combination caused similar signaling activation to that of Upd alone, and it was significantly higher than the intermediate signal stimulated from separately expressed ligands ($p < 0.05$, two-tailed T-test). This result suggests that co-expression was required for the cooperative function between Upd and Upd3 to achieve higher signaling intensity. Although Upd and Upd3 did not function in a simple additive manner when co-expressed, they did not exhibit strong synergy either. JAK signaling activation from none of the ligand combinations was significantly higher than the one from Upd alone, and the co-expressed ligand combinations with Upd: Upd3 ratios of 3:1 and 1:1 did not stimulate significantly higher JAK signaling activity than separately expressed ligands. Both of these results could be caused by several technical limitations of the luciferase assay, which will be discussed in details at the end of this chapter.

Functional domains in Upd3

One possible underlying mechanism for the cooperative function between Upd and Upd3 is through an Upd/Upd3 oligomer. To test this hypothesis, the Upd3 alanine substitution mutants were subjected to a luciferase assay to assess their ability in signaling induction, since all of them slightly affected the interaction strength of Upd3, as shown in the previous chapter. In addition to amino acid substitutions made in individual domains, a big domain swap was also generated in Upd3 by replacing the region comprising domain 3, 4 and 5 with the corresponding region from Upd. The resulting chimeric protein was named Upd3³¹³. To create a negative control for this domain study, the same alanine substitutions were also made in five amino acids

located in a non-conserved region at the N-terminus of Upd3, and the resulting protein was named Upd3^{NCAS} (non-conserved alanine substitution). All modified Upd3 coding sequences were fused with the CFPC155 tag at their C-terminus, allowing the proteins to be detected by anti-GFP polyclonal antibodies in western analysis. The luciferase assay was repeated 5 times and the results were consistent. All six alanine substitution mutant proteins showed dramatically reduced JAK signaling potency compared to wild-type Upd3 (Figure 3.5A; $p < 0.0001$ T-test with Bonferroni correction). Upd3^{AS1} was the only substitution mutant capable of stimulating a signal that was distinguishable from the baseline, although the signaling intensity was only about 1/5 of that stimulated by wild-type Upd3. All other alanine substitutions totally abolished the reporter activity to the baseline level. The big domain swap, Upd3³¹³ also failed to elicit any JAK signaling activity. However, Upd3^{NCAS} was able to stimulate JAK signaling to the same level as wild-type Upd3.

The deficiency of Upd3 substitutions in activating the pathway could be due to their modified ability in Upd3 homotypic interaction, but it can also be caused by other reasons. First of all, amino acid substitutions made at certain domains might result in improper protein folding and consequently lead to a higher rate of protein degradation. To test this possibility, co-cultured cells left from the luciferase assay were lysed in cold RIPA buffer and the cell lysate was subjected to western blot analysis. Most of the Upd3 mutants showed similar protein abundance as wild-type Upd3, except for Upd3^{AS4} and the big domain swap protein (Upd3³¹³). A trace amount of Upd3^{AS4} protein in the cell lysate could be detected on the western blot at long exposure times, whereas Upd3³¹³ was not detected at all (Figure 3.5B). The DNA constructs expressing these alanine substitution mutants were sequenced around the substitution sites and confirmed that no additional mutation was introduced during cloning. In addition, the trace amount of Upd3^{AS4} detected on the western blot was at the same size as wild-type Upd3, suggesting the gene product was in the correct reading frame. Domain 4 resides in a helix structure located in the middle of Upd3, but the poly-alanine substitution of this domain did not change the secondary structure of the protein, as predicted by the

psipred server (Kruger et al. 2013). The reduction of protein accumulation could be caused by changes in RNA production, if, for example, this mutation altered the splicing pattern of *upd3* mRNA. Or it might be caused by changes in the protein tertiary structure, which can lead to improper folding and quicker degradation of the protein. The lack of protein accumulation of these two mutants was likely the cause for their deficiency in signaling activation as well as ligand interaction.

Additionally, altered ECM association could be another mechanism for the reduced signaling intensity of the Upd3 substitution mutants. Upd associates with the ECM through Dally, a HSPG molecule (Hayashi et al. 2012). Loss of Dally in mosaic clones reduced JAK signaling activation in a cell non-autonomous manner in egg chambers. Upd3 shows similar ECM association as Upd in cell culture and loss of this ECM association could also alter Upd3 ability to stimulate the pathway. The previous western blot used cold RIPA buffer to extract proteins that remain inside cells but it did not include preparation of proteins bound to the extracellular matrix or in the conditioned medium. To assay these pools of the mutant proteins also, a second western blot was performed using different cell lysis protocols to separately extract proteins from inside the cell, the extracellular matrix, and the conditioned medium. In these experiments, Upd3^{AS1} showed more accumulation in the conditioned medium in comparison to wild-type Upd3, at the expense of protein abundance in the extracellular matrix (Figure 3.5C). Therefore, the first conserved domain may be critical for Upd3 association with the ECM. The first conserved domains of Upd-family ligands are enriched with basic amino acids, including arginines and lysines, which could be important for Upd-family ligands to bind to negatively charged ECM molecules, such as HSPGs. Moreover, a similar stretch of basic amino acids has been identified previously at the N-terminus of Dpp, and removing multiple amino acids from this basic domain released Dpp from Dally (Akiyama et al. 2008), indicating the importance of this basic domain in Dpp association with the ECM. The lack of ECM association of Upd3^{AS1} might contribute to the low JAK signaling activation of this mutant.

No synergy was exhibited between Upd and Upd3 in vivo

The luciferase assay in cell culture suggested that co-expressed Upd and Upd3 might be able to stimulate higher signaling intensity than individual ligands alone, although only weak synergy was observed. In order to understand if the small intensity difference detected *in vitro* can cause any functional consequence *in vivo*, JAK signaling intensity stimulated by single or combined ligands was assessed qualitatively in egg chambers, using ectopic border cell specification as an indicator of high levels of JAK signaling activation. Upd plays a pivotal role in border cell specification. The lack of *upd* expression in *upd* hypomorphic mutants converts some border cells into stretched cells and slows down the migration of the remaining border cells (Silver and Montell 2001, Xi et al. 2003). On the other hand, overexpression of *upd* is sufficient to induce ectopic border cell specification in stretched cell and centripetal cell populations (Xi et al. 2003). All these observations are in line with the idea that Upd functions as a morphogen to specify follicle cell fates. However, *upd* overexpression in main body cells at the center of egg chambers failed to induce border cell specification. It has been speculated that some other proteins, accumulated at the pole but absent at the center of egg chambers, might be needed to function together with Upd to achieve the highest JAK signaling activation needed for border cell specification. Upd3 is an excellent candidate of such proteins. It is co-expressed from polar cells with Upd (Wang 2009) and anticipated to have limited diffusion distance into egg chambers due to its association with the ECM. Moreover, Upd3 is also involved in border cell specification (McGregor et al. 2002, Sexton 2009). Null mutants of *upd3* contain a slightly reduced number of border cells, and these border cells, although still properly migrating, show some defects in micropyle formation (Michelle Giedt, personal communication). Therefore, whether co-expressing Upd and Upd3 together is able to induce ectopic border cells in the main body cell population was tested. If true, this would support the idea of synergistic activities of the two ligands in this context.

Ligand overexpression was carried out using a flip-out cassette (Ito et al. 1997). Small clones of cells misexpressing Upd, Upd3 or both were generated randomly in egg

chambers, marked by the expression of a UAS-GFP reporter. A lacZ enhancer trap marker, 5A7, was also expressed in flies to specifically label border cells. Ectopically induced border cells were distinguished from endogenous border cells based on the position and morphology of surrounding cells. Overexpression of *upd3* alone in egg chambers did not induce ectopic border cells in any other type of follicular epithelial cells (Figure 3.6 B). *upd* overexpression induced ectopic border cell formation in presumptive stretched cells (Figure 3.6 A, arrowhead) and centripetal cells (Figure 3.6 A, arrow). These ectopic border cells not only expressed the border cell specific 5A7 marker, but also adopted a border cell-like morphology. The ectopic co-expression of *upd* and *upd3* caused very similar results to those of overexpressing *upd* alone that ectopic border cells were detected in presumptive stretched cells and centripetal cells (Figure 3.6 C). However, neither Upd alone nor Upd and Upd3 together were able to cause ectopic border cell formation in the main body cell population.

Upd exhibited narrower distribution in upd3 mutant egg chambers

In addition to the regulation of signaling intensity, another potential consequence of ligand oligomerization is affecting the signaling activity range. Different types of ligand oligomers might have distinct distribution patterns in tissues. To compare the localization patterns of protein oligomers, a multi-colored BiFC assay is potentially an excellent choice, since it is able to show multiple pairs of protein interactions and their tissue localizations at once. *In vivo* BiFC detecting homotypic and heterotypic interactions of Upd and Upd3 has been tried in *Drosophila* embryos, but unfortunately, the BiFC signal could not be consistently detected (not shown). This might be due to the fact that BiFC had limited ability to detect protein interactions in the ECM as indicated in the cell culture study, or that the VenusN and CFPC tagged Upd and Upd3 proteins might not be properly expressed in flies. Therefore, oligomer distribution patterns were assessed indirectly by detecting the distribution of Upd in various *upd3*-expressing backgrounds, under the assumption that if the distribution pattern differs between different oligomers, manipulating the expression level of one ligand should change the oligomer composition and consequently alter the distribution

pattern of the other ligand. Changing the expression level of one protein alters the localization pattern of an interacting protein has been observed with Dpp and Scw. Dpp accumulation at the dorsal midline of embryos is lost in *scw* mutants (Shimmi et al. 2005), indicating a role of Dpp/Scw heterodimerization in Dpp distribution.

Upd distribution was tested in *upd3* mutant, *upd3* overexpression and wild-type backgrounds. The *upd3* mutant used in this study, *upd3*^{d232a}, was created by a P-element imprecise excision deleting the entire last exon of *upd3* (Wang 2009). *upd3*^{d232a} flies are viable and fertile, but have several obvious defects, including smaller eyes and outstretched wings. A P-element precise excision line, *upd3*^{x37e}, was used as the control since it is wild-type for *upd3* and has similar genetic background to that of *upd3*^{d232a}. Overexpression of *upd3* was achieved utilizing another P-element, P{XP}d04951, inserted upstream of the *upd3* coding sequence (Wright et al. 2011). P{XP}d04951 contains a UAS site, so that it can result in *upd3* overexpression in polar cells in the present of Upd-Gal4. Because Upd-GAL4 can drive the ectopic expression of *upd3* in many other loci besides polar cells during development, to avoid the potential detrimental effect from *upd3* overexpression, a temperature sensitive GAL80 was expressed in flies to suppress the activity of Upd-GAL4 until adulthood, when female flies were switched to higher temperature to turn on ectopic *upd3* expression (McGuire et al. 2003). An extracellular immunohistological staining protocol was followed to detect Upd distribution in egg chambers (Strigini and Cohen 2000, Sexton 2009). Unlike conventional immunostaining, which detects both extracellular and intracellular proteins, the extracellular staining protocol detects only extracellular proteins by incubating tissues with primary antibodies before fixation.

Upd was detected at the apical surface of the follicular epithelium at the two poles. At the anterior, Upd was localized into a very narrow region, making it hard to recognize the pattern of the concentration gradient. The concentration gradient can be more prominently detected at the posterior, starting from stage 5. Stronger staining can be observed in later stage chambers (Figure 3.7), but it coupled with higher background

signals surrounding the oocyte. Stage 7 chambers showed the most consistent staining results and therefore were chosen to compare Upd distribution in different *upd3* backgrounds. Upd showed grossly similar location and gradient pattern in the three backgrounds (Figure 3.8 A). To quantitatively compare Upd distribution, the width of the *upd* distribution in each egg chamber was measured and normalized to the perimeter of the egg chamber using the Image J software. This experiment was performed blindly and repeated three times. The Upd distribution range was consistently narrower in *upd3* mutants (*upd3^{d232a}*) and broader in *upd3* overexpressing flies (Upd-GAL4>Upd3^{d04951}) compared to wild-type flies (*upd3^{x37e}*). In the representative experiment shown in figures 3.8, Upd distribution was quantified in over 10 egg chambers for each genotype and it showed a 14% reduction in *upd3^{d232a}* and a 19% increase in *upd3^{d04951}* in comparison to the distribution in the wild-type *upd3^{x37e}*. Although the difference was not large, it was statistically significant (Figure 3.8 B; $p < 0.05$, two-tailed T-test).

Since Upd distribution was shown to be narrower in *upd3^{d232a}* egg chambers at the posterior end compared to the wild-type control, it was questioned whether cell specification of follicular cells at the posterior termini of egg chambers was affected. There is only one type of follicle cells at the posterior, called posterior cells, the specification of which requires high levels of both JAK and EGFR signaling (Xi et al. 2003). Posterior cells can be identified using a Pnt-lacZ marker, which is expressed strongly in posterior cells, with a graded reduction towards the center of the egg chamber (Roth et al. 1995). *upd3^{d232a}* egg chambers showed narrower staining of the Pnt-lacZ marker compared to wild-type *upd3^{x37e}* egg chambers (Figure 3.9). To quantify the result, 3 to 4 confocal images were taken at the middle sections of each egg chamber, where the diameter of the egg chamber appears to be at its largest. The number of cells showing the expression of Pnt-lacZ was counted and normalized to the total number of follicle cells covering the oocyte. Staining was repeated independently three times, and in total over thirty egg chambers at stage 10 were scored for each genotype. *upd3^{d232a}* showed a 17% reduction in posterior cell population in comparison to the wild-type, and the difference was statistically significant ($p < 0.0001$, two-tailed T-test).

Loss of Upd3 caused stronger impact on Upd distribution than JAK signaling intensity

Both *in vitro* and *in vivo* functional assays suggested that loss of *upd3* might have a mild effect on JAK signaling intensity but alter the activity range of this pathway. This is different from the function of Dpp and Scw heterodimers in embryos but resembles that of Dpp heterodimers with another BMP ligand, Glass bottom boat (Gbb), during *Drosophila* wing development (Shimmi et al. 2005). Both Dpp and Gbb are necessary for posterior crossvein formation. However, Gbb alone, Dpp alone and the two ligands together elicit similar signaling induction *in vitro*, indicating that heterodimerization is not necessary for achieving high signaling intensity during this process. Instead, because no ligand is expressed in the crossvein region and heterodimers of Gbb and Dpp bind more strongly than homodimers to extracellular proteins needed for ligand distribution, Dpp/Gbb heterodimers can be more effectively transported to the crossvein region to stimulate BMP signaling activation. To directly test whether Upd3 has a stronger impact on the signaling activity range than signaling intensity, the composition of anterior follicle cells was compared between wild-type and *upd3*^{d232a} egg chambers (Figure 3.11). If Upd3 has a stronger effect on the overall JAK signaling intensity in egg chambers, when it is lost, the number of border cells, which require the highest amount of JAK signaling activation, will be reduced most significantly compared to other cell types. The number of cells requiring the lowest levels of JAK signaling activity, in this case main body cells, will increase correspondingly. Cells requiring the intermediate levels of JAK signaling activation, stretched cells and centripetal cells, are expected to change slightly or stay the same, depending on the level of signaling reduction. Such changes in anterior follicle cell distribution were observed in *upd* and *hop* mutants. A combination of an *upd* hypomorphic allele, *upd*^{siscG20}, and a null allele, *upd*^{YM55}, produced egg chambers with dramatically reduced border cell numbers from 5 to 2 on average, and the remaining border cells showed migratory defects. However, the numbers of stretched cells and centripetal cells were roughly the same compared to wild-type egg chambers (Xi 2002). A combination of two hypomorphic *hop* alleles, *hop*^{msv} and *hop*^{m4}, causes a further reduction in JAK signaling intensity. In egg chambers of these mutants, the border cell

population was totally lost, and the number of stretched cells was also slightly reduced. The number of centripetal cells stayed the same, while the main body cell number increased significantly (Xi et al. 2003). Alternatively, if Upd3 has a stronger effect on controlling the signaling range than signaling intensity, the change of anterior follicle cell fates in response to the loss of *upd3* will be different. In this model, since the concentration of Upd stays high near the source but decays more rapidly along the diffusion path, the number of border cells should not change significantly, but instead, the number of stretched and centripetal cells would be predicted to decrease. To compensate for the loss of these two cell types, the number of main body cells should increase.

Anterior follicle cells were compared individually between *upd3* mutant (*upd3^{d232a}*) and wild-type using cell specific markers in flies no more than 5 days of age. Border cells were labeled using 5A7 and counted in over 70 egg chambers of each genotype. The average border cell number showed only a slight decrease in *upd3* mutants compared to wild-type, from 5.2 to 5.0, and the difference was not statistically significant (Figure 3.10 A; two-tailed T-test). Dpp-lacZ was used to label both stretched cells and centripetal cells. *dpp* expression in egg chambers can be observed starting from the end of stage 8, but the number of dpp-expressing cells keeps increasing until the end of stage 9 (Twombly et al. 1996). Therefore, the numbers of Dpp-lacZ labeled cells were only counted in stage 10 egg chambers. At this stage, stretched cells and centripetal cells can be distinguished based on cell position and morphology. Compared to wild-type, the numbers of stretched cells and centripetal cells were reduced 17% and 24% respectively in *upd3* mutant egg chambers, and both changes were statistically significant (Figure 3.10 B; $p < 0.0001$, two-tailed T-test). In addition, MA33 is another lacZ enhancer trap line that expresses only in stretched cells. The staining of MA33 revealed consistent results as Dpp-lacZ staining that *upd3* mutant had a 20% reduction in the number of stretched cells compared to wild-type (Figure 3.10 C; $p < 0.0001$ two-tailed T-test). Main body cells were detected by mirr-lacZ. This marker is strongly expressed in main body cells from stage 6 to 8, but from stage 9, its expression is restricted to follicle

cells located at the dorsal anterior region of the oocyte (Jordan et al. 2000). Therefore, only stage 7 and 8 egg chambers were analyzed for the main body cell population in this study. The spread of *mirr-lacZ* positive cells in terms of cell diameters was counted and normalized to total number of cells surrounding the egg chamber. 18 and 22 egg chambers were analyzed in wild-type and *upd3* mutant backgrounds, respectively, and *upd3* mutant egg chambers showed a 12% increase in the main body cell population in comparison to that in wild-type chambers ($p < 0.01$, two-tailed T-test) (Figure 3.10 D).

Upd3 might affect the concentration gradient of JAK signaling through complex mechanisms

The loss of *upd3* narrowed the distribution distance of Upd in egg chambers, and resulted in a steeper slope of the JAK signaling gradient. Since Upd and Upd3 are co-expressed from polar cells and able to form homotypic and heterotypic interactions, Upd3 might facilitate the distribution of Upd through ligand interactions (Figure 3.12 A). Under this assumption, hetero-oligomers of Upd/Upd3 are speculated to have longer distribution distance than homo-oligomers of Upd, analogous to the distribution of BMP ligand dimers. Heterodimers of Dpp/Scw in embryos and heterodimers of Dpp/Gbb in wing discs are transported over a longer distance in comparison to the respective homodimers, mediated by enzymatic reactions between extracellular proteins (O'Connor et al. 2006). Different distribution distances of Upd-family ligand oligomers might also be established by some extracellular proteins, although no such protein has been identified yet. Alternatively, different distribution distances may be established by ECM molecules. Numerous ECM molecules are present in the cell membrane and exhibit diverse functions to regulate signaling transductions (Nybakken and Perrimon 2002). Upd and Upd3 could bind to different ECM molecules in egg chambers and are consequently transported to different distances from polar cells. Or, even if they bind to the same ECM molecule, the difference in their binding affinity to the shared ECM molecule can result in different distribution distances of the two ligands.

However, the observed effect of Upd3 on Upd distribution could also be explained by other mechanisms as well. For example, since both Upd and Upd3 are associated with ECM and activate the pathway through the same receptor, they might compete for binding to the receptor or certain molecules in the ECM. Under this assumption, the loss of *upd3* opens up more binding sites near polar cells to Upd and consequently, the Upd distribution appears to be more restricted in *upd3* mutant egg chambers. On the other hand, overexpressed Upd3 may outcompete Upd for the binding sites close to polar cells and force Upd to diffuse further away from the source (Figure 3.12 B). Alternatively, since Upd-family ligand binding to Dome triggers endocytosis of the ligand/receptor complex (Devergne et al. 2007, Vidal et al. 2010), it is possible that different ligands disassociate from the receptor at different speed in the endosome. If Upd3 disassociates from Dome slower than Upd, overexpression of *upd3* would trap more receptor in the endocytic pathway and result in less receptors at the cell membrane. Consequently, Upd would have to travel further to bind to Dome (Figure 3.12 C). Finally, in a previous study, mosaic clones of *dally* mutants created near polar cells resulted in a sharp decline of Upd concentration at the distal side of the clones relative to the pole (Hayashi et al. 2012). The rapid loss rather than a shallower gradient of Upd suggested that binding to Dally might be crucial for Upd to be stabilized at the cell membrane, and the unbound ligands might be degraded by proteases. Because of the protein similarity between the two ligands, Upd3 is likely to be subjected to the same cleavage reaction as Upd after secretion. Therefore, the presence of Upd3 may protect Upd from being cleaved and stabilize Upd in egg chambers. Under this assumption, the loss of *upd3* would also result in a shorter distribution of Upd (Figure 3.12 D).

To test if other mechanisms besides ligand oligomerization are involved in controlling Upd distribution, ectopic expression of *upd3* was induced outside of polar cells but still in the path of Upd distribution. If ligand interaction is the sole element, or the most important one, to control ligand distribution, the ectopically expressed *upd3* outside polar cells will not affect the distribution of Upd, assuming hetero-oligomers can

only be formed when the two ligands are expressed from the same cell. On the other hand, if other factors are involved to determine the ligand distribution range, since the ectopic expression of *upd3* inside or outside of polar cells has the same effect on these factors, *upd3* expressed from these small clones will further the distribution of Upd. Egg chambers with clones generated at only one side of polar cells were imaged and the Upd intensity profiles of these egg chambers were plotted (Figure 3.12 A''' B'''). From each plot, the Upd distribution distance at the side containing *upd3* expression clones was measured and divided by the Upd distribution distance on the other side of the same egg chamber. In total, 10 egg chambers were analyzed. Seven of them were at stage 8 and three of them were at stage 7. The difference in egg chamber stage did not seem to affect the result. The average ratio of Upd distribution distance was 1.24, and it was not statistically different from 1 ($p=0.1864$, one-sample T-test). However, the ectopic expression of *upd3* showed two opposite effects on Upd distribution in different egg chambers. In half of the egg chambers analyzed, the ectopically expressed *upd3* seemed to destabilize Upd in egg chamber, causing the Upd staining to decline more sharply beyond the clone site compared to the corresponding region on the other side of the egg chamber (Figure 3.12 A-A'''). This result was not anticipated but can be explained by the proposed mechanism involving ligand competition for extracellular binding sites. Since *upd3* was expressed near the end of the Upd gradient, the trace amount of Upd that failed to bind to the ECM might get lost instead of traveling further away to bind as predicted. However, the other five egg chambers showed that the ectopically expressed *upd3* extended the distance of Upd distribution, and two out of the five egg chambers even showed greater than a 2-fold change (Figure 3.12 C). Moreover, the Upd distribution profile of these five egg chambers showed a similar pattern in which Upd intensity kept steady across the *upd3* clones instead of declining as showed at the corresponding region on the other side of the egg chamber (Figure 3.12 B-B'''). This pattern disagreed with the idea of ligand competition, in which Upd intensity at the *upd3* overexpressing sites should be lower. Instead, it argued that the underlying mechanism might be Upd3 protecting Upd from proteolytic cleavage.

Notably, the variations in results could also be introduced by technical reasons. First of all, asymmetric distribution of Upd can also be found in wild-type egg chambers. In addition, the size and the position of the *upd3* overexpression clones cannot be controlled in this experiment but might influence the results. Therefore, enlarging the sample size as well as analyzing the variation of Upd distribution in wild-type chambers may help to draw a clearer conclusion. Based on the 10 egg chambers analyzed, since the ectopic expression of *upd3* led to diverse outcomes of Upd distribution, it suggested that the Upd gradient might be regulated through complex or multiple mechanisms.

Discussion

No strong synergistic effect was detected between Upd and Upd3

In the *in vitro* luciferase assay, expression of *upd* and *upd3* together caused slightly higher signaling intensity than what was expected if the two ligands function independently. Moreover, this weak synergistic effect was only observed when the two ligands were co-expressed instead of separately expressed, consistent with the model that ligand association only occurs within the cell and it is the basis for synergy. However, the synergistic effect between Upd and Upd3 was not as strong as what was observed between Dpp and Scw. Heterodimers of Dpp and Scw elicit 10 fold higher signaling intensity than homodimers as measured by the phosphorylation level of the transcriptional factor, Mad. In contrast, co-expressed Upd and Upd3 caused signaling induction to a similar level as Upd alone. The failure to show a clear synergy between Upd and Upd3 might be caused by several technical limitations of this assay. First of all, the linear induction of reporter activity was only demonstrated up to the level of Upd stimulation. The system could have already been close to saturation upon Upd stimulation and was not able to show further signaling activation by co-expressed Upd and Upd3. To avoid the saturation point, the amount of ligands presented to the reporter cells was lowered by transfecting less ligand expressing plasmids into cells or incorporating less ligand expressing cells in the co-culture. In addition, the duration of the co-culture period was shortened from 3 to 2 days. However, none of these attempts helped to show a clearer synergistic effect between the two ligands. Secondly, in contrast to the purified Dpp/Scw heterodimers used in the other study (Shimmi et al. 2005), the co-expression of Upd and Upd3 presumably resulted in a mixture of both homotypic and heterotypic oligomers. Especially, since both BiFC and yeast two-hybrid assays indicated that Upd3 homotypic interaction is stronger than Upd and Upd3 heterotypic interaction, the mixture of ligands resulted from Upd and Upd3 co-expression was likely to contain more Upd3 homo-oligomers than Upd/Upd3 hetero-oligomers. The presence of homo-oligomers could mask the potential synergistic effect from the hetero-oligomers. Last but not least, high variation was seen in luciferase

signals between technical replicates. Each experimental group contained three replicates, which were made by pipetting co-cultured cells multiple times to re-suspend them and using the same volume of cells from the mixture in the luciferase assay. Variations might be introduced during this process for technical reasons. For example, it is possible that the co-cultured cells were not re-suspended to a completely homogeneous mixture. Even though the luciferase assay suggested that the co-expressed Upd and Upd3 might be able to stimulate slightly higher JAK signaling than individual ligands, no synergistic effect between the two ligands was observed when they were tested for the ability to generate ectopic border cells in the main body cell population in egg chambers. However, a caveat to this experiment is that the EGFR signaling expressed from the posterior of the egg chamber can possibly suppress high levels of JAK signaling activation in main body cells and mask the difference in signaling intensity stimulated by Upd alone or Upd/Upd3 together.

JAK signaling stimulation is controlled by complex regulatory machinery

Signaling cascades are often considered as an on/off switch to control downstream gene expression in diverse biological processes. However, this oversimplified understanding of signaling pathways cannot explain how a simple pathway, such as *Drosophila* JAK signaling, utilizes only a few signaling activators to achieve signaling specificity as well as diversity. Signaling pathways not only need to be controlled at the level of signaling intensity, but also at the levels of the activity range and signaling kinetics. The morphogen capacity of the JAK/STAT pathway in determining anterior follicle cell fates provides an excellent model to separate these aspects of signaling activation and understand their individual impacts on signaling outcomes. The present study argued that Upd3 does not contribute to the regulation of signaling intensity in follicle cells, since loss of *upd3* did not cause a significant change in border cell numbers and the overexpression of *upd* and *upd3* together showed the same effect on border cell specification as the overexpression of *upd* alone. Instead, Upd3 seems to facilitate the distribution of Upd and by changing the activity range, Upd3 can affect the composition of follicle cells. Although the loss of *upd3* caused only mild change on

follicle cell numbers and there was no obvious morphological defect observed in *upd3* mutant egg chambers, this study suggested that the three Upd-family ligands might stimulate signaling activation at different distances. This functional distinction between Upd-family ligands may play a role in the choice of ligands during diverse biological processes. For example, Upd2 is the only ligand in the family not strongly associated with the ECM but more freely diffused in medium in cell culture (Wright et al. 2011). Therefore, it is presumably capable of traveling longer distance in tissues than the other two ligands, and this might be the reason why Upd2 is evolutionarily selected from the Upd-family to be sent from fat body cells to the brain to maintain homeostasis of the organism (Rajan and Perrimon 2012).

Signaling pathways are constantly under complex regulations and the balance between all regulatory elements needs to be re-established when the pathway is utilized in a different biological context. This highly dynamic regulation of signaling pathways is the key to achieving signaling diversity and specificity. The observed function of Upd3 on anterior follicle cell specification in this study represents a snapshot of the total effect from multiple regulatory forces on this particular process. Upd3 may play different functions in signaling regulation during other developmental processes. In many tissues, Upd3 is required to maintain the signaling intensity. For example, under septic injury, hemocyte-specific *upd3* expression is highly elevated, and it triggers JAK signaling activation in fat body cells to express antimicrobial peptides (Agaisse et al. 2003). During this process, the expression of *upd2* was not detected and the defect in *upd* expression did not significantly change the expression level of antimicrobial peptides. Therefore, Upd3 appears to be the main ligand responsible for elevating the signaling intensity during this process. In addition, not only does Upd3 exhibit different functions between tissues, but within the same tissues, its effect on JAK signaling can be altered during fly aging. Only young flies within 5 days of age were analyzed in this study, and Upd3 did not seem to contribute to the signaling intensity. However, several lines of evidence have suggested that Upd3 is necessary for maintaining signaling intensity in egg chambers when flies age (Sexton 2009). First of all, JAK signaling activation is

necessary for stalk and polar cell specification during early oogenesis. Reduction of JAK signaling intensity decreases the number of stalk cells and expands the number of polar cells. Reduction of stalk cells often leads to egg chamber fusion. When analyzed at day 12 and day 18 after eclosion, *upd3* mutants exhibited significantly higher rates of egg chamber fusion compared to wild-type flies, indicating a reduction in JAK signaling intensity. Secondly, the number of border cells was compared between *upd3* mutants and wild-type flies at age 13 and 23 days. At both time points, the numbers of border cells were slightly less in *upd3* mutants than in the wild-type, but this difference is statistically significant. Moreover, from day 13 to day 23, the number of border cells showed an 11% reduction in *upd3* mutants, but only a 3% reduction in the wild-type. The Upd3 function differences between young and old flies might be due to the different signaling potency and protein stabilities between Upd and Upd3 during fly aging. Both the luciferase assay and the ectopic border cell assay in egg chambers suggested that Upd3 has much lower signaling potency than Upd. On the other hand, although no study has been performed to directly compare the abundance of Upd and Upd3 in old flies, there is evidence suggesting that the expression of *upd* does decrease in the fly testis during aging (Boyle et al. 2007, Toledano et al. 2012). If the aging process has a stronger impact on Upd abundance than on Upd3, when there is still sufficient Upd available in younger flies, Upd3 function in stimulating the pathway would be masked by Upd. However, as the fly ages, the amount of Upd might not be enough to achieve the required signaling activation and the presence of Upd3 would become necessary to maintain the signaling intensity, especially given that co-expressed Upd and Upd3 at a ratio that is mostly Upd3 can still stimulate similar signaling intensity as Upd alone. Overall, these studies on Upd3 functions in different developmental processes illustrate that signaling regulation is a highly dynamic process that shows much tissue and developmental stage specificity.

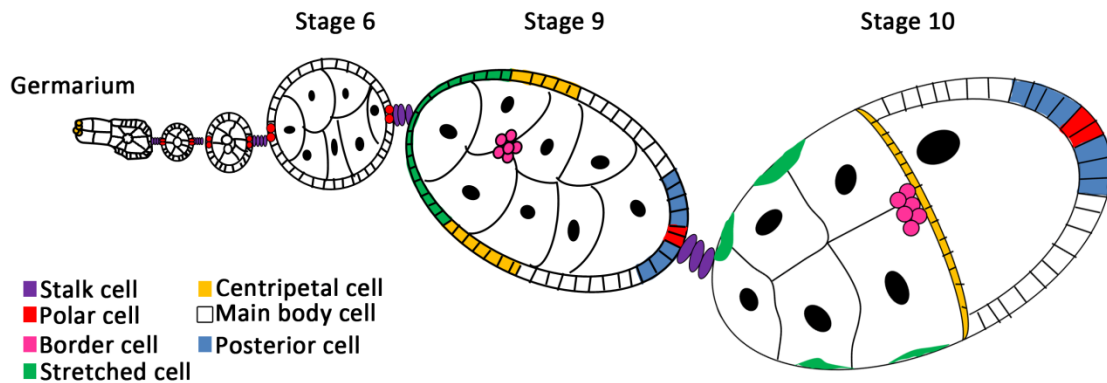


Figure 3.1 A schematic diagram of follicular cell specification during egg chamber development.

Polar cells (red) and stalk cells (purple) are specified early during oogenesis when the 16 cell cyst exits from the germarium. The other follicular epithelial cells start to differentiate from stage 7. Controlled by the level the JAK signaling they receive, the anterior follicular cells are specified into border cells (magenta), stretch cells (green), and centripetal cells (yellow). Cells located to the posterior end of egg chamber are specified into posterior cells (blue). The remaining cells located at the center of egg chambers, receiving lowest JAK signaling, become main body cells (white).

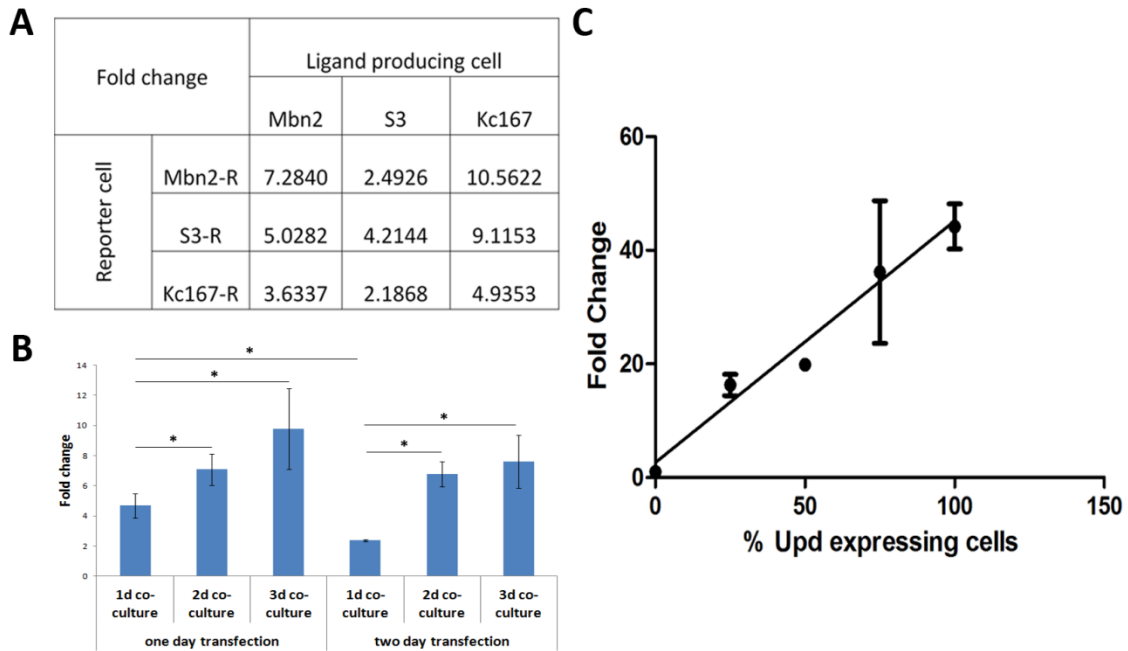


Figure 3.2. Optimization of the luciferase assay. In the paracrine luciferase assay, ligand producing cells expressing Upd were co-cultured with reporter cells expressing 6x2xDrafluc-firefly, a JAK signaling reporter. Ligand producing cells with no exogenous plasmid transfected was co-cultured with the same reporter cells and used as mock. **(A)** *Drosophila* mbn2, S3 and Kc167 cells were tested in combinations to stimulate JAK signaling activation. The fold change of luciferase activity compared to respective mock groups was shown for each combination. The combination with Kc167 as the ligand producing cell and mbn2 as the reporter cell showed the highest JAK signaling induction, and it was used in all other luciferase assays. **(B)** Cells were incubated with plasmids and transfection reagents for one or two days. Then ligand producing cells and reporter cells were co-cultured for one, two or three days before lysed for measuring luminescence. Shorter incubation of cells with the transfection reagent and longer incubation during co-culture was optimal for showing high JAK signaling induction. Error bars, SD; * $p < 0.05$, two-tailed T-test. **(C)** Different fractions of Upd-expressing cells were co-cultured with a constant number of reporter cells. This co-culture system showed JAK signaling induction in a dosage dependent way. Error bars, SEM.

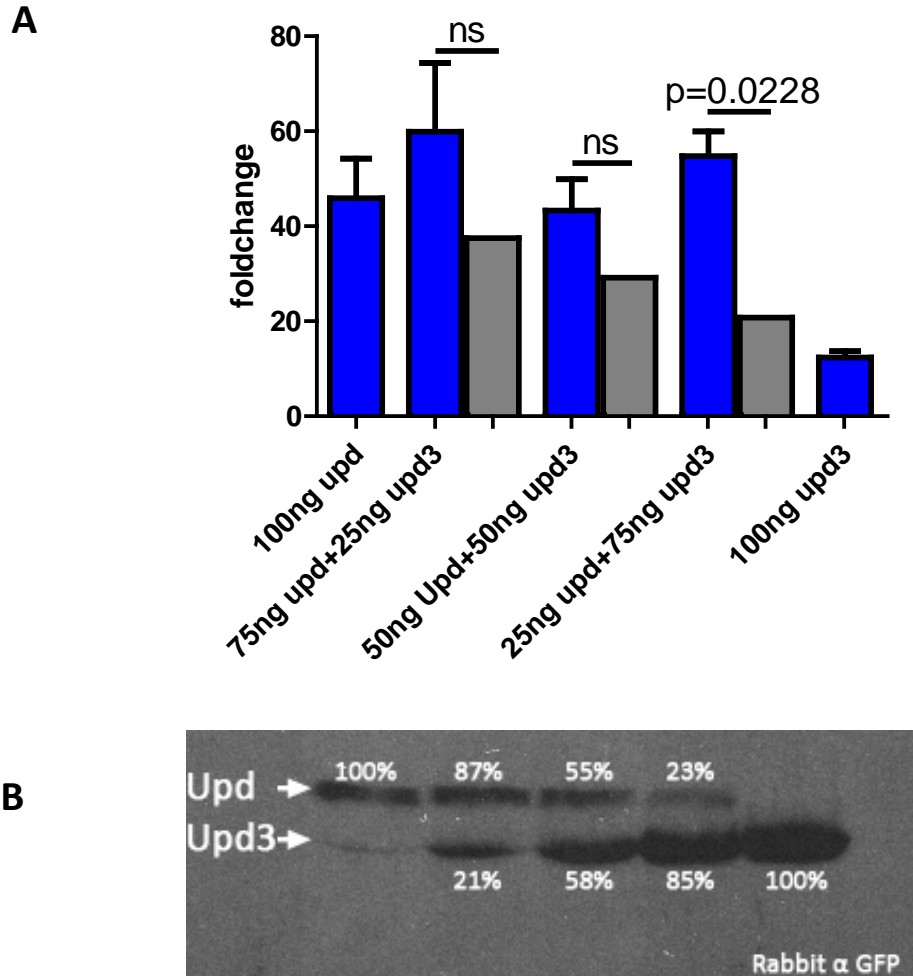


Figure 3.3. JAK signaling activation stimulated by different proportions of Upd and Upd3. A. Cells expressing Upd, Upd3 or combinations of the two ligands in different ratios were used to stimulate JAK signaling activation in a luciferase assay. The amount of the two plasmids used in transfection is indicated for each group. Gray bars represent the anticipated luciferase activities under the assumption that Upd and Upd3 function independently to stimulate the pathway, and Blue bars are the actual observed results. Error bars, SEM; ns= not significant, one sample T-test. **B.** A portion of the co-cultured cells from the luciferase assay was lysed and the protein lysate was subjected to western blot analysis. Protein band intensities were analyzed using the Image Studio Lite software. Protein band intensities of the single ligand expressing groups were normalized to 100%, and the relative protein band intensities of *upd* and *upd3* co-expressed groups were calculated and shown above each band.

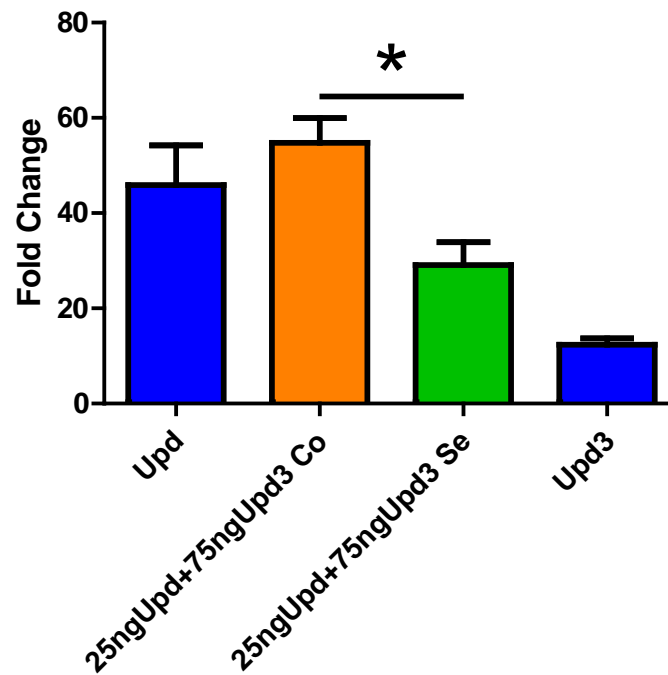


Figure 3.4 Different ligand expression strategies caused distinct JAK signaling activation. Co-expressed (orange) and separately expressed (green) Upd and Upd3 were used to stimulate JAK signaling activation in a luciferase assay. Co-expressed ligands stimulated significantly higher luciferase activity compared to separately expressed ligands. Error bars, SEM; * $p < 0.05$, two-tailed T-test.

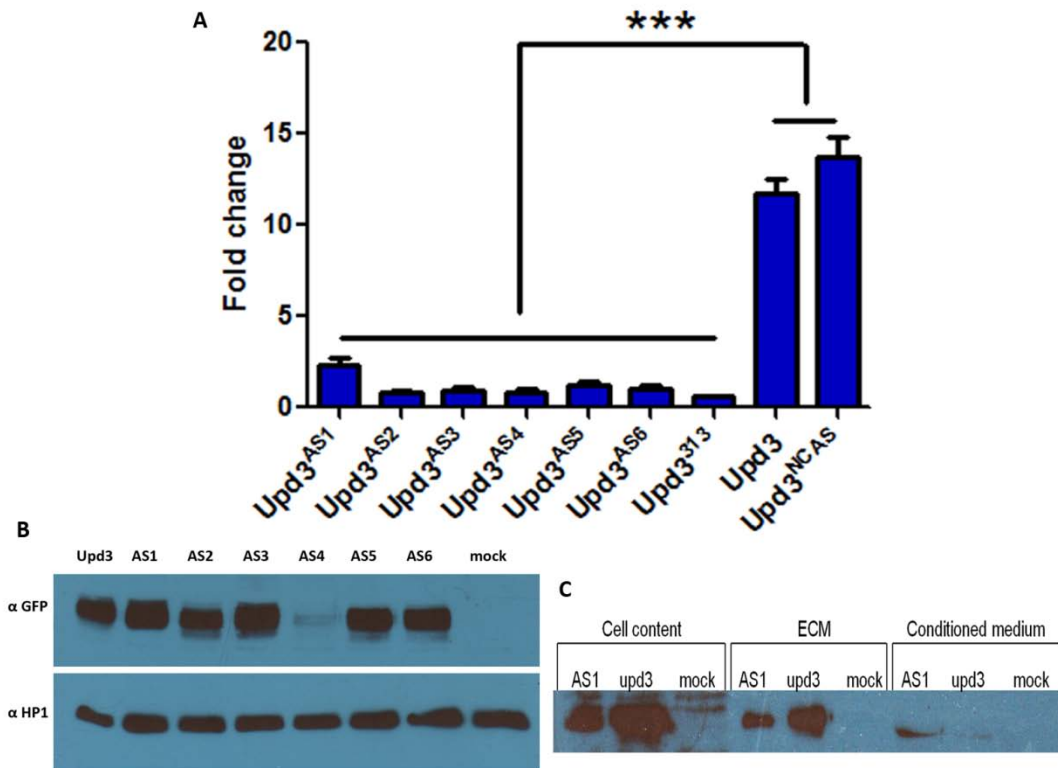


Figure 3.5. Functional domains in Upd3. (A) The ability of Upd3 mutants to stimulate JAK signaling activation was tested in a luciferase assay. All proteins were fused with the CFPC155 tag at the C-terminus. Upd3 domain substitution mutants (Upd3^{AS1-6}) and a big domain swap between Upd and Upd3 (Upd3³¹³) resulted in significantly lower JAK signaling intensity compared to wild-type Upd3. Alanine substitutions made in a non-conserved region (Upd3^{NCA5}) did not affect Upd3 function in JAK signaling activation. Error bars, SEM; $p < 0.0001$, one way ANOVA; *** $p < 0.0001$, t-test with Bonferroni correction. (B) Upd3^{AS1-6}-expressing cells used in the luciferase assay were subjected to immunoblot analysis. Upd3 mutants were detected by rabbit anti-GFP antibodies. HP1 was used as the loading control. Upd3^{AS4} has dramatically reduced protein abundance in cells. All other Upd3 mutants have similar expression levels to wild-type Upd3. (C) Proteins located inside the cell, the extracellular matrix and the conditioned medium were separately extracted from *upd3* and *upd3*^{AS1} expressing cells. Protein accumulation in different cell compartment was compared through immunoblot analysis using rabbit anti-GFP antibodies.

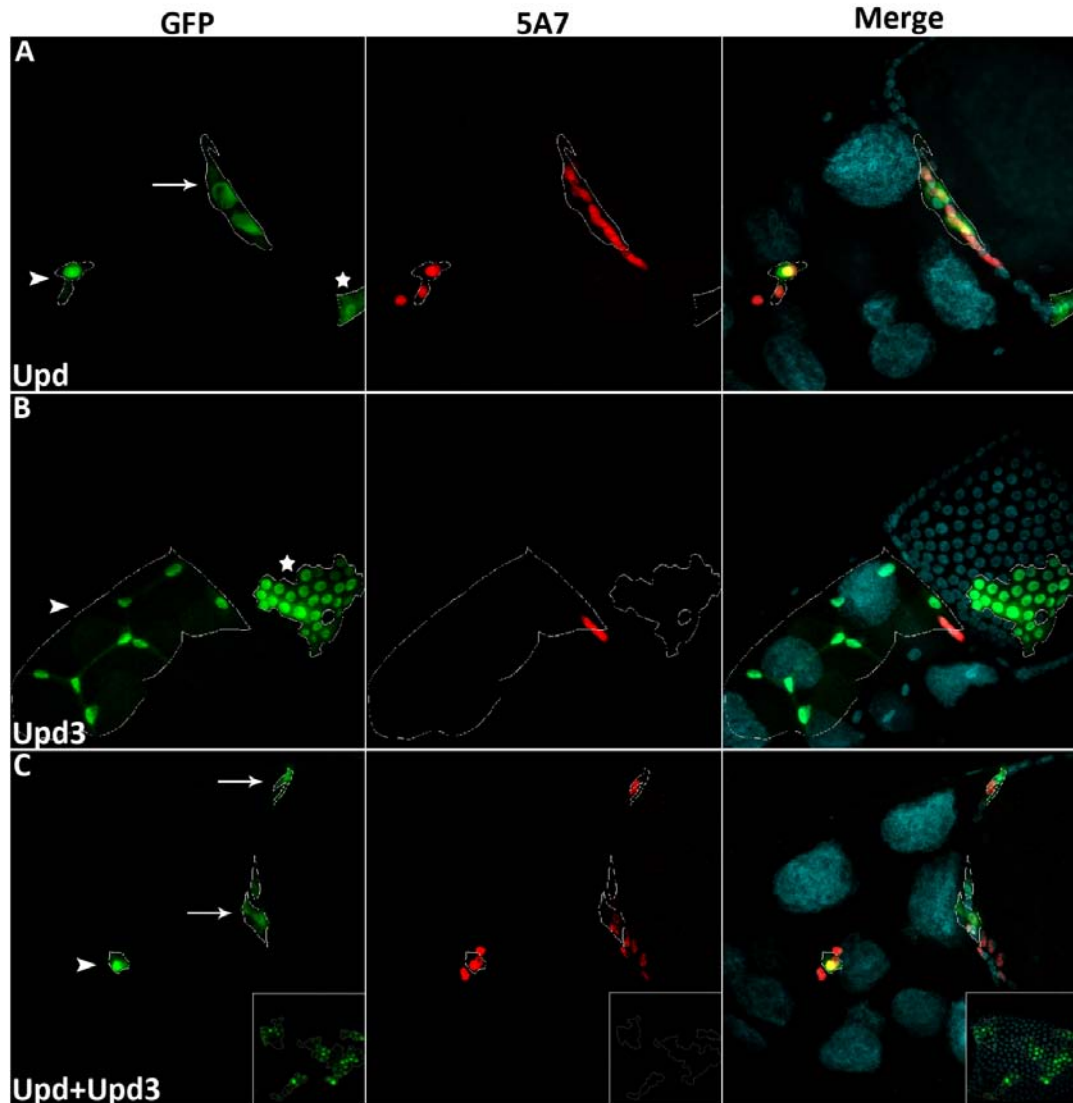


Figure 3.6 Ectopic border cell formation caused by the overexpression of Upd-family ligands. Ectopic expression clones of *upd*, *upd3* or the two ligands together were generated by a flip-out cassette and marked by GFP. Egg chambers at stage 10b were assessed for the formation of ectopic border cells, which were marked by a border cell specific marker, 5A7. Overexpression of *upd3* in any of follicle cells did not cause ectopic border cell formation (B). Overexpression of *upd* (A) or the two ligands together (C) caused ectopic border cell specification in presumptive stretch cells (arrowhead) and centripetal cells (arrow), but not in main body cells (star). Inset shows the clones created in main body cells in the same egg chamber. All egg chambers are oriented with anterior pointed towards the lower left.

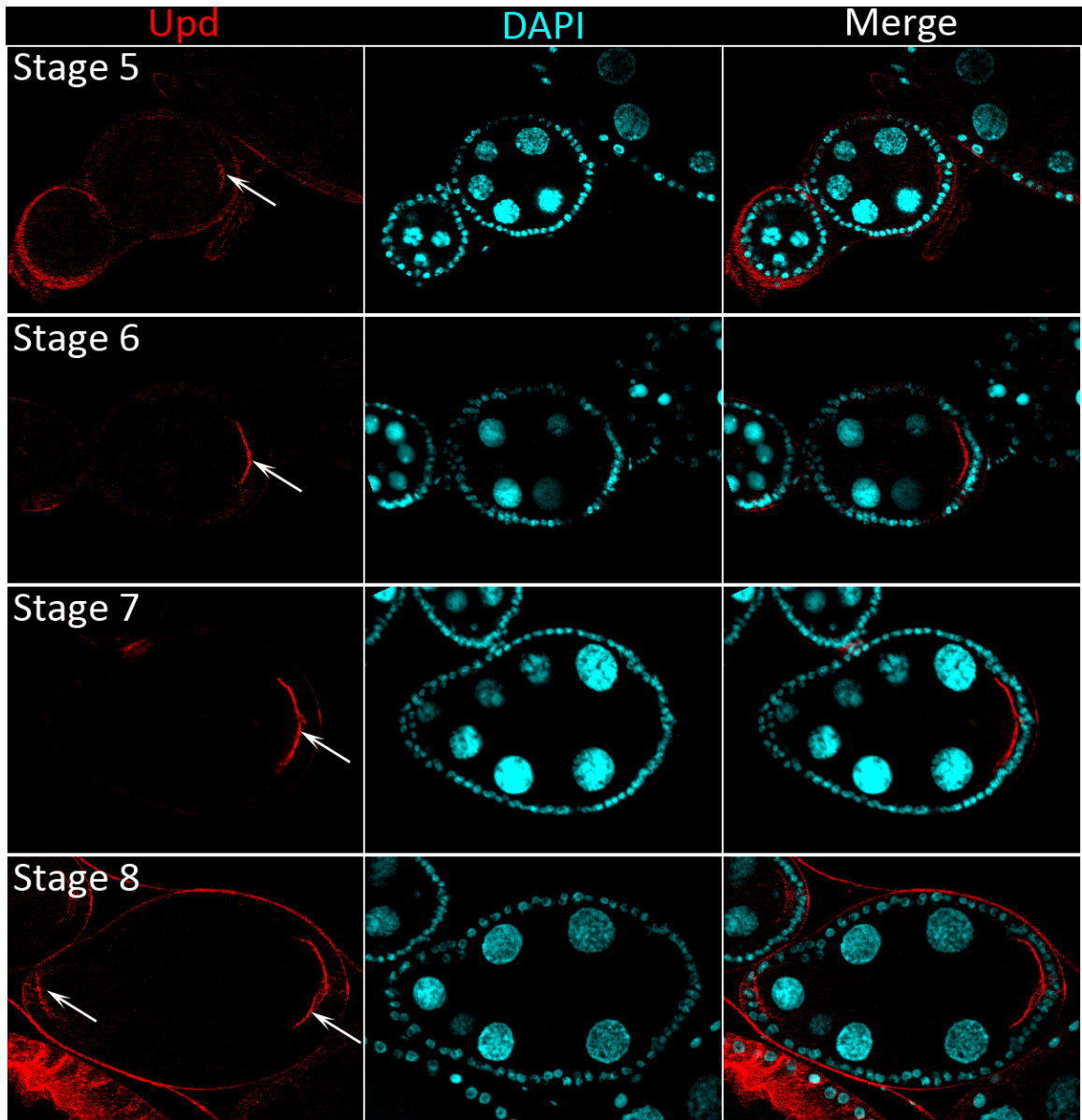


Figure 3.7 Upd localization on different stages of egg chambers. Upd was detected by anti-Upd polyclonal antibodies at the apical surface of follicle cells of egg chambers from stage 5 (shown as red staining, arrow). After stage 8, high background staining starts to show surrounding the oocyte. Upd localization at the anterior of the egg chambers can be rarely detected.

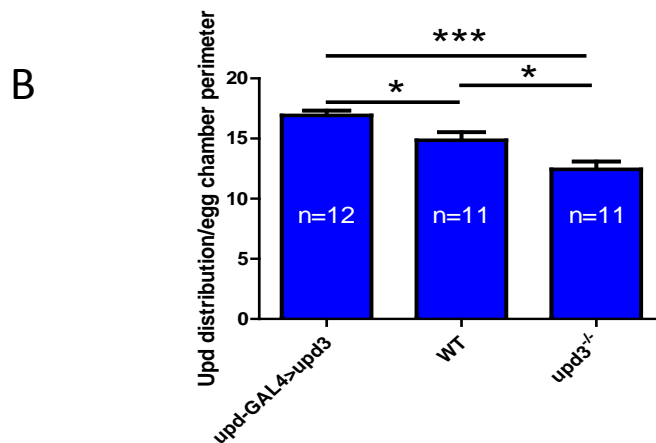
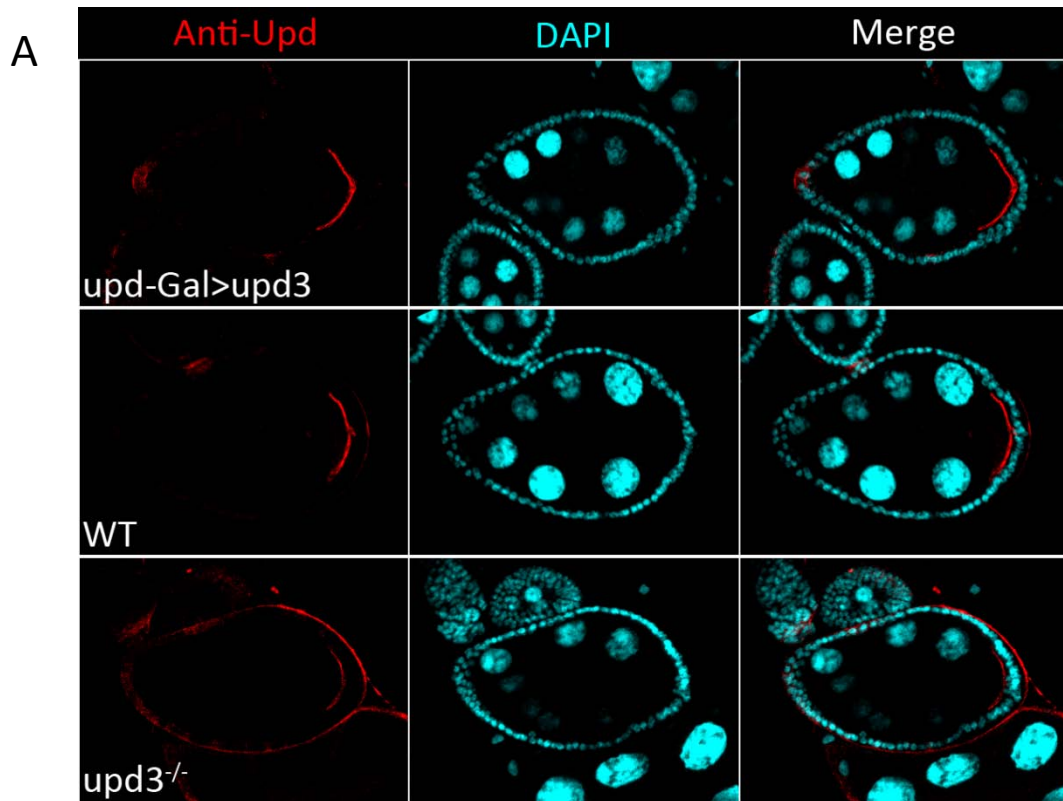


Figure 3.8 Upd3 expression affects Upd distribution in egg chambers. (A) Upd distribution (red staining) at the posterior of egg chambers was compared between *upd3* overexpression, *upd3* null mutant and wild-type egg chambers. **(B)** Compared to the wild-type, Upd showed wider distribution in *upd3* overexpression and narrower distribution in *upd3* mutant egg chambers. Error bars, SEM; $p < 0.0001$, one-way ANOVA; * $p < 0.05$, *** $p < 0.0001$, T-test with Bonferroni correction.

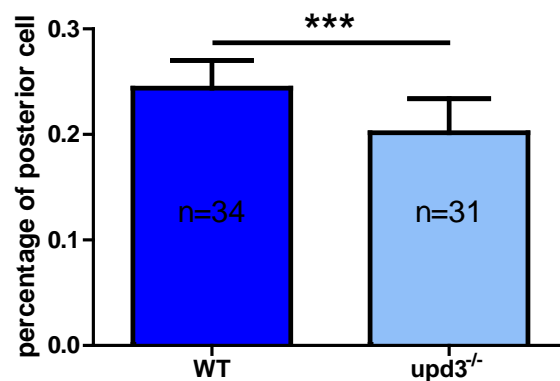
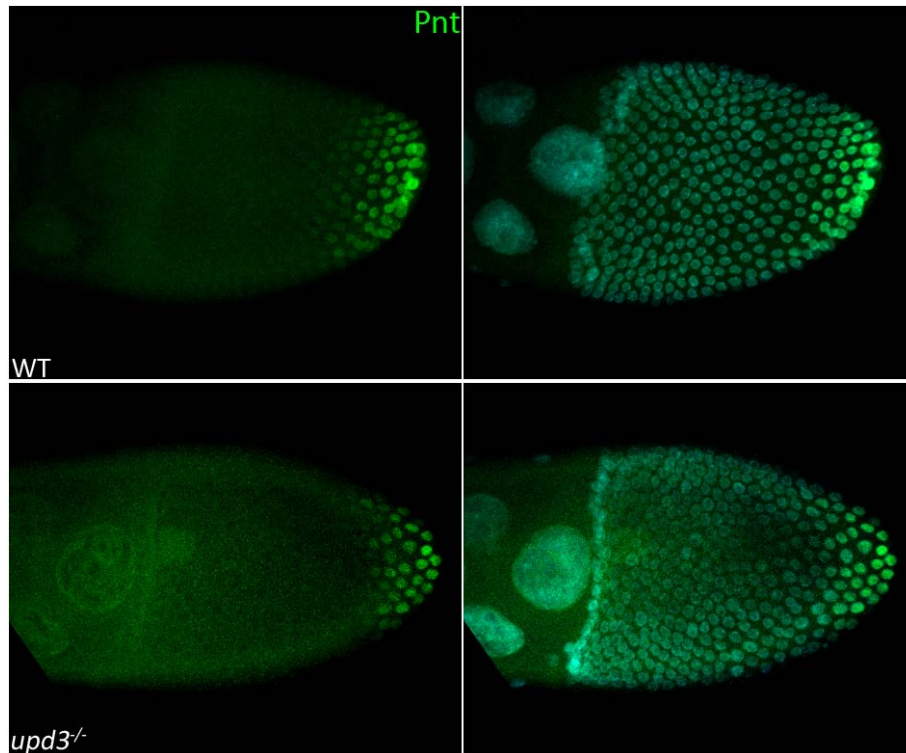


Figure 3.9 Posterior cell population is reduced in *upd3* null mutants. Posterior cells were identified by a Pnt-lacZ marker (green) in both wild-type and *upd3* mutant egg chambers. The range of the posterior cell population was quantified by counting the number of Pnt-lacZ positive cells in the middle confocal section of each egg chamber, where the diameter of egg chambers appears to be at its largest, and normalizing it to the total number of follicle cells surrounding the oocyte in the same confocal section. The Pnt-lacZ marker showed significantly wider distribution in wild-type than *upd3* mutant egg chambers. Error bars, SEM; *** $p < 0.0001$, two tailed T-test.

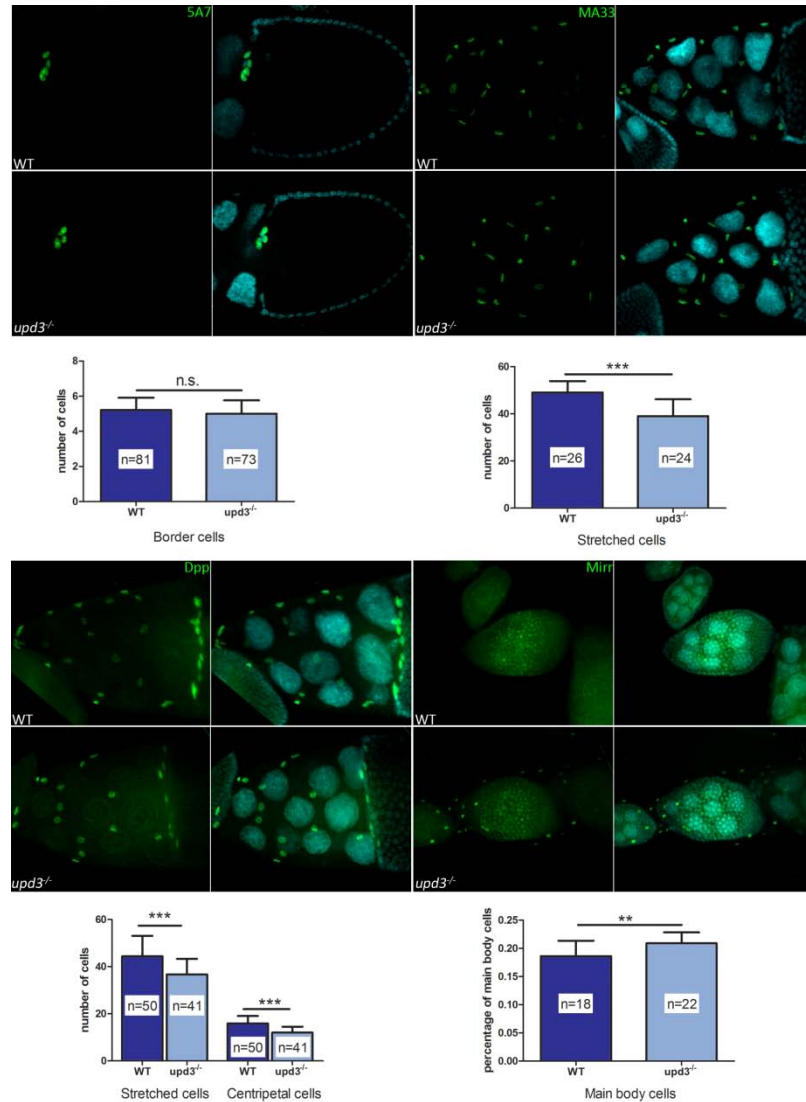


Figure 3.10 Loss of *upd3* changes anterior follicle cell fates. (A) Border cells were identified using a cell specific marker, 5A7. The numbers of border cells were counted in *upd3* mutant and wild-type egg chambers. **(B)** Stretched cells and centripetal cells were marked by *dpp-lacZ*, and they were distinguished based on cell morphology and location. The numbers of these two cell types were compared between wild-type and *upd3* mutants. **(C)** The numbers of stretched cells in wild-type and *upd3* mutants were counted based on a MA33 marker. **(D)** *Mirr-lacZ* marks main body cells. The spread of *mirr-lacZ* marker in terms of cell diameters was normalized to the total number of cells surrounding the egg chamber and compared between wild-type and *upd3* mutants. Error bars, SD; * $p < 0.05$, ** $p < 0.01$, *** $p < 0.0001$, n.s. not significant.

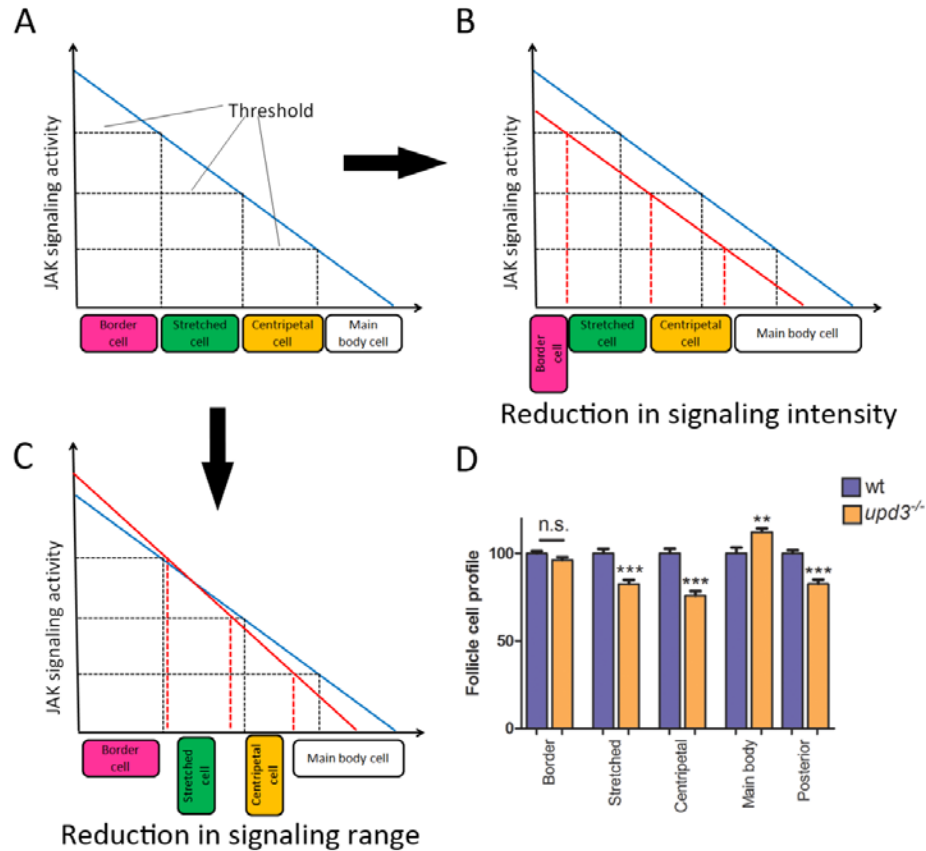


Figure 3.11 Upd3 has a stronger effect on JAK signaling activity range than signaling intensity. **(A)** Anterior follicle cell fates are determined by the JAK signaling gradient (blue line). **(B)** Changing the JAK signaling gradient (red line) to cause reduction in overall signaling intensity in egg chambers should reduce the number of border cells. The number of stretched cells should stay the same or decrease slightly, while the centripetal cell number should stay the same. The main body cell population should expand. **(C)** Reducing the signaling activity range (red line) will cause only slight change in the number of border cells, but reduce the number of stretched cells and centripetal cells. The number of main body cells is expected to increase. **(D)** To summarize the data of follicle cell specification shown individually in the previous figure, the quantification of each cell type in wild-type chambers is normalized to 100% and the relative cell abundance in *upd3* mutants was calculated. The composition change of follicle cells in *upd3* mutants fitted with the idea that the loss of *upd3* altered the activity range of JAK signaling in egg chambers.

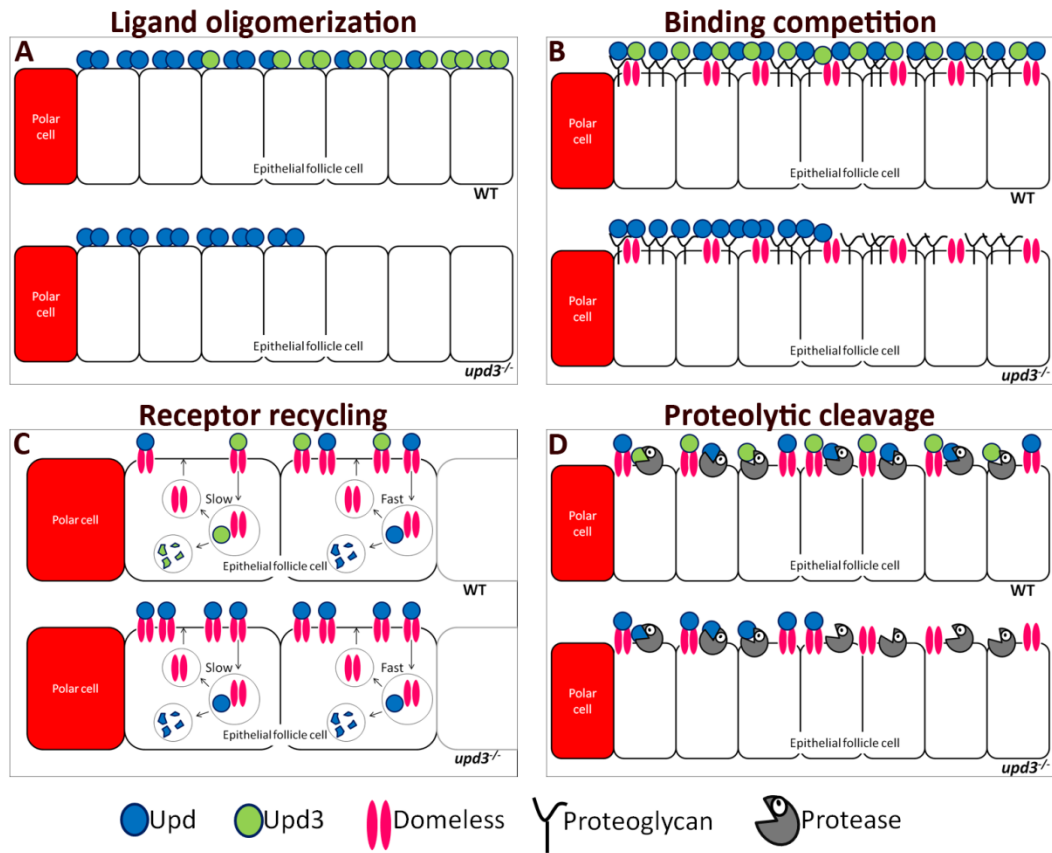


Figure 3.12 Potential mechanisms underlying the Upd3 effect on Upd distribution in egg chambers. (A) Upd3 may facilitate the distribution of Upd through physical interaction. In this model, homo-oligomers of Upd are located closer to polar cells compared to hetero-oligomers between Upd and Upd3. Homo-oligomers of Upd3 might be able to distribute the longest distance. **(B)** Upd3 may compete with Upd for binding to the Dome receptor and proteoglycans in the extracellular matrix. Loss of *upd3* would open more binding sites for Upd near polar cells. **(C)** Upd3 may have a slower disassociation rate from the receptor compared to Upd and thus delay receptor recycling to the membrane. In the absence of Upd3, receptors would be recycled back to the membrane more quickly and bind to more Upd near polar cells. **(D)** Upd3 may buffer the reaction of proteolytic cleavage of Upd on the cell membrane. In the absence of Upd3, more Upd would be processed by proteases, resulting in shorter distribution of Upd.

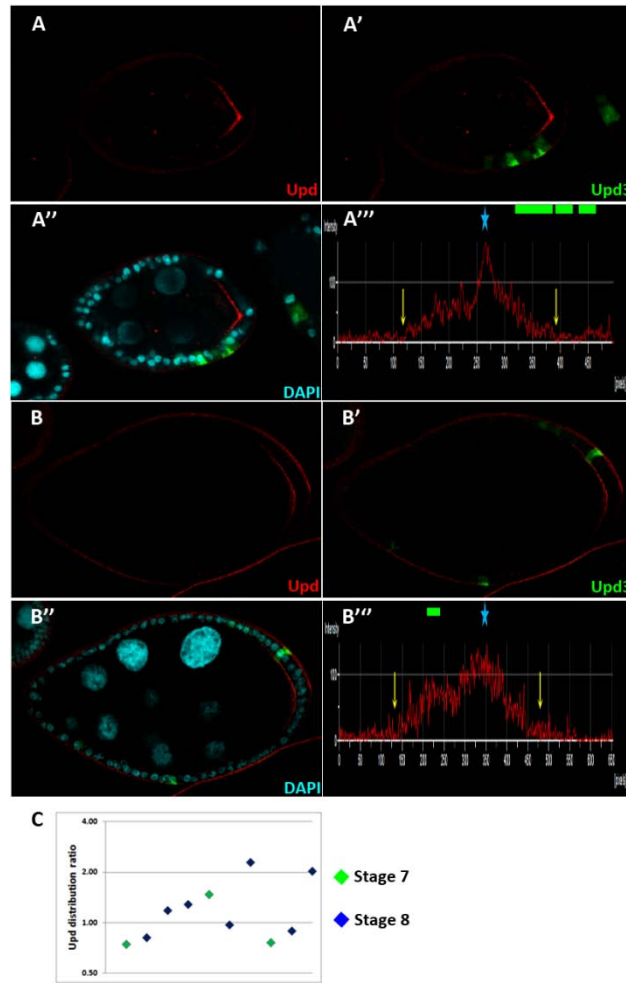


Figure 3.13 *upd3* overexpression outside of polar cells. Ectopic expression of *upd3* was created in mosaic clones, marked by GFP. The endogenous Upd gradient was detected at the posterior of egg chambers using rabbit anti-Upd antibodies (red). The ectopically expressed *upd3* showed different effects on Upd distribution in egg chambers. **(A-A''')** Overexpression of *upd3* shortens the distribution of Upd. **(B-B''')** Overexpression of *upd3* extends the distribution of Upd. **(A''',B''')** The intensity profiles of Upd gradients in egg chambers were shown. Green bars indicate the position of *upd3* overexpression clones. The asterisk marks the position of polar cells. Yellow arrows indicate the ends of Upd distribution. **(C)** Upd distribution distances at both sides of polar cells were measured in 10 egg chambers. The ratio of Upd distribution was calculated as Upd distribution distance over *upd3* overexpression clones divided by Upd distribution distance on the other side of the same egg chamber with no clone.

Chapter 4: Conclusions and Discussion

The overlapping expression patterns and similar functions of Upd-family ligands led to the hypothesis that the three ligands can physically interact with each other. The aim of this project was to examine the possibility of protein interactions between Upd-family ligands and to explore the biological consequences of ligand interactions. The work presented in the thesis reveals the formation of homotypic and heterotypic interactions between Upd-family ligands, with the exception of heterotypic interactions between Upd2 and Upd3. These interactions exhibited different strengths: homotypic interactions of Upd2 and Upd3 were stronger than their respective heterotypic interactions with Upd, and homotypic interactions of Upd might be the weakest. My findings also argue that in egg chambers, Upd3 plays a more important role in controlling the distribution range of JAK signaling than signaling intensity. Furthermore, substituting the conserved domains identified in Upd-family ligands with poly-alanine in Upd3 reduced ligand activity, suggesting the requirement of these domains for Upd3 function.

Interactions between Upd-family ligands are mediated by weak strength

Protein-protein interactions between ligands can be mediated by various covalent and non-covalent bonds. Notably, domains 2 and 5 each contain a highly conserved cysteine residue, which might be involved in the formation of disulfide bonds. These two cysteines are not only conserved within Upd-family ligands but also in all Upd homologs from several other insect species (Loehlin and Werren 2012). Moreover, a couple of amino acids surrounding the two cysteines are also strikingly conserved, suggesting the importance of domains 2 and 5 in Upd-family ligand functions. Disulfide bonds have been shown to mediate protein oligomerization in some cytokines, such as IL-5 (Kusano et al. 2012). However, alanine substitutions within domain 5 caused only minor decreases in the Upd3 homotypic interaction strength and substitutions in domain2 even enhanced the interaction, suggesting that Upd3/Upd3 interaction is not likely to be mediated by disulfide bonds formed between these two cysteine residues.

Instead, intramolecular disulfide bonds might be formed within Upd3 to stabilize the protein structure. In addition, since both the BiFC and the yeast two-hybrid assays indicated that the interaction strength between Upd-family ligands was weak, it is more likely that the interaction is mediated by non-covalent interaction, such as hydrogen bonds, van der Waal interactions, and hydrophobic effects.

The weak interactions between Upd-family ligands, however, might be beneficial to allow ligand oligomerization with different interaction strengths. In the BiFC assay, homotypic interactions of Upd2 and Upd3 were shown to be stronger than their heterotypic interactions with Upd respectively, and the homotypic interaction of Upd was the weakest. Moreover, among all possible interactions involving Upd and Upd3, only the strongest interaction, Upd3/Upd3 interaction, was shown in the yeast two-hybrid assay. The failure to detect other types of interactions between Upd and Upd3 in yeast two-hybrid was likely due to the high stringency of this assay as discussed in chapter 2, but it was an additional indirect indication that interactions between Upd-family ligands were formed at different strengths. The difference in interaction strength between Upd-family ligand oligomers might be involved in the regulation of the JAK signaling pathway in some aspects. For example, the relatively stronger interaction of homo-oligomers of Upd2 and Upd3 might be partially accounted for their low signaling potency compared to Upd, especially given that Upd3^{AS2}, which showed stronger interaction compared to wild-type Upd3 in both BiFC and yeast two-hybrid, had significantly lower signaling potency. The strong ligand interactions within Upd2 and Upd3 homo-oligomers might interfere with the interaction capacity of ligands with receptors by steric hindrance. Or, the strong ligand interaction might affect signaling intensity by interfering with ligand binding to the ECM. Upd is strongly associated with the ECM through Dally, which functions as a co-receptor to stabilize Upd at the cell membrane (Hayashi et al. 2012). Upd2 is not associated with the ECM, and Upd3 was speculated to have a weaker ECM association compared to Upd in cell culture (Wright et al. 2011). The weaker ECM association of Upd2 and Upd3 might be in part attributed to their strong ligand interactions. On the other hand, if ligand oligomerization can affect

ligand affinity to the receptor or the ECM, it can influence not only the signaling intensity but also the signaling distribution range. Ligands with weaker binding strength to the receptor and/or the ECM might be able to diffuse over longer distance in tissues and set up a wider activity range of JAK signaling. Besides signaling intensity and the activity range, different interaction strengths between ligands could possibly play a role in other signaling aspects as well, and therefore, it potentially adds another layer of control to the regulation of the pathway.

Physical interactions between Upd-family proteins expand the reservoir of JAK signaling ligands. Consequently, the more diversified pool of ligands could be utilized by a wider array of environmental cues to elicit JAK signaling more specifically. However, it is not known how much ligand interactions expand the pool of ligands, because ligand interactions can lead to the formation of ligand dimers, oligomers or even higher order multimers. Neither the BiFC nor the yeast two-hybrid assay was able to show the size of these ligand complexes, which can be determined through native western blot analysis or size exclusion chromatography. If Upd-family ligands can form oligomers or multimers, the differences in the size and composition of these protein complexes can further enlarge the diversity of ligands in comparison to dimers, such that the signaling pathway can be responsive to an even wider range of stimuli.

Interactions between Upd-family ligands are likely to happen intracellularly

Ligand interactions can occur either inside or outside the cell in different signaling pathways. In the *Drosophila* BMP signaling pathway, heterodimerization between Dpp and Scw only happens inside cells. Ligands mixed in the conditioned medium cannot form heterodimers, and they consequently lose their synergistic effects in stimulating the BMP pathway (Shimmi et al. 2005). In contrast, oligomerizations of several other ligands occur outside of cells, often mediated by ECM molecules. For example, most mammalian chemokines are basic in nature and bind to glycosaminoglycans in the ECM. This ECM association is critical for concentrating chemokines at the cell membrane and promoting chemokine multimerization, which is a

prerequisite for establishing a chemotaxis gradient to control nearby cell migration (Hoogewerf et al. 1997, Wang et al. 2013). Several observations from the current study implied that Upd-family ligand oligomerization might occur inside cells. First of all, in BiFC assays, fluorescent signals were accumulated into punctate structures inside cells, presumably in Golgi or ER compartments in the secretory pathway. Secondly, co-expressed Upd and Upd3 stimulated significantly higher JAK signaling activity in the luciferase assay compared to separately expressed ligands, also implying interactions between the two ligands might only occur inside cells. However, the Upd3^{AS1} data may suggest otherwise. Upd3^{AS1} showed not only weaker association with the ECM but also reduced Upd3/Upd3 interaction strength in comparison to wild-type Upd3. It is possible that the first conserved domain in Upd3 can affect ligand association with the ECM and ligand interaction separately, or the alanine substitutions of it impaired proper protein folding and caused the reduction in ligand interaction strength indirectly. However, another interpretation of the Upd3^{AS1} data could be that oligomerization of Upd-family ligands occur outside of cells, facilitated by molecules in the ECM. To test whether Upd-family ligand oligomers are exclusively formed inside cells, ligands can be co-expressed or separately expressed from cells, and the conditioned medium collected from these two expression systems can be subjected to a co-immunoprecipitation experiment to detect the formation of ligand oligomers. If Upd-family ligand oligomerization occurs exclusively inside cells, ligand oligomers should only be detected in the conditioned medium of ligand co-expressed cells but not separately expressed cells. If ligand oligomerization of Upd-family ligands occurs in similar locations to some other more extensively studied ligands, such as Dpp/Scw and chemokines, some regulatory mechanisms observed with those ligands may be also applied to Upd-family ligands.

Functional domains of Upd-family ligands

Six conserved domains were identified previously between Upd-family ligands (Wang 2009). In the current study, five alanines were used to substitute amino acids at the cores of the 6 domains in Upd3 and the substitution mutants were subjected to

several functional assays to determine domains critical for ligand association with the ECM, ligand/ligand interaction and signaling activation. Based on the results, all six domains were shown to be essential for JAK signaling activation, but the underlying mechanisms were likely to be different. The first and fourth conserved domains might influence JAK signaling activation by maintaining Upd3 association with the ECM and Upd3 stability, respectively. All the domains, except for domain 4, might be involved in Upd3/Upd3 homotypic interaction, since alanine substitutions of these domains altered the interaction strength between Upd3 proteins. Especially, alanine substitutions of domains 3 and 6 most significantly weakened the Upd3 homotypic interaction. These data seemed to imply that the Upd3/Upd3 interaction interface is constituted by several discrete domains and ligand interaction is essential for JAK signaling activation. However, if this is true, mutation of any of these domains should reduce, but not abolish, Upd3 ability to stimulate the pathway, which is contradictory to what was observed from the luciferase assay. Therefore, some of these domains might not be directly involved in Upd3/Upd3 interaction but control other aspects of ligand functions. For example, as aforementioned, an intramolecular disulfide bond might be formed between the two conserved cysteines residues in domain 2 and domain 5 respectively, and this disulfide bond is presumably important for stabilizing the protein. Alanine substitution made in these two domains would then destabilize the protein and consequently affect Upd3 behavior in several ways, such as ligand interaction and ligand binding to the receptor. The latter effect is more likely to be the direct cause for the reduced signaling intensity. To test if some of the conserved domains mediate ligand binding to the receptor, a BiFC assay can be used. In the BiFC assay, since the N-terminus of Dome is displayed outside of cells to be bound by ligands, the truncated fluorescent protein tags will need to be inserted between the signal peptide and the transmembrane domain of Dome. The ligand/receptor interactions can be tested by incubating the Dome expressing cells with culture medium condition by Upd3 or its domain substitution mutants. BiFC signals in this proposed experiment should be localized at the cell membrane. Alternatively, the ligand/receptor interaction can also be tested using co-immunoprecipitation. Besides

the binding capacity to Dome, if alanine substitutions made in domains 2 and 5 impair protein stability, they might also influence ligand interactions with other proteins, such as chaperone proteins and protein modification enzymes, all of which can be critical for signaling activation. Therefore, the six conserved domains might be essential for Upd3 activity because of their importance in other aspects of Upd3 behaviors than the few examined in this study.

Because the six domains studied in Upd3 are conserved within the Upd-family, some of the corresponding domains in Upd and Upd2 might play similar roles. For example, the fourth conserved domain could also be essential for maintaining protein abundance of the other two ligands. On the other hand, it is possible that the small variations of amino acid composition in the conserved domains might account for the differences in ligand function. For example, the first conserved domains of all three proteins are composed of stretches of basic amino acids, enriched with arginines. The first domains in both Upd (Dustin Perry, personal communication) and Upd3 (shown here) mediate ligand association with the ECM. A similar stretch of amino acids at the N-terminus of Dpp, composing high percentage of arginines, is also responsible for Dpp association with the ECM (Akiyama et al. 2008). However, the corresponding conserved domain in Upd2 does not cause the ligand to be localized to the ECM. Instead, Upd2 is more freely diffused in the conditioned medium in cell culture (Hombría et al. 2005). The first domain in Upd2 is not short of arginines compared to the other two ligands, but a couple of other amino acids in this region might be responsible for the weak ligand association with the ECM. For example, there is a glutamic acid residue close to this domain, which introduces a negative charge to this region. In addition, there is also a threonine residue that could get phosphorylated to introduce a negative charge. Moreover, the phosphorylation of this threonine residue might be controlled and thus provides a mechanism to regulate ligand interactions with the ECM depending on tissue or developmental signals. On the other hand, amino acid variations between the three ligands in the domains that are involved in Upd3 homotypic interaction might account for the difference in interaction strengths between ligand oligomers.

Lastly, the six domains likely cover the regions that are responsible for common features of the three Upd-family ligands, such as protein secretion and receptor binding. Amino acid domains important for functional differences between the three ligands might be located outside of the six domains. For example, additional interaction domains might be present in Upd2 and Upd3 to stabilize ligand interactions and the absence of such domains in Upd could help to establish the difference in ligand interaction strengths.

Upd3 facilitates the establishment of the Upd concentration gradient in egg chambers

In comparison to Upd alone, Upd and Upd3 together did not stimulate significantly higher JAK signaling activity in either the *in vitro* luciferase assay or in follicular cell fate specification in egg chambers. However, the diffusion distance of Upd in egg chambers was shown to be narrower in *upd3* null mutants and wider in *upd3* overexpressing flies compared to wild-type. Consistent with the shorter distribution of Upd, loss of *upd3* caused reduction in the size of the posterior cell population at the posterior of egg chambers, and at the anterior, caused significant decrease in the numbers of stretched and centripetal cells but not border cells. Collectively, these data suggest that Upd3 seems to function primarily to regulate the range of JAK signaling activity more than signaling intensity in egg chambers.

Ligand oligomerization of Upd and Upd3 is a potential mechanism underlying the Upd3 effect on Upd distribution. However, there are several other possible mechanisms that would cause a similar effect, as discussed in chapter 3. For example, Upd and Upd3 might compete for binding to the ECM, and in this scenario, the loss of *upd3* would leave more binding sites available for Upd and also result in a shorter distribution of Upd. To test this potential mechanism, flies expressing *upd3*^{AS1} from polar cells can be utilized. Since Upd3^{AS1} showed compromised binding capacity to the ECM in comparison to wild-type Upd3 (Figure 3.5 C), it should not be able to compete as effectively as wild-type Upd3 over Upd for binding to the ECM and therefore, the overexpression of *upd3*^{AS1} should result in a shorter Upd distribution than that caused

by the overexpression of wild-type Upd3. On the other hand, if binding competition to the ECM is not a major mechanism but ligand oligomerization is, the overexpression of *upd3^{AS1}* may cause Upd to diffuse even further than wild-type Upd3 does. However, this experiment also faces several potential challenges. First of all, the alanine substitution of a few amino acids at the core of the first domain did not completely eliminate Upd3 association with the ECM. There was still a significant amount of Upd3^{AS1} bound to the ECM shown in figure 3.5 C and the weak interaction with the ECM could potentially diminish the difference between Upd3^{AS1} and wild-type Upd3 in affecting Upd distribution. Additionally, Upd3^{AS1} showed reduced Upd3/Upd3 interaction strength compared to wild-type Upd3. It does not necessarily indicate that Upd3^{AS1} has impaired interaction with Upd, but if it does, the two mechanisms might be hard to distinguish using Upd3^{AS1}.

Upd distribution in egg chambers is worth extensive study because it functions as a morphogen, a pivotal molecule in development to provide positional information to cells and instruct cell specification based on its concentration. Several secreted proteins have been identified as morphogen molecules, and the shape of each morphogen gradient is under an array of regulations to ensure the signaling sensitivity and robustness. Some of the regulatory mechanisms are shared between pathways, but many of them are unique to particular morphogens. On the other hand, the same morphogen gradient may utilize different regulatory mechanisms in different developmental processes to accommodate the respective constraints in each tissue. For example, the first validated secreted morphogen, Dpp, is capable of generating long-range morphogen gradients in both embryogenesis and wing disc development, but through different mechanisms. During embryogenesis, *dpp* mRNA is evenly expressed in a broad domain of the embryonic ectoderm, but the protein distribution is restricted into a graded pattern with the highest concentration shown at the dorsal most region of the embryo (Wang and Ferguson 2005). In wing discs, the expression of *dpp* mRNA is rather limited to a stripe at the anterior-posterior compartment boundary and the protein is distributed to a larger region to establish concentration gradients towards

both the anterior and posterior of the wing disc (Entchev et al. 2000, Teleman and Cohen 2000). Moreover, in some other tissues, the distribution of Dpp is restricted to a very limited distance. Such short-range Dpp distribution is observed in egg chambers where Dpp is secreted from cap cells, the somatic niche of stem cells, to the adjacent germline stem cells to maintain the stem cell identity (Xie and Spradling 2000). The short distribution distance of Dpp is required to control the balance between the number of stem cells and the number of differentiated cystoblasts in egg chambers. To ensure proper establishment of Dpp gradients in these different tissues, diverse regulatory mechanisms are utilized, including proprotein cleavage (Sopory et al. 2010), enzymatic reactions between extracellular modulators (Shimmi et al. 2005), ECM facilitation (Akiyama et al. 2008), and many more. One mechanism used repetitively during development by the BMP pathway is ligand oligomerization. As described in chapter 1 and chapter 3, Dpp forms heterodimers with Scw (Shimmi et al. 2005) and Gbb (Shimmi et al. 2005) respectively during embryogenesis and larval posterior crossvein development. Heterodimers of Dpp/Scw and Dpp/Gbb can be transported over longer distance compared to homodimers in both tissues by extracellular modulators. However, strong synergistic effect was observed between Dpp and Scw but not between Dpp and Gbb.

Ligand oligomerization might also be a mechanism to regulate the morphogen gradient of the JAK/STAT signaling pathway in egg chambers, with a stronger impact on the signaling range than signaling intensity, but the underlying mechanism is not known. A similar example of ligand oligomerization controlling signaling activity range has been reported for the Hedgehog pathway in both *Drosophila* (Vyas et al. 2008) and vertebrates (Zeng et al. 2001). Hh protein acts in both short range and long range to elicit responses of the pathway. Hh mutants with impaired ability in multimerization maintain signaling activity in short range, but fail to stimulate the pathway over long distances (Chen et al. 2004). Hh proteins have two covalently linked lipid moieties: a palmitate moiety at the N-terminus and a cholesterol moiety at the C-terminus, which are essential for the protein multimerization as well as signaling activation. Some

studies suggest that the lipid modifications are hidden inside Hh multimers but exposed on the surface of monomers, anchoring Hh monomers to the cell membrane. There are other studies suggesting that Hh multimerization is a requisite for its binding to HSPGs, which incorporate Hh into a lipoprotein complex and enhance its mobility (Panakova et al. 2005). Although there are still controversies on the regulatory mechanisms of Hh distribution, studies of this pathway provide valuable insights into how ligand oligomerization could influence morphogen distribution. Upd-family ligands might follow similar strategies or adopt completely different ones to regulate the JAK signaling range. First of all, Upd-family ligands might achieve better solubility and mobility as oligomers compared to monomers. Although, there has been no lipid modification reported on any of the Upd-family ligands, a predicted palmitoylation site in Upd2 is suggested by the CSS-Palm server (Ren et al. 2008). This palmitoylate, if it exists, might be essential for the homotypic oligomerization of Upd2 and the high mobility of this ligand compared to the other family members. Secondly, similar to Upd, Upd3 distribution is also likely to be influenced by HSPGs and different binding affinities of Upd and Upd3 to the ECM might be the key to the different distribution distances of oligomers. Finally, it is also possible that certain Upd and Upd3 oligomers can be selectively transported by some extracellular proteins, similar to the localization strategy used by the BMP signaling pathway.

Protein oligomerization has been observed between many mammalian cytokines as well, such as the aforementioned chemokines (Wang et al. 2013) and IL-3 family cytokines: IL-3 (Dey et al. 2009), IL-5 (Kusano et al. 2012) and GM-CSF (Hansen et al. 2008). Disruption of protein oligomerization affects the function of some of these cytokines. For example, disrupting IL-5 dimerization by mutating the critical cysteines needed for disulfide bonds can totally abolish IL-5 signaling activity (Milburn et al. 1993, Kusano et al. 2012). However, the detailed mechanism of how cytokine oligomerization is involved in the signaling regulation is not clear. Although there has been no report indicating that these mammalian cytokines function as morphogens, like Upd-family ligands, they are capable of stimulating JAK signaling in autocrine, paracrine and

endocrine manners. Therefore, ligand oligomerization might be also a strategy utilized by mammalian cytokines to regulate their migration distance and activity range.

Chapter 5: Materials and Methods

Cell culture maintenance

Kc167, S3 and ML-DmD32 cells were purchased from the Drosophila Genomic Resource Center (DGRC). Mbn2 cells are a generous gift from Dr. Subba Palli. Sf9 cells are a generous gift from Dr. Grace Jones. Kc167, mbn2 and S3 cells were maintained in Schneider's medium (made from powder or Gibco liquid Schneider's medium) supplemented with 10% FBS (Gibco). Clone 8 cells were maintained in Schneider's medium supplemented with 10% FBS and 2.5% fly extract (Cherbas 2012). ML-DmD32 cells were maintained in M3+BPYE medium (Cherbas 2008) supplemented with 10% FBS and 10ug/ml insulin. Sf9 cells were grown in Sf-900 II SFM medium (Gibco) with no FBS added. All cells were maintained at 28°C.

Bimolecular Fluorescence Complementation (BiFC)

Cell transfection was performed in Kc167 cells, following the Effectene manual (Qiagen). Cells were loaded into a 24-well plate one day before transfection at the concentration of 600,000 cells/ml and they reached about 50%-70% confluency on the day of transfection. Before incubated with transfection reagents, cells were washed one and sit in 350 µl fresh medium in each well. To compose the transfection complex, 100 ng *armadillo-Gal4* (a generous gift from Dr. Joseph Duffy), 100 ng VenusN173 tagged plasmid, 100 ng CFPC155 tagged plasmid and 35 ng *pacpal-cherry* were mixed with 2.68 µl enhancer in 60 µl buffer EC and the mixture was incubated at room temperature for 5 minutes. After incubation, 5 µl Effectene was added into the mixture and incubated for another 10 minutes to allow the transfection complex to form. Then the transfection complexes were mixed with 350 µl fresh medium and applied to cells. Two days after transfection, monensin was added directly to cells to a final concentration of 20 nM to block exocytosis. Cells were resuspended by pipetting and transferred into a chamber slide. Cells were seated in the chamber slide for 30 minutes to 1 hour before microscopic observation. To analyze the results of BiFC, the number of cherry positive cells and the number of total cells were counted by the Image J program (Schneider et al.

2012). To count the number of BiFC positive cells, a threshold of green fluorescence intensity was set by Image J and the number of cells having signals above the threshold was counted manually.

Yeast two-hybrid assay

Upd Δ SS was amplified from pENTR-Upd using a primer pair: UpdTr-attB-F (GGGGACAAGTTTGTACAAAAAAGCAGGCT TGC GCAGCACCACCAGCAGCG) and UpdTr-attB-R (GGGGACCACTTTGTACAAGAAAGCTGGGTTACAGTGCCTGCACGCGCTT). Upd3 Δ SS was amplified from pENTR-Upd3 using a primer pair: Upd3Tr-attB-F (GGGGACAAGTTTGTACAAAAAAGCAGGCT TGGGTTGTGGCGTCTCAGCGGC) and Upd3Tr-attB-R (GGGGACCACTTTGTACAAGAAAGCTGGGTTACAGAGTTTCTTCTGGATCGCCTTTGGC). Upd Δ SS, Upd3 Δ SS and the full length Upd3 coding sequences were constructed into GAL4 activation domain containing vector pACT-GW and GAL4 DNA binding domain containing pAS2-GW (Nakayama et al. 2002) through Gateway cloning (Invitrogen). pACT-GW and pAS2-GW vectors are generous gifts from Dr. Susan Baserga. Plasmids were transformed into yeast PJ69-4A host cells and successful transformants were selected by tryptophan/leucine double selective plates. The interaction strength was scored by colony size at 30°C on –adenine, –histidine, and –histidine plus 5mM 3-aminotriazole plates.

Upd3 alanine substitution constructs

The Upd3 coding sequence was amplified from the pACT-Upd3 construct (a generous gift from Dr. Martin Zeidler) and inserted into pENTR vector through Gateway cloning. Alanine substitution was made in pENTR-Upd3 construct via InFusion cloning technology (clontech). Primers used are:

U3-XcmI-5F: CGGCCAGAACCAGGAATCCAGTG

U3-Del1-F: GCCGCTGCTGCAGCTGCGGCCAACTTCCGGCTGAC

U3-Del1-R: AGCTGCAGCAGCGGCTAGGTGCTTCAGGGGATTGGTG

U3-Del2-F: GCCGCTGCTGCAGCTATCTGAAGCCCACGGGTCTG

U3-Del2-R: AGCTGCAGCAGCGGCGTCCAGATGCGTACTGCTGGC

U3-Bam-5F: GCAAGAAACGCCAAAGGATCCTGC

U3-Del3-F: GCCGCTGCTGCAGCTCGTCTGAATCTCACTAGCAAACAG

U3-Del3-R: AGCTGCAGCAGCGGCGTTTCCCTTATAGAATCGCCACTTG

U3-Del4-F: GCCGCTGCTGCAGCTGGCGCCTTCACGTACATGC

U3-Del4-R: AGCTGCAGCAGCGGCGTCGCGATGGGCGTGCC

U3-BstEII-3R: GCGGCAGTATCTTGTAGGTGAC

U3-Del5-F: GCCGCTGCTGCAGCTGAGGAGGCC

U3-Del5-R: AGCTGCAGCAGCGGCCTCGCGGGCGGACTTCC

U3-Del6-F: GCCGCTGCTGCAGCTAAGAGTATCCGCAAGATACTCGC

U3-Del6-R: AGCTGCAGCAGCGGCCTTCAGTTTGGTGAAGAGGGCG

U3-PmlI-3R: CTTCTGGATCGCCTTTGGCACG

PCR reactions were performed using Phusion DNA polymerase (NEB). PCR products were examined on an agarose gel and then treated with Cloning Enhancer for 15 minutes at 37°C, followed by inactivation of the Cloning Enhancer for another 15 minutes at 80°C. Then the InFusion cloning reaction was set up following the manual. Upd3 substitution mutants in the pENTR vector were subcloned into expression vectors UAS-DEST-VenusN173 and UAS-DEST-CFPC155 through Gateway cloning.

Upd3 substitutions tested in the yeast two-hybrid assay have the signal peptide removed using Upd3Tr-attB-F and Upd3Tr-attB-R primers. The PCR products were cloned into the pAS2-GW vector through Gateway cloning.

Luciferase Assay

Luciferase constructs: 6x2xDrafLuc (Muller et al. 2005) and actin-renilla are generous gifts from Dr. Martin Zeidler.

Linear signaling induction upon Upd stimulation

Mbn2 cells and Kc167 cells were seeded in a 12-well plate one day before transfection. Mbn2 cells were transfected with 240 ng 6x2xDrafLuc, 240 ng CaspeR4 (Thummel and Pirrotta 1991) and 12 ng actin-renilla. Kc167 cells were transfected with 150 ng arm-GAL4 and 150 ng UAS-upd. One day after transfection, cells were washed once and resuspended in fresh medium. Cell concentration was measured using hemocytometer. Transfected Kc167 cells were mixed with untransfected Kc167 cells to create cell mixtures containing 0%, 25%, 50%, 75% and 100% of transfected Kc167 cells. 500 μ l mbn2 cells at the concentration of 625,000 cells/ml were combined with 500 μ l mixed Kc167 cells at the concentration of 827,500 cells/ml and grown in a 24-well plate. Cells were co-cultured for two days. 45 μ l co-cultured cells were subjected to the luciferase assay. The luciferase assay was performed following the Dual-luciferase reporter assay manual (Promega).

Paracrine luciferase assay

Mbn2 cells were seeded in 12-well plates at 800,000 cells/ml and Kc167 cells were seeded in 24-well plates at 600,000 cells/ml on the day before transfection. mbn2 cells were transfected with 240 ng 6x2xDrafLuc, 240 ng CaspeR4 and 12 ng actin-renilla. Kc167 cells were transfected with 100ng of ligand expressing constructs and 100ng of armadillo-GAL4. One day after transfection, 500 μ l mbn2 cells at the concentration of 800,000 cells/ml and 300 μ l Kc167 cells at the concentration of 750,000 cells/ml were combined and seeded in 12-well plates. Cells were co-cultured for 3 days. 45 μ l cells were subjected to luciferase measurement. The rest cells were lysed in RIPA buffer (Harrison et al. 1998) and protein concentration was measured by BCA assay. Then cell lysate containing same amount of total proteins was used for western blot analysis. In

western blot, rabbit anti-GFP primary antibody (Torrey pines biolabs) was used at 1:5000 and HRP anti-rabbit secondary antibody (Santa cruz biotechnology) was used at 1:10000. Protein bands were detected by SuperSignal West Pico Chemiluminescent Substrate Kit (Thermo Scientific), and the intensity was quantified using the Image Studio Lite Ver3.1 software (LI-COR Biosciences).

Cellular fractionation

Kc167 cells were grown in 12-well plates or 35mm cell culture dishes and transfected with 150 ng UAS-upd3CFPC155 (wild-type or alanine substitutions) and 150 ng arm-GAL4. One day after transfection, cells were washed and grown in plain Schneider's medium (without FBS) for 24 hours. Conditioned medium was centrifuged at full speed to get rid of floating cells and the supernatant was incubated with 1% volume of 2mg/ml sodium deoxycholate on ice for 30 minutes. Then 10% volume of 100% Trichloroacetic acid was added to the mixture and incubated for another 30 minutes to precipitate proteins. Protein pellets were washed three times with 80% acetone before dissolved in hot laemmli buffer (Laemmli 1970). To extract proteins inside cells, cells were washed twice with PBS and lysed in 50 μ l ice-cold RIPA buffer for 10 minutes. Protein concentration was measured using a BCA assay. To extract proteins from the extracellular matrix, the plate was washed once with 2M urea and three times with PBS before scraped in 90°C laemmli buffer. Western blot was performed in the same way as in the luciferase assay.

Fly strains and markers

Flies were raised at 25 °C unless otherwise stated. *upd3*^{d04951} has a P-element inserted at the 5' end of *upd3*, containing a UAS site (Wang 2009). *upd3*^{d232a} and *upd3*^{x37e} were created through P-element mutagenesis (Wang 2009). *upd3*^{d232a} contains a deletion covering the entire last exon. *upd3*^{x37e} is a precise excision of the P-element. Gal-E132 (Upd-Gal4) is an enhancer trap in the *upd* locus (Tsai and Sun 2004). All markers used to label follicular epithelial cells are lacZ enhancer traps. 5A7, MA33, Mirr, and H2O labels

border cells, stretched cells, main body cells and posterior cells respectively (Roth et al. 1995, Gonzalez-Reyes and St Johnston 1998, Jordan et al. 2000). Dpp-lacZ marks both stretched cells and centripetal cells (Twombly et al. 1996).

Generation of misexpression clones

To overexpress *upd3* in polar cells, flies carrying Upd-Gal4 was crossed to *upd3*^{d04951} flies. Ectopic expression clones of *upd* and *upd3* in follicle cells were created using a flip-out cassette (Struhl and Basler 1993). Clones were induced by a 20 minutes heat shock in a 37 °C water bath. Flies were put on yeast paste and raised at 25 °C for 40 hours before ovaries were dissected out. The genotypes of the misexpressing clones are:

*W*¹¹¹⁸hsFLP1/+; [Act>y>Gal4][UAS-GFP]/[UAS-GFP]; [UAS-Upd]PK9/5A7

upd3^{d04951}hsFLP1/+; [Act>y>Gal4][UAS-GFP]/+; 5A7/TM3

upd3^{d04951}hsFLP1/+; [Act>y>Gal4][UAS-GFP]/+; [UAS-Upd]PK9/5A7

Immunological staining

Extracellular Staining

Flies within 2-day old were raised on yeast paste for two days at 30 °C. Ovaries were dissected in ice cold M3+BPYE medium and incubated with rabbit anti-Upd antibodies diluted in the same medium for 4 hours at 4 °C. After primary incubation, ovaries were washed two times in M3+BPYE medium and three times in PBS. Ovaries were fixed in 3.7% formaldehyde in PBS for 20 minutes on ice, followed by 2 washes with PBS and 2 washes with PBT. Ovaries were blocked in 5% BSA diluted in PBT. Secondary antibodies were incubated with ovaries overnight at 4 °C. Ovaries were washed 5 times with PBT and DAPI was added to the PBT wash in the second wash. Ovaries were mounted in 70% glycerol with addition of 2.5% Dabco in 1XPBS.

Conventional Staining

Ovaries were dissected from flies within 4 days old in PBT and fixed in 4% methanol-free formaldehyde for 3-5 minutes at room temperature. Ovaries were washed 5 times after

fixation and permeabilized in 2% TritonX-100 for 1 hour with rotation. Then ovaries were washed 5 times and blocked in 5% BSA for 1.5-2 hours at room temperature. Primary antibodies were incubated with ovaries overnight at 4 °C. Secondary antibodies were incubated with ovaries for 3 hours at room temperature before ovaries were mounted in the mounting medium.

Primary antibodies and dilutions used were: rabbit anti-Unpaired (Harrison et al. 1998) at 1:250, rabbit anti- β -Gal at 1:500, Dylight 488 conjugated goat anti-GFP (Rockland) at 1:1000. Secondary antibodies were: Alexa Fluor 488 anti-rabbit (Jackson immune research), alexa 555 anti-rabbit (Molecular probes), Cy5 anti-rabbit (Jackson immune research), Dylite 488 anti-goat (Jackson immune research), and they were all used at 1:1000.

Image capture and processing

BiFC images were captured using a SPOT camera on a Nikon E800 microscope. Images were analyzed using the Image J software (Schneider et al. 2012). Yeast images were taken using a CanoScan LiDE 90 scanner and processed in Adobe Photoshop CS5.

Confocal images of follicle cells were collected on a Leica TCS-SP laser scanning confocal microscope. Images were processed in Image J and Photoshop. Quantification of Upd staining intensity in egg chambers was performed using Nikon Elements software.

Reference

- Agaisse, H. and N. Perrimon (2004). "The roles of JAK/STAT signaling in Drosophila immune responses." Immunological Reviews **198**(1): 72-82.
- Agaisse, H., U.-M. Petersen, M. Boutros, B. Mathey-Prevot and N. Perrimon (2003). "Signaling Role of Hemocytes in Drosophila JAK/STAT-Dependent Response to Septic Injury." Developmental Cell **5**(3): 441-450.
- Akiyama, T., K. Kamimura, C. Firkus, S. Takeo, O. Shimmi and H. Nakato (2008). "Dally regulates Dpp morphogen gradient formation by stabilizing Dpp on the cell surface." Developmental Biology **313**(1): 408-419.
- Arbouzova, N. I. and M. P. Zeidler (2006). "JAK/STAT signalling in Drosophila: insights into conserved regulatory and cellular functions." Development **133**(14): 2605-2616.
- Atmakuri, K., Z. Ding and P. J. Christie (2003). "VirE2, a Type IV secretion substrate, interacts with the VirD4 transfer protein at cell poles of *Agrobacterium tumefaciens*." Molecular Microbiology **49**(6): 1699-1713.
- Bai, J., Y. Uehara and D. J. Montell (2000). "Regulation of Invasive Cell Behavior by Taiman, a Drosophila Protein Related to AIB1, a Steroid Receptor Coactivator Amplified in Breast Cancer." Cell **103**(7): 1047-1058.
- Bartee, E. and G. McFadden (2013). "Cytokine synergy: An underappreciated contributor to innate anti-viral immunity." Cytokine(0).
- Bastock, R. and D. St Johnston (2008). "Drosophila oogenesis." Current Biology **18**(23): R1082-R1087.
- Batard, P., M. Jordan and F. Wurm (2001). "Transfer of high copy number plasmid into mammalian cells by calcium phosphate transfection." Gene **270**(1-2): 61-68.
- Binari, R. and N. Perrimon (1994). "Stripe-specific regulation of pair-rule genes by hopscotch, a putative Jak family tyrosine kinase in Drosophila." Genes & Dev. **8**(3): 300-312.
- Boulay, J.-L., J. J. O'Shea and W. E. Paul (2003). "Molecular Phylogeny within Type I Cytokines and Their Cognate Receptors." Immunity **19**(2): 159-163.
- Boyle, M., C. Wong, M. Rocha and D. L. Jones (2007). "Decline in Self-Renewal Factors Contributes to Aging of the Stem Cell Niche in the Drosophila Testis." Cell Stem Cell **1**(4): 470-478.
- Brown, S., N. Hu and J. C.-G. Hombria (2001). "Identification of the first invertebrate interleukin JAK/STAT receptor, the Drosophila gene domeless." Current Biology **11**(21): 1700-1705.
- Buijs, J. T., G. van der Horst, C. van den Hoogen, H. Cheung, B. de Rooij, J. Kroon, M. Petersen, P. G. M. van Overveld, R. C. M. Pelger and G. van der Pluijm (2012). "The BMP2/7 heterodimer inhibits the human breast cancer stem cell subpopulation and bone metastases formation." Oncogene **31**(17): 2164-2174.
- Butler, S. J. and J. Dodd (2003). "A Role for BMP Heterodimers in Roof Plate-Mediated Repulsion of Commissural Axons." Neuron **38**(3): 389-401.
- Campanella, G. S. V., J. Grimm, L. A. Manice, R. A. Colvin, B. D. Medoff, G. R. Wojtkiewicz, R. Weissleder and A. D. Luster (2006). "Oligomerization of CXCL10 Is Necessary for Endothelial Cell Presentation and In Vivo Activity." The Journal of Immunology **177**(10): 6991-6998.
- Chen, H. W., X. Chen, S. W. Oh, M. J. Marinissen, J. S. Gutkind and S. X. Hou (2002). "mom identifies a receptor for the Drosophila JAK/STAT signal transduction pathway and encodes a protein distantly related to the mammalian cytokine receptor family." Genes Dev **16**(3): 388-398.

- Chen, M.-H., Y.-J. Li, T. Kawakami, S.-M. Xu and P.-T. Chuang (2004). "Palmitoylation is required for the production of a soluble multimeric Hedgehog protein complex and long-range signaling in vertebrates." Genes & Development **18**(6): 641-659.
- Cherbas, L. (2008, Oct. 21). "Tissue Culture Medium." Drosophila Genomic Resource Center Retrieved Jun. 27, 2014, from <https://dgrc.cgb.indiana.edu/include/file/TissueCultureMedium.pdf>.
- Cherbas, L. (2012, Jun. 18). "Additions to Tissues Culture Medium." Drosophila Genomic Resource Center Retrieved Jun. 28, 2014, from https://dgrc.cgb.indiana.edu/include/file/additions_to_medium.pdf.
- Cherbas, L., A. Willingham, D. Zhang, L. Yang, Y. Zou, B. D. Eads, J. W. Carlson, J. M. Landolin, P. Kapranov, J. Dumais, A. Samsonova, J.-H. Choi, J. Roberts, C. A. Davis, H. Tang, M. J. van Baren, S. Ghosh, A. Dobin, K. Bell, W. Lin, L. Langton, M. O. Duff, A. E. Tenney, C. Zaleski, M. R. Brent, R. A. Hoskins, T. C. Kaufman, J. Andrews, B. R. Graveley, N. Perrimon, S. E. Celniker, T. R. Gingeras and P. Cherbas (2011). "The transcriptional diversity of 25 *Drosophila* cell lines." Genome Research **21**(2): 301-314.
- Cherbas, P., L. Cherbas, S. S. Lee and K. Nakanishi (1988). "26-[125I]iodoponasterone A is a potent ecdysone and a sensitive radioligand for ecdysone receptors." Proceedings of the National Academy of Sciences **85**(7): 2096-2100.
- Criekinge, W. and R. Beyaert (1999). "Yeast two-hybrid: State of the art." Biological Procedures Online **2**(1): 1-38.
- Cui, Y., G. Riedlinger, K. Miyoshi, W. Tang, C. Li, C. X. Deng, G. W. Robinson and L. Hennighausen (2004). "Inactivation of Stat5 in mouse mammary epithelium during pregnancy reveals distinct functions in cell proliferation, survival, and differentiation." Mol Cell Biol **24**(18): 8037-8047.
- Darnell, J. E. K., Ian M. and G. R. Stark (1994). "Jak-STAT Pathways and Transcriptional Activation in Response to IFNs and Other Extracellular Signaling Proteins." Science **264**(5164): 1415-1421.
- Devergne, O., C. Ghigliione and S. Noselli (2007). "The endocytic control of JAK/STAT signalling in *Drosophila*." J Cell Sci **120**(19): 3457-3464.
- Dey, R., K. Ji, Z. Liu and L. Chen (2009). "A Cytokine–Cytokine Interaction in the Assembly of Higher-Order Structure and Activation of the Interleukine-3:Receptor Complex." PLoS ONE **4**(4): e5188.
- Dey, R., J. Kunmei, L. Zhigang and C. Lin (2009). "A Cytokine-Cytokine Interaction in the Assembly of Higher-Order Structure and Activation of the Interleukine-3:Receptor Complex." PLoS ONE **4**(4): 1-12.
- dos Remedios, C. G. and P. D. J. Moens (1995). "Fluorescence Resonance Energy Transfer Spectroscopy Is a Reliable "Ruler" for Measuring Structural Changes in Proteins: Dispelling the Problem of the Unknown Orientation Factor." Journal of Structural Biology **115**(2): 175-185.
- Duffy, J. B. (2002). "GAL4 system in *Drosophila*: a fly geneticist's Swiss army knife." Genesis **34**(1-2): 1-15.
- Dyrløv Bendtsen, J., H. Nielsen, G. von Heijne and S. Brunak (2004). "Improved Prediction of Signal Peptides: SignalP 3.0." Journal of Molecular Biology **340**(4): 783-795.
- Entchev, E. V., A. Schwabedissen and M. González-Gaitán (2000). "Gradient Formation of the TGF- β Homolog Dpp." Cell **103**(6): 981-992.
- Gateff, E., L. Gissmann, R. Shrestha, N. Plus, H. Pfister, J. Schroder and H. Z. Hausen (1980). "Characterization of two tumorous blood cell lines of *Drosophila melanogaster* and the

- viruses they contain." Invertebrate Systems in Vitro. Fifth International Conference on Invertebrate Tissue Culture, Rigi-Kaltbad, Switzerland, 1979: 517-533.
- Gilbert, M. M., B. K. Weaver, J. P. Gergen and N. C. Reich (2005). "A novel functional activator of the Drosophila JAK/STAT pathway, unpaired2, is revealed by an in vivo reporter of pathway activation." Mechanisms of Development **122**(7-8): 939-948.
- Giot, L., J. S. Bader, C. Brouwer, A. Chaudhuri, B. Kuang, Y. Li, Y. L. Hao, C. E. Ooi, B. Godwin, E. Vitols, G. Vijayadamar, P. Pochart, H. Machineni, M. Welsh, Y. Kong, B. Zerhusen, R. Malcolm, Z. Varrone, A. Collis, M. Minto, S. Burgess, L. McDaniel, E. Stimpson, F. Spriggs, J. Williams, K. Neurath, N. Ioime, M. Agee, E. Voss, K. Furtak, R. Renzulli, N. Aanensen, S. Carrola, E. Bickelhaupt, Y. Lazovatsky, A. DaSilva, J. Zhong, C. A. Stanyon, R. L. Finley, K. P. White, M. Braverman, T. Jarvie, S. Gold, M. Leach, J. Knight, R. A. Shimkets, M. P. McKenna, J. Chant and J. M. Rothberg (2003). "A Protein Interaction Map of Drosophila melanogaster." Science **302**(5651): 1727-1736.
- Gohl, C., D. Banovic, A. Grevelhörster and S. Bogdan (2010). "WAVE Forms Hetero- and Homooligomeric Complexes at Integrin Junctions in Drosophila Visualized by Bimolecular Fluorescence Complementation." Journal of Biological Chemistry **285**(51): 40171-40179.
- Gonzalez-Reyes, A. and D. St Johnston (1998). "Patterning of the follicle cell epithelium along the anterior-posterior axis during Drosophila oogenesis." Development **125**(15): 2837-2846.
- Grinberg, A. V., C.-D. Hu and T. K. Kerppola (2004). "Visualization of Myc/Max/Mad Family Dimers and the Competition for Dimerization in Living Cells." Mol. Cell. Biol. **24**(10): 4294-4308.
- Haerry, T. E. (2010). "The interaction between two TGF- β type I receptors plays important roles in ligand binding, SMAD activation, and gradient formation." Mechanisms of Development **127**(7-8): 358-370.
- Hansen, G., T. R. Hercus, B. J. McClure, F. C. Stomski, M. Dottore, J. Powell, H. Ramshaw, J. M. Woodcock, Y. Xu, M. Guthridge, W. J. McKinstry, A. F. Lopez and M. W. Parker (2008). "The Structure of the GM-CSF Receptor Complex Reveals a Distinct Mode of Cytokine Receptor Activation." Cell **134**(3): 496-507.
- Harrison, D., R. Binari, T. Nahreini, M. Gilman and N. Perrimon (1995). "Activation of a Drosophila Janus kinase (JAK) causes hematopoietic neoplasia and developmental defects." EMBO J **14**(12): 2857-2865.
- Harrison, D. A., P. E. McCoon, R. Binari, M. Gilman and N. Perrimon (1998). "Drosophila unpaired encodes a secreted protein that activates the JAK signaling pathway." Genes Dev **12**(20): 3252-3263.
- Hayashi, Y., T. R. Sexton, K. Dejima, D. W. Perry, M. Takemura, S. Kobayashi, H. Nakato and D. A. Harrison (2012). "Glypicans regulate JAK/STAT signaling and distribution of the Unpaired morphogen." Development **139**(22): 4162-4171.
- Hayashi, Y., T. R. Sexton, K. Dejima, D. W. Perry, M. Takemura, S. Kobayashi, H. Nakato and D. A. Harrison (2012). "Glypicans regulate JAK/STAT signaling and distribution of the Unpaired morphogen." Development **139**(22): 4162-4171.
- Hiatt, S. M., Y. J. Shyu, H. M. Duren and C.-D. Hu (2008). "Bimolecular fluorescence complementation (BiFC) analysis of protein interactions in Caenorhabditis elegans." Methods **45**(3): 185-191.
- Hombría, J. C.-G., S. Brown, S. Häder and M. P. Zeidler (2005). "Characterisation of Upd2, a Drosophila JAK/STAT pathway ligand." Developmental Biology **288**(2): 420-433.
- Hoogewerf, A. J., G. S. V. Kuschert, A. E. I. Proudfoot, F. Borlat, I. Clark-Lewis, C. A. Power and T. N. C. Wells (1997). "Glycosaminoglycans Mediate Cell Surface Oligomerization of Chemokines." Biochemistry **36**(44): 13570-13578.

- Horstman, A., I. A. Tonaco, K. Boutilier and R. G. Immink (2014). "A Cautionary Note on the Use of Split-YFP/BiFC in Plant Protein-Protein Interaction Studies." Int J Mol Sci **15**(6): 9628-9643.
- Hou, S. X., Z. Zheng, X. Chen and N. Perrimon (2002). "The JAK/STAT Pathway in Model Organisms: Emerging Roles in Cell Movement." Developmental Cell **3**(6): 765-778.
- Hou, X. S., M. B. Melnick and N. Perrimon (1996). "marelle Acts Downstream of the Drosophila HOP/JAK Kinase and Encodes a Protein Similar to the Mammalian STATs." Cell **84**(3): 411-419.
- Hu, C.-D., Y. Chinenov and T. K. Kerppola (2002). "Visualization of Interactions among bZIP and Rel Family Proteins in Living Cells Using Bimolecular Fluorescence Complementation." Molecular Cell **9**(4): 789-798.
- Hu, C.-D. and T. K. Kerppola (2003). "Simultaneous visualization of multiple protein interactions in living cells using multicolor fluorescence complementation analysis." Nat Biotech **21**(5): 539-545.
- Igaz, P., S. Tóth and A. Falus (2001). "Biological and clinical significance of the JAK-STAT pathway; lessons from knockout mice." Inflammation Research **50**(9): 435-441.
- Issigonis, M., N. Tulina, M. de Cuevas, C. Brawley, L. Sandler and E. Matunis (2009). "JAK-STAT Signal Inhibition Regulates Competition in the Drosophila Testis Stem Cell Niche." Science **326**(5949): 153-156.
- Ito, K., W. Awano, K. Suzuki, Y. Hiromi and D. Yamamoto (1997). "The Drosophila mushroom body is a quadruple structure of clonal units each of which contains a virtually identical set of neurones and glial cells." Development **124**(4): 761-771.
- Ito, T., T. Chiba, R. Ozawa, M. Yoshida, M. Hattori and Y. Sakaki (2001). "A comprehensive two-hybrid analysis to explore the yeast protein interactome." Proc Natl Acad Sci U S A **98**(8): 4569-4574.
- James, P., J. Halladay and E. A. Craig (1996). "Genomic Libraries and a Host Strain Designed for Highly Efficient Two-Hybrid Selection in Yeast." Genetics **144**(4): 1425-1436.
- Jiang, H., P. H. Patel, A. Kohlmaier, M. O. Grenley, D. G. McEwen and B. A. Edgar (2009). "Cytokine/Jak/Stat Signaling Mediates Regeneration and Homeostasis in the Drosophila Midgut." Cell **137**(7): 1343-1355.
- Johansen, H., A. van der Straten, R. Sweet, E. Otto, G. Maroni and M. Rosenberg (1989). "Regulated expression at high copy number allows production of a growth-inhibitory oncogene product in Drosophila Schneider cells." Genes & Development **3**(6): 882-889.
- Johnsson, N. and A. Varshavsky (1994). "Split ubiquitin as a sensor of protein interactions in vivo." Proceedings of the National Academy of Sciences **91**(22): 10340-10344.
- Jordan, K. C., N. J. Clegg, J. A. Blasi, A. M. Morimoto, J. Sen, D. Stein, H. McNeill, W.-M. Deng, M. Tworoger and H. Ruohola-Baker (2000). "The homeobox gene mirror links EGF signalling to embryonic dorso-ventral axis formation through Notch activation." Nat Genet **24**(4): 429-433.
- Kallio, J., H. Myllymaki, J. Gronholm, M. Armstrong, L. M. Vanha-aho, L. Makinen, O. Silvennoinen, S. Valanne and M. Ramet (2010). "Eye transformer is a negative regulator of Drosophila JAK/STAT signaling." FASEB J **24**(11): 4467-4479.
- Karpusas, M., M. Nolte, C. B. Benton, W. Meier, W. N. Lipscomb and S. Goelz (1997). "The crystal structure of human interferon β at 2.2-Å resolution." Proceedings of the National Academy of Sciences **94**(22): 11813-11818.
- Kershaw, N. J., J. M. Murphy, I. S. Lucet, N. A. Nicola and J. J. Babon (2013). "Regulation of Janus kinases by SOCS proteins." Biochem Soc Trans **41**(4): 1042-1047.

- Kisseleva, T., S. Bhattacharya, J. Braunstein and C. W. Schindler (2002). "Signaling through the JAK/STAT pathway, recent advances and future challenges." Gene **285**(1-2): 1-24.
- Kiu, H. and S. E. Nicholson (2012). "Biology and significance of the JAK/STAT signalling pathways." Growth Factors **30**(2): 88-106.
- Klingmüller, U., U. Lorenz, L. C. Cantley, B. G. Neel and H. F. Lodish (1995). "Specific recruitment of SH-PTP1 to the erythropoietin receptor causes inactivation of JAK2 and termination of proliferative signals." Cell **80**(5): 729-738.
- Kodama, Y. and C.-D. Hu (2010). "An improved bimolecular fluorescence complementation assay with a high signal-to-noise ratio." Biotechniques **49**(5): 793-805.
- Kothes, K. (1997). "Structure-function studies on human macrophage colony-stimulating factor (M-CSF)." Molecular Reproduction and Development **46**(1): 31-38.
- Krogan, N. J., G. Cagney, H. Yu, G. Zhong, X. Guo, A. Ignatchenko, J. Li, S. Pu, N. Datta, A. P. Tikuisis, T. Punna, J. M. Peregrín-Alvarez, M. Shales, X. Zhang, M. Davey, M. D. Robinson, A. Paccanaro, J. E. Bray, A. Sheung, B. Beattie, D. P. Richards, V. Canadien, A. Lalev, F. Mena, P. Wong, A. Starostine, M. M. Canete, J. Vlasblom, S. Wu, C. Orsi, S. R. Collins, S. Chandran, R. Haw, J. J. Rilstone, K. Gandi, N. J. Thompson, G. Musso, P. St Onge, S. Ghanny, M. H. Y. Lam, G. Butland, A. M. Altaf-Ul, S. Kanaya, A. Shilatifard, E. O'Shea, J. S. Weissman, C. J. Ingles, T. R. Hughes, J. Parkinson, M. Gerstein, S. J. Wodak, A. Emili and J. F. Greenblatt (2006). "Global landscape of protein complexes in the yeast *Saccharomyces cerevisiae*." Nature **440**(7084): 637-643.
- Kruger, D. M., P. C. Rathi, C. Pflieger and H. Gohlke (2013). "CNA web server: rigidity theory-based thermal unfolding simulations of proteins for linking structure, (thermo-)stability, and function." Nucleic Acids Res **41**(Web Server issue): W340-348.
- Krüger, D. M., P. C. Rathi, C. Pflieger and H. Gohlke (2013). "CNA web server: rigidity theory-based thermal unfolding simulations of proteins for linking structure, (thermo-)stability, and function." Nucleic Acids Research **41**(W1): W340-W348.
- Kusano, S., M. Kukimoto-Niino, N. Hino, N. Ohsawa, M. Ikutani, S. Takaki, K. Sakamoto, M. Hara-Yokoyama, M. Shirouzu, K. Takatsu and S. Yokoyama (2012). "Structural basis of interleukin-5 dimer recognition by its α receptor." Protein Science **21**(6): 850-864.
- Laemmli, U. K. (1970). "Cleavage of structural proteins during the assembly of the head of bacteriophage T4." Nature **227**(5259): 680-685.
- Leonard, W. J. and J. J. O'Shea (1998). "JAKS AND STATS: Biological Implications*." Annual Review of Immunology **16**(1): 293-322.
- Lin, G., N. Xu and R. Xi (2010). "Paracrine Unpaired Signaling through the JAK/STAT Pathway Controls Self-renewal and Lineage Differentiation of *Drosophila* Intestinal Stem Cells." J Mol Cell Biol **2**(1): 37-49.
- Liu, B., J. Liao, X. Rao, S. A. Kushner, C. D. Chung, D. D. Chang and K. Shuai (1998). "Inhibition of Stat1-mediated gene activation by PIAS1." Proceedings of the National Academy of Sciences **95**(18): 10626-10631.
- Loehlin, D. W. and J. H. Werren (2012). "Evolution of Shape by Multiple Regulatory Changes to a Growth Gene." Science **335**(6071): 943-947.
- Lokker, N. A., N. R. Movva, U. Strittmatter, B. Fagg and G. Zenke (1991). "Structure-activity relationship study of human interleukin-3. Identification of residues required for biological activity by site-directed mutagenesis." Journal of Biological Chemistry **266**(16): 10624-10631.
- López-Onieva, L., A. Fernández-Miñán and A. González-Reyes (2008). "Jak/Stat signalling in niche support cells regulates dpp transcription to control germline stem cell maintenance in the *Drosophila* ovary." Development **135**(3): 533-540.

- Makki, R., M. Meister, D. Pennetier, J. M. Ubeda, A. Braun, V. Daburon, J. Krzemien, H. M. Bourbon, R. Zhou, A. Vincent and M. Crozatier (2010). "A short receptor downregulates JAK/STAT signalling to control the Drosophila cellular immune response." *PLoS Biol* **8**(8): e1000441.
- Maurisse, R., D. De Semir, H. Emamekhoo, B. Bedayat, A. Abdolmohammadi, H. Parsi and D. Gruenert (2010). "Comparative transfection of DNA into primary and transformed mammalian cells from different lineages." *BMC Biotechnology* **10**(1): 9.
- McGregor, J. R., R. Xi and D. A. Harrison (2002). "JAK signaling is somatically required for follicle cell differentiation in Drosophila." *Development* **129**(3): 705-717.
- McGuire, S. E., P. T. Le, A. J. Osborn, K. Matsumoto and R. L. Davis (2003). "Spatiotemporal Rescue of Memory Dysfunction in Drosophila." *Science* **302**(5651): 1765-1768.
- Milburn, M. V., A. M. Hassell, M. H. Lambert, S. R. Jordan, A. E. I. Proudfoot, P. Graber and T. N. C. Wells (1993). "A novel dimer configuration revealed by the crystal structure at 2.4 [angst] resolution of human interleukin-5." *Nature* **363**(6425): 172-176.
- Morrison, K. L. and G. A. Weiss (2001). "Combinatorial alanine-scanning." *Current Opinion in Chemical Biology* **5**(3): 302-307.
- Muller, P., D. Kutteneuler, V. Gesellchen, M. P. Zeidler and M. Boutros (2005). "Identification of JAK/STAT signalling components by genome-wide RNA interference." *Nature* **436**(7052): 871-875.
- Nakagawa, C., K. Inahata, S. Nishimura and K. Sugimoto (2011). "Improvement of a Venus-Based Bimolecular Fluorescence Complementation Assay to Visualize bFos-bJun Interaction in Living Cells." *Bioscience, Biotechnology, and Biochemistry* **75**(7): 1399-1401
- Nakayama, M., R. Kikuno and O. Ohara (2002). "Protein-Protein Interactions Between Large Proteins: Two-Hybrid Screening Using a Functionally Classified Library Composed of Long cDNAs." *Genome Research* **12**(11): 1773-1784.
- Nüsslein-Volhard, C. and E. Wieschaus (1980). "Mutations affecting segment number and polarity in Drosophila." *Nature* **287**(5785): 795-801.
- Nybakken, K. and N. Perrimon (2002). "Heparan sulfate proteoglycan modulation of developmental signaling in Drosophila." *Biochim Biophys Acta* **1573**(3): 280-291.
- O'Connor, M. B., D. Umulis, H. G. Othmer and S. S. Blair (2006). "Shaping BMP morphogen gradients in the Drosophila embryo and pupal wing." *Development* **133**(2): 183-193.
- Olins, P. O., S. C. Bauer, S. Braford-Goldberg, K. Sterbenz, J. O. Polazzi, M. H. Caparon, B. K. Klein, A. M. Easton, K. Paik, J. A. Klover, B. R. Thiele and J. P. McKearn (1995). "Saturation Mutagenesis of Human Interleukin-3." *Journal of Biological Chemistry* **270**(40): 23754-23760.
- Opdenakker, G., P. M. Rudd, M. Wormald, R. A. Dwek and J. Van Damme (1995). "Cells regulate the activities of cytokines by glycosylation." *Faseb j* **9**(5): 453-457.
- Ouyang, X., T. Gulliford, G. Huang and R. J. Epstein (1999). "Transforming growth factor-alpha short-circuits downregulation of the epidermal growth factor receptor." *Journal of Cellular Physiology* **179**(1): 52-57.
- Panakova, D., H. Sprong, E. Marois, C. Thiele and S. Eaton (2005). "Lipoprotein particles are required for Hedgehog and Wingless signalling." *Nature* **435**(7038): 58-65.
- Pandit, S., B. Lynn and B. C. Rymond (2006). "Inhibition of a spliceosome turnover pathway suppresses splicing defects." *Proceedings of the National Academy of Sciences* **103**(37): 13700-13705.
- Parrish, J. R., K. D. Gulyas and R. L. Finley Jr (2006). "Yeast two-hybrid contributions to interactome mapping." *Current Opinion in Biotechnology* **17**(4): 387-393.

- Peel, D. and M. Milner (1990). "The diversity of cell morphology in cloned cell lines derived from *Drosophila* imaginal discs." Roux's archives of developmental biology **198**(8): 479-482.
- Pelletier, J. N., F.-X. Campbell-Valois and S. W. Michnick (1998). "Oligomerization domain-directed reassembly of active dihydrofolate reductase from rationally designed fragments." Proceedings of the National Academy of Sciences **95**(21): 12141-12146.
- Petersen, T. N., S. Brunak, G. von Heijne and H. Nielsen (2011). "SignalP 4.0: discriminating signal peptides from transmembrane regions." Nat Meth **8**(10): 785-786.
- Phizicky, E. M. and S. Fields (1995). "Protein-protein interactions: methods for detection and analysis." Microbiological Reviews **59**(1): 94-123.
- Proudfoot, A. E. I., T. M. Handel, Z. Johnson, E. K. Lau, P. LiWang, I. Clark-Lewis, F. Borlat, T. N. C. Wells and M. H. Kosco-Vilbois (2003). "Glycosaminoglycan binding and oligomerization are essential for the in vivo activity of certain chemokines." Proceedings of the National Academy of Sciences **100**(4): 1885-1890.
- Rajan, A. and N. Perrimon (2012). "Drosophila cytokine unpaired 2 regulates physiological homeostasis by remotely controlling insulin secretion." Cell **151**(1): 123-137.
- Ray, R. P. and T. Schüpbach (1996). "Intercellular signaling and the polarization of body axes during *Drosophila* oogenesis." Genes & Development **10**(14): 1711-1723.
- Ren, J., L. Wen, X. Gao, C. Jin, Y. Xue and X. Yao (2008). "CSS-Palm 2.0: an updated software for palmitoylation sites prediction." Protein Engineering Design and Selection **21**(11): 639-644.
- Rio, D. C. and G. M. Rubin (1985). "Transformation of cultured *Drosophila melanogaster* cells with a dominant selectable marker." Molecular and Cellular Biology **5**(8): 1833-1838.
- Rossi, F., C. A. Charlton and H. M. Blau (1997). "Monitoring protein-protein interactions in intact eukaryotic cells by β -galactosidase complementation." Proceedings of the National Academy of Sciences **94**(16): 8405-8410.
- Roth, S., F. Shira Neuman-Silberberg, G. Barcelo and T. Schüpbach (1995). "cornichon and the EGF receptor signaling process are necessary for both anterior-posterior and dorsal-ventral pattern formation in *Drosophila*." Cell **81**(6): 967-978.
- Schneider, C. A., W. S. Rasband and K. W. Eliceiri (2012). "NIH Image to ImageJ: 25 years of image analysis." Nat Meth **9**(7): 671-675.
- Schneider, I. (1972). "Cell lines derived from late embryonic stages of *Drosophila melanogaster*." Journal of Embryology and Experimental Morphology **27**(2): 353-365.
- Sexton, T. (2009). "The distribution of Unpaired during *Drosophila* oogenesis." Thesis.
- Shimmi, O., A. Ralston, S. S. Blair and M. B. O'Connor (2005). "The crossveinless gene encodes a new member of the Twisted gastrulation family of BMP-binding proteins which, with Short gastrulation, promotes BMP signaling in the crossveins of the *Drosophila* wing." Developmental Biology **282**(1): 70-83.
- Shimmi, O., D. Umulis, H. Othmer and M. B. O'Connor (2005). "Facilitated Transport of a Dpp/Scw Heterodimer by Sog/Tsg Leads to Robust Patterning of the *Drosophila* Blastoderm Embryo." Cell **120**(6): 873-886.
- Shuai, K. and B. Liu (2003). "Regulation of JAK-STAT signalling in the immune system." Nat Rev Immunol **3**(11): 900-911.
- Shyu, Y. J., H. Liu, X. Deng and C.-D. Hu (2006). "Identification of new fluorescent protein fragments for bimolecular fluorescence complementation analysis under physiological conditions." BioTechniques **40**: 61-66.
- Silver, D. L., E. R. Geisbrecht and D. J. Montell (2005). "Requirement for JAK/STAT signaling throughout border cell migration in *Drosophila*." Development **132**(15): 3483-3492.

- Silver, D. L. and D. J. Montell (2001). "Paracrine Signaling through the JAK/STAT Pathway Activates Invasive Behavior of Ovarian Epithelial Cells in *Drosophila*." Cell **107**(7): 831-841.
- Singh, S. R., W. Liu and S. X. Hou (2007). "The adult *Drosophila* malpighian tubules are maintained by multipotent stem cells." Cell Stem Cell **1**(2): 191-203.
- Sopory, S., S. Kwon, M. Wehrli and J. L. Christian (2010). "Regulation of Dpp activity by tissue-specific cleavage of an upstream site within the prodomain." Developmental Biology **346**(1): 102-112.
- Sprang, S. R. and J. Fernando Bazan (1993). "Cytokine structural taxonomy and mechanisms of receptor engagement: Current opinion in structural biology 1993, 3:815–827." Current Opinion in Structural Biology **3**(6): 815-827.
- Strigini, M. and S. M. Cohen (2000). "Wingless gradient formation in the *Drosophila* wing." Current Biology **10**(6): 293-300.
- Struhl, G. and K. Basler (1993). "Organizing activity of wingless protein in *Drosophila*." Cell **72**(4): 527-540.
- Takeda, K., K. Noguchi, W. Shi, T. Tanaka, M. Matsumoto, N. Yoshida, T. Kishimoto and S. Akira (1997). "Targeted disruption of the mouse Stat3 gene leads to early embryonic lethality." Proc Natl Acad Sci U S A **94**(8): 3801-3804.
- Teleman, A. A. and S. M. Cohen (2000). "Dpp gradient formation in the *Drosophila* wing imaginal disc." Cell **103**(6): 971-980.
- Thummel, C. S. and V. Pirrotta (1991). "Technical Notes: New pCaSpeR P-element vectors." Drosophila Information Newsletter **2**.
- Toledano, H., C. D'Alterio, B. Czech, E. Levine and D. L. Jones (2012). "The let-7-Imp axis regulates ageing of the *Drosophila* testis stem-cell niche." Nature **485**(7400): 605-610.
- Tsai, Y. C. and Y. H. Sun (2004). "Long-range effect of Upd, a ligand for Jak/STAT pathway, on cell cycle in *Drosophila* eye development." Genesis **39**(2): 141-153.
- Tseng, W.-C., F. R. Haselton and T. D. Giorgio (1997). "Transfection by Cationic Liposomes Using Simultaneous Single Cell Measurements of Plasmid Delivery and Transgene Expression." Journal of Biological Chemistry **272**(41): 25641-25647.
- Tulina, N. and E. Matunis (2001). "Control of stem cell self-renewal in *Drosophila* spermatogenesis by JAK- STAT signaling." Science **294**(5551): 2546-2549.
- Twombly, V., R. K. Blackman, H. Jin, J. M. Graff, R. W. Padgett and W. M. Gelbart (1996). "The TGF-beta signaling pathway is essential for *Drosophila* oogenesis." Development **122**(5): 1555-1565.
- Udy, G. B., R. P. Towers, R. G. Snell, R. J. Wilkins, S. H. Park, P. A. Ram, D. J. Waxman and H. W. Davey (1997). "Requirement of STAT5b for sexual dimorphism of body growth rates and liver gene expression." Proc Natl Acad Sci U S A **94**(14): 7239-7244.
- Uetz, P., L. Giot, G. Cagney, T. A. Mansfield, R. S. Judson, J. R. Knight, D. Lockshon, V. Narayan, M. Srinivasan, P. Pochart, A. Qureshi-Emili, Y. Li, B. Godwin, D. Conover, T. Kalbfleisch, G. Vijayadamodar, M. Yang, M. Johnston, S. Fields and J. M. Rothberg (2000). "A comprehensive analysis of protein-protein interactions in *Saccharomyces cerevisiae*." Nature **403**(6770): 623-627.
- Ui, K., R. Ueda and T. Miyake (1987). "Cell lines from imaginal discs of *Drosophila melanogaster*." In Vitro Cellular and Developmental Biology **23**: 707-711.
- Ungureanu, D., P. Saharinen, I. Junttila, D. J. Hilton and O. Silvennoinen (2002). "Regulation of Jak2 through the Ubiquitin-Proteasome Pathway Involves Phosphorylation of Jak2 on Y1007 and Interaction with SOCS-1." Molecular and Cellular Biology **22**(10): 3316-3326.

- Vaughn, J. L., R. H. Goodwin, G. J. Tompkins and P. McCawley (1977). "The Establishment of Two Cell Lines from the Insect *Spodoptera frugiperda* (Lepidoptera; Noctuidae)." *In Vitro* **13**(4): 213-217.
- Vidal, O. M., W. Stec, N. Bausek, E. Smythe and M. P. Zeidler (2010). "Negative regulation of *Drosophila* JAK-STAT signalling by endocytic trafficking." *J Cell Sci* **123**(Pt 20): 3457-3466.
- Villalobos, V., S. Naik and D. Piwnica-Worms (2007). "Current State of Imaging Protein-Protein Interactions In Vivo with Genetically Encoded Reporters." *Annual Review of Biomedical Engineering* **9**(1): 321-349.
- Vyas, N., D. Goswami, A. Manonmani, P. Sharma, H. A. Ranganath, K. VijayRaghavan, L. S. Shashidhara, R. Sowdhamini and S. Mayor (2008). "Nanoscale Organization of Hedgehog Is Essential for Long-Range Signaling." *Cell* **133**(7): 1214-1227.
- Wang, L. (2009). "Functional characterization of Upd3 in *Drosophila* development." Thesis.
- Wang, X., J. S. Sharp, T. M. Handel and J. H. Prestegard (2013). Chapter Twenty - Chemokine Oligomerization in Cell Signaling and Migration. *Progress in Molecular Biology and Translational Science*. G. Jesús and C. Francisco, Academic Press. **Volume 117**: 531-578.
- Wang, Y.-C. and E. L. Ferguson (2005). "Spatial bistability of Dpp-receptor interactions during *Drosophila* dorsal-ventral patterning." *Nature* **434**(7030): 229-234.
- Ward, L. D., A. Hammacher, G. J. Howlett, J. M. Matthews, L. Fabri, R. L. Moritz, E. C. Nice, J. Weinstock and R. J. Simpson (1996). "Influence of Interleukin-6 (IL-6) Dimerization on Formation of the High Affinity Hexameric IL-6-Receptor Complex." *Journal of Biological Chemistry* **271**(33): 20138-20144.
- Wawersik, M., A. Milutinovich, A. L. Casper, E. Matunis, B. Williams and M. Van Doren (2005). "Somatic control of germline sexual development is mediated by the JAK/STAT pathway." *Nature* **436**(7050): 563-567.
- Wright, V. M., K. L. Vogt, E. Smythe and M. P. Zeidler (2011). "Differential activities of the *Drosophila* JAK/STAT pathway ligands Upd, Upd2 and Upd3." *Cellular Signalling* **23**(5): 920-927.
- Xi, R. (2002). "The roles of the JAK pathway in follicular patterning in *Drosophila* " Thesis.
- Xi, R., J. R. McGregor and D. A. Harrison (2003). "A Gradient of JAK Pathway Activity Patterns the Anterior-Posterior Axis of the Follicular Epithelium." *Developmental Cell* **4**(2): 167-177.
- Xie, T. and A. C. Spradling (2000). "A niche maintaining germ line stem cells in the *Drosophila* ovary." *Science* **290**(5490): 328-330.
- Yang, J. and M. Reth (2012). *Drosophila* S2 Schneider Cells: A Useful Tool for Rebuilding and Redesigning Approaches in Synthetic Biology. *Synthetic Gene Networks*. W. Weber and M. Fussenegger, Humana Press. **813**: 331-341.
- Zeng, X., J. A. Goetz, L. M. Suber, W. J. Scott, C. M. Schreiner and D. J. Robbins (2001). "A freely diffusible form of Sonic hedgehog mediates long-range signalling." *Nature* **411**(6838): 716-720.

VITA

Author's name

Qian Chen

Place of birth

Beijing, China

Education

B.S. in Biological Sciences (2007)
Fudan University

Employment

Teaching / Research Assistant (2007-2013)
University of Kentucky

Awards and certificates

Academic Year Fellowship (2013)
University of Kentucky

Ribble Mini-grant Award (2009, 2013)
Department of Biology, University of Kentucky

Ren Min Scholarship (2006)
Fudan University

Publications

1. Chen Q, Giedt M, Tang L, Harrison D. Tools and methods for studying the Drosophila JAK/STAT pathway. *Method* 68, 160-172
2. Chen Q and Harrison D. The functional interaction among the JAK/STAT signaling ligands in *Drosophila melanogaster*. (In preparation)